AD-A125 400 ANALYSIS OF THE LARGE URBAN FIRE ENVIRONMENT PART II PARAMETRIC ANALYSIS A..(U) PACIFIC-SIERRA RESEARCH CORP LOS ANGELES CA D A LARSON ET AL. NOV 82 PSR-1210-PT-2 EMW-C-0747 1/2

UNCLASSIFIED F/G 15/6 NL

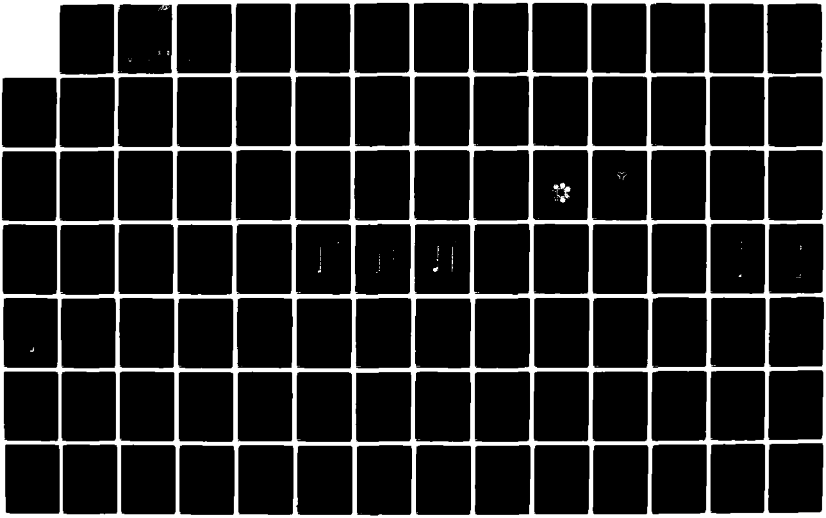

M-2

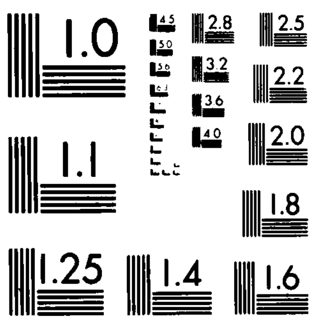

MICROCOPY RESOLUTION TEST CHART
NATIONAL BUREAU OF STANDARDS 1963 A

PSR Report 1210

ANALYSIS OF THE LARGE URBAN FIRE ENVIRONMENT

Part II. Parametric Analysis and Model City Simulations

By
D. A. Larson
R. D. Small

November 1982

Final Report
Contract EMW-C-0747, Work Unit 2564E

For
Federal Emergency Management Agency
National Preparedness Programs
Washington, D.C. 20472

Approved for Public Release: Distribution Unlimited

PACIFIC-SIERRA RESEARCH CORP.
12340 Santa Monica Blvd. • Los Angeles, CA 90025 • (213) 820-2200

PSR Report 1210

ANALYSIS OF THE LARGE URBAN FIRE ENVIRONMENT

Part II. Parametric Analysis and Model City Simulations

By
D. A. Larson
R. D. Small

November 1982

Final Report
Contract EMW-C-0747, Work Unit 2564E

For
Federal Emergency Management Agency
National Preparedness Programs
Washington, D.C. 20472

FEMA Review Notice

This report has been reviewed in the Federal Emergency Management Agency and approved for publication. Approval does not signify that the contents necessarily reflect the views and policies of the Federal Emergency Management Agency.

Approved for Public Release: Distribution Unlimited

PACIFIC-SIERRA RESEARCH CORP.
12340 Santa Monica Blvd. • Los Angeles, CA 90025 • (213) 820-2200

SECURITY CLASSIFICATION OF THIS PAGE (When Data Entered)

REPORT DOCUMENTATION PAGE

READ INSTRUCTIONS BEFORE COMPLETING FORM

1. REPORT NUMBER PSR Report 1210	2. GOVT ACCESSION NO. AD-A125 400	3. RECIPIENT'S CATALOG NUMBER
4. TITLE (and Subtitle) ANALYSIS OF THE LARGE URBAN FIRE ENVIRONMENT PART II. PARAMETRIC ANALYSIS AND MODEL CITY SIMULATIONS		5. TYPE OF REPORT & PERIOD COVERED Final Report Sept. 1981 - Sept. 1982 6. PERFORMING ORG. REPORT NUMBER PSR Report 1210
7. AUTHOR(s) D. A. Larson, R. D. Small		8. CONTRACT OR GRANT NUMBER(s) EMW-C-0747
9. PERFORMING ORGANIZATION NAME AND ADDRESS Pacific-Sierra Research Corporation 12340 Santa Monica Boulevard Los Angeles, California 90025		10. PROGRAM ELEMENT, PROJECT, TASK AREA & WORK UNIT NUMBERS Work Unit 2564E
11. CONTROLLING OFFICE NAME AND ADDRESS Federal Emergency Management Agency National Preparedness Programs Washington, D.C. 20472		12. REPORT DATE November 1982 13. NUMBER OF PAGES 120
14. MONITORING AGENCY NAME & ADDRESS(if different from Controlling Office)		15. SECURITY CLASS. (of this report) Unclassified 15a. DECLASSIFICATION/DOWNGRADING SCHEDULE

16. DISTRIBUTION STATEMENT (of this Report)

Approved for public release: distribution unlimited.

17. DISTRIBUTION STATEMENT (of the abstract entered in Block 20, if different from Report)

18. SUPPLEMENTARY NOTES

19. KEY WORDS (Continue on reverse side if necessary and identify by block number)

Fire	Nuclear effects
Large area fire	Fire model
Mass fire	Combustion zone
Firestorm	Urban fire

20. ABSTRACT (Continue on reverse side if necessary and identify by block number)

This report considers the fire environment that would result from a megaton-yield nuclear weapon explosion. An analysis (developed in Part I) that treats the physics of the burning zone and the volume immediately above it (turning region) is used to predict the velocity, temperature, and pressure fields of large area fires.

A sensitivity study explores the influence of turbulence, radiation, fire size, and burning intensity on the mean temperature levels and velocity fields. The results show hurricane-force velocities developing as the fire size or

DD FORM 1473, 1 JAN 73 EDITION OF 1 NOV 65 IS OBSOLETE

SECURITY CLASSIFICATION OF THIS PAGE (When Data Entered)

BLOCK 20 (cont.)

burning rate is increased. A sample calculation illustrates the change in fire-wind velocities as the fire evolves over time.

Calculations of the burning region for three model urban areas show the influence of building density and urban sprawl on the resulting fire environment. An additional set of predictions accounts for reduction of the fire intensity by blast in the urban center. For the latter cases, the temperature distribution is changed markedly, though the magnitude of the induced fire winds is not appreciably reduced.

PREFACE

This report is the second of the two-part documentation of Pacific-Sierra Research Corporation's analysis of the large urban fire environment. This part presents calculations of the characteristics of nuclear-weapon-ignited fires. Part I develops the theory underlying the analysis. All work was performed for the Federal Emergency Management Agency under contract EMW-C-0747; the technical monitor was Dr. David Bensen.

The authors gratefully acknowledge the contributions of Dr. Harold L. Brode.

SUMMARY

This report considers the large-fire environment that would occur in an urban area subject to a nuclear weapon explosion. The effects of system parameters are explored in a sensitivity study, and results for three model cities are presented.

The examples are characterized by extensive areas simultaneously burning, strong buoyancy, and large temperature gradients. Several such fires occurred during World War II. Though those fires were dramatic in intensity and destructiveness, each involved a relatively small area. A nuclear weapon explosion could generate a far larger area fire and a more severe fire environment. This report is intended to define such large fires. The results should be applicable for damage evaluation, formulation of shelter requirements, and rescue planning.

The calculations are based on the theory developed in Part I of this report, which is applicable to the fire zone and the volume immediately above it (turning region). The effects of variable area heating, turbulence, strong buoyancy, large temperature changes, and radiation are treated. The induced fire winds and rapid temperature changes at the fire periphery are uniquely determined by the use of jump conditions. Simulations of the Hamburg firestorm and a large Flambeau fire agreed well with available data.

The parametric analysis considers a large area fire and the effects of fire size, heating rates, mixing coefficients, and hot gas/smoke radiation. The results show the influence of those variables on the induced fire winds, mean temperature, and pressure gradients. In general, an increase in either the fire size or heating rate raises the mean temperature levels and the induced fire-wind velocities. For the larger heat release rates or fire sizes, the attendant increases in mean temperature and velocity are limited by compressibility effects.

Fires such as may result from a megaton-yield explosion are analyzed for three model urban areas. Each city is characterized by

a high-density center, a surrounding belt of mixed residential/industrial construction, and a lower density suburban belt. Each model city portrays a different degree of building density and urban sprawl. The results illustrate how a particular city geometry affects the velocity and temperature fields for a given fire. An additional series of computations considers reduction of the fire area by severe blast damage and debris formation. For those calculations, complete burning was allowed in an annular area, with the fire intensity significantly reduced in the center.

Finally, the model is employed to estimate the behavior of the velocity and temperature fields as a function of fire evolution. Those calculations may indicate the most appropriate periods for effecting rescue operations as well as provide an estimate of time-dependent shelter loadings.

CONTENTS

FIGURES

TABLES

SYMBOLS

MATHEMATICAL SYMBOLS

A = dimensionless constant, gH/U^2

c_p = specific heat capacity at constant pressure

E_B = average heat released per unit weight of all combustibles

$\mathcal{E}_1$ = effective kinematic viscosity (for turbulent flow)

f_{Bu} = building density (ratio of area covered by buildings to total area)

F = dimensionless measure of QH [defined by Eq. (13)]

g = gravitational acceleration

H = maximum height of flames

k^* = reciprocal of graybody radiation mean free path

k_1 = effective thermal conductivity (for turbulent flow)

K_1 = dimensionless heat-diffusion coefficient

L_s = average fuel loading per building story

L_T = average areal fuel loading

M_1 = dimensionless momentum-diffusion coefficient

N_s = average number of building stories

P = perturbation pressure (dimensionless)

P_a = ground-level atmospheric pressure in far field

P_{max} = maximum perturbation pressure

q = dimensionless spatial distribution of volumetric heat-addition rate

Q = volumetric heat-addition-rate scale

Q_A = areal heat-addition rate

r = radial position coordinate (dimensionless, except in Figs. 24 through 26)

R = fire radius

T = temperature (dimensionless)

T_a = ground-level atmospheric temperature in far field

T_{max} = maximum temperature

u = radial velocity (dimensionless)

u_{max} = maximum radial velocity

U = radial velocity scale

v = vertical velocity (dimensionless)

v_{max} = maximum vertical velocity

y = vertical position coordinate (dimensionless)

γ = specific heat ratio

δ = dimensionless constant, $U^2/(P_a/\rho_a)$

ϕ = radial dependence of model-city heat release rates in blast-modified cases

ρ = density (dimensionless)

ρ_a = ground-level atmospheric density in far field

σ = radiation coefficient (dimensionless constant), $4\pi\hat{\sigma}T_a^4k^*/Q$

$\hat{\sigma}$ = Stefan's constant

SYMBOLS[†] USED IN DOCUMENTATION OF PREDICTION ALGORITHM

E_j = intermediate variable [defined by Eq. (A.37)]

$\vec{F}, \vec{G}, \vec{H}$ = vectors of functions that are to be driven to zero (by proper choice of $\vec{x}$) in Newton iterations, and that represent discretized model equations on individual lines of constant y

---

[†]Mathematical variables only--not FORTRAN labels.

G_i, H_i = *ith* components of $\vec{G}$ and $\vec{H}$

i = radial position index ($1 \leq i \leq M + 1$)

j = vertical position index ($1 \leq j \leq N + 1$)

J = $\partial\vec{F}/\partial\vec{x}$ Jacobian matrix

k = vector component index ($1 \leq k \leq 2M$)

ℓ = index for α, β, γ, δ Jacobian elements ($1 \leq \ell \leq M$)

m, n = iteration counters in Newton and shooting iterations

M, N = number of finite difference cells in radial and vertical directions, respectively (see footnote, p. 68)

p = index for α, β, γ, δ Jacobian elements ($0 \leq p \leq 2$)

$P_{i,j}$ = $P(r_i, y_j)$

P_{old}, P_{new} = successive discretized forms of P in shooting iterations

$(Qq)_{max}$ = maximum value of Qq

r_i = $(i - 1)\,\Delta r$

R_i = sum of all terms in G_i, for any line $y = y_j$, j fixed, that depend only on $y = y_{j-1}$ data

t = time

$\vec{T}$ = vector of discrete T values for line of constant y

$T_{i,j}$ = $T(r_i, y_j)$

T_{old}, T_{new} = successive discretized forms of T in shooting iterations

$\vec{u}$ = vector of discrete u values for line of constant y

$u_{i,j}$ = $u(r_i, y_j)$

u_{old}, u_{new} = successive discretized forms of u in shooting iterations

$v_{i,j}$ = $v(r_i, y_j)$

w = generic variable

$w_{i,j}$ = generic finite-difference variable

$\vec{x}$ = vector of discrete u and T values for line of constant y

$\tilde{x}_k$ = *k*th component of $\vec{x}$

$\vec{x}_{old}$, $\vec{x}_{new}$ = successive discretized forms of $\vec{x}$ in Newton iterations

y_j = $(j - 1)\ \Delta y$ for $j \le 5M + 1$; $5 + (j - 5M - 1)(2\ \Delta r)$ for $j > 5M + 1$

y_{max} = maximum value of y considered

$\alpha_{p,\ell}$ = nonzero element in $\partial\vec{G}/\partial\vec{u}$ Jacobian ($0 \le p \le 2$, $1 \le \ell \le M$)

$\beta_{p,\ell}$ = nonzero element in $\partial\vec{G}/\partial\vec{T}$ Jacobian ($0 \le p \le 2$, $1 \le \ell \le M$)

$\gamma_{p,\ell}$ = nonzero element in $\partial\vec{H}/\partial\vec{u}$ Jacobian ($0 \le p \le 2$, $1 \le \ell \le M$)

$\vec{\delta}$ = vector difference between successive values of $\vec{x}$ in Newton iterations

δ_k = *k*th component of $\vec{\delta}$

$\delta_{p,\ell}$ = nonzero element in $\partial\vec{H}/\partial\vec{T}$ Jacobian ($0 \le p \le 2$, $1 \le \ell \le M$)

Δr, Δy = cell width and height, respectively

Π_i = sum of all terms in H_i, for any line $y = y_j$, j fixed, that depend only on $y = y_{j-1}$ data

$\rho_{i,j}$ = $\rho(r_i, y_j)$

ω = relaxation coefficient in shooting iterations

I. INTRODUCTION

This report presents predictions of the temperatures, pressures, and high-speed winds created by large urban fires. The dependence of those quantities on fire size, burning rate, and various other parameters is explored, and fires in model U.S. cities are examined. Simulations in which nuclear-weapon-ignited fires are extinguished in the center by blast are compared with those in which the fires continue to burn. The model developed in Part I of this report was used to calculate all values. That model may be readily extended to obtain estimates of oxygen depletion and noxious gas buildup as well and, hence, a fairly complete baseline description of the environment facing civil defense personnel when large urban areas are burning.

Most previous research concerning the hydrothermodynamics of free-burning fires has been restricted to the weakly buoyant free-convection plume. The resulting theories describe the basic flow in the middle and upper parts of a long, thin plume over a small fire, and may be relevant to some portion of the convection column generated over a large urban fire [e.g., Morton, Taylor, and Turner, 1956; Murgai and Emmons, 1960; Yokoi, 1960; Nielsen and Tao, 1965]. However, as discussed in Part I, such theories are inapplicable in and around the combustion zone, so they cannot be used to predict the environment and high-speed surface winds induced by large fires.

Smith, Morton, and Leslie [1975] present global computations of the hydrothermodynamic environment near the combustion zone as well as above it. In their calculations, all components of the fire-generated flow field--e.g., surface inflow, the convection column, the far field--are considered collectively, and the strong coupling between dynamic forces and the induced surface winds is demonstrated. In and around the combustion zone, however, density changes are assumed to be small (Boussinesq approximation), heat is input at the boundary rather than in volume, and not much resolution is sought.

Further, the computations are not specifically designed for the analysis of large urban fires.

In a more recent study, Brode, Larson, and Small [1982] adopt the basic computational approach of Smith, Morton, and Leslie in studying the mesoscale motions generated by large fires, but eliminate some of the stated deficiencies. Their work is directly aimed at the definition of the large urban fire environment, and arbitrary changes in temperature and density are allowed in the near-fire region. The resolution in that region is still rather coarse, however.

The component analysis introduced by Small, Larson, and Brode [1981] provides an alternative to the global-calculation analysis in which fine resolution near the fire can be obtained economically. Using that approach, the components of the flow field are analyzed separately, and then combined by means of appropriate matching conditions. The special features of each component are thus considered in greater detail, and resolution is enhanced.

The key element in the component analysis is the description of the environment in and around the fire, since the entire flow is driven by the hydrothermodynamic interactions in that region. The turning-region model developed in Part I provides the key description. That model decouples from those for the other flow components, and thus can be used independently to make detailed predictions of the near-fire environment. Such a capability extends our understanding of fire dynamics and is the basis for the present analysis.

We use the turning-region model to generate the large urban fire predictions. In that model, a volume heat source represents the net effect of the combustion process, and the induced flow is taken to be axisymmetric and quasi-steady. The flow is also assumed compressible, to permit arbitrary changes in temperature and density. A one-parameter eddy-viscosity model is used to describe the turbulent transfer of heat and momentum, and a graybody approximation to model hot gas and smoke radiation. Finally, jump conditions are derived to account for the rapid changes in physical quantities at the fire periphery. They effect model problem closure, and decouple the turning-region analysis from that of other component flows. An iterative finite-difference scheme, documented in the Appendix, is employed to solve the resultant boundary value problem.

We study the large urban fire environment in two ways--by varying parameters and by simulating three model cities. In the parametric analysis, excursions are made about a baseline in which the fire radius is taken to be 10 km and the characteristic heat release rate is consistent with that of the 1943 Hamburg firestorm [DCPA, 1973]. Predictions of hurricane-force winds are typical in the parameter excursions as well as the model city simulations, which consider fires of radius 12 km with spatially varying heating rates on the order of those in the parametric analysis. That is believed to be about the size of the fire that would result from a near-surface nuclear burst of about 1 Mt [Johnson and Larson, 1982].

Section II presents the results of the parametric analysis. As expected, temperatures and fire-wind velocities increase with an increase in either fire size or burning rate, though the fire-wind variations are not as rapid as the linear scaling law of Part I suggests. Also as expected, temperatures and winds increase with a decrease in radiation intensity; winds also increase with a decrease in the magnitude of the eddy coefficient for turbulent momentum transfer. The temperature field is relatively insensitive to changes in that coefficient, however, and both winds and temperature are relatively insensitive to changes in the corresponding coefficient for turbulent heat transfer.

The basic flow pattern also seems to be relatively insensitive to variations in the specific dependence of the heat release rate on spatial position, though such variations modify velocities slightly and may significantly change the temperature field. That behavior is found when model predictions for a uniformly heated, circular fire are compared with those for an annular fire. The comparison indicates how partial blast extinguishment would modify the hydrothermodynamic environment generated by a nuclear-weapon-ignited fire. It also provides a first look at the catastrophic effect of multiple weapon bursts.

Section III describes the model city simulations. Three model cities are defined: one that is lightly built-up, intended to represent new, sprawling cities; one that is heavily built-up, intended to represent old, congested cities; and one of intermediate building density. For each city, spatially dependent fuel loadings and peak-period burning rates for a baseline fire are estimated, and the resulting temperatures, pressures, and fire winds predicted. Those calculations are repeated for a scenario in which the fire is ignited by a nuclear burst and the city partially destroyed by the attendant blast.

Somewhat surprisingly, despite a significant difference in model-city temperature predictions for the "blast" and "no blast" simulations, the corresponding difference in induced fire winds is fairly small. Such behavior suggests that the winds and wind damage resulting from nuclear-weapon-ignited fires may be relatively independent of the degree of blast extinguishment--unless, of course, extinguishment is nearly complete.

As expected, however, temperatures and fire-wind velocities all increase with building density. For a given fire size, the large-fire threat facing civil defense workers will thus be more severe in the tall, heavily loaded cities than in the short, lightly loaded cities. In general, however, the shorter cities sprawl out over greater land areas than do taller ones of comparable population, and are thus capable of supporting larger fires. The large-fire threat for any given population size may thus be greatest in some of the shorter cities, especially if the fires result from multiple nuclear bursts. Comparisons between specific cities must be made individually.

Finally, Sec. IV presents a sample application of the quasi-steady model of Part I to obtain time-dependent predictions. The sample case considers multiple-fuel-bed Flambeau fires, the largest area fires for which a reasonable body of technical data exists [Countryman, 1969; Palmer, 1981].

II. PARAMETRIC ANALYSIS OF LARGE-FIRE ENVIRONMENT

Using the turning-region model of Part I, this section explores the dependence of the large-fire environment on fire size (height and radius), burning rate (spatial average and form), degree of turbulent mixing, and degree of hot-gas radiation.

Briefly, with r, y, u, v, ρ, T, and P denoting dimensionless radial and vertical position, radial and vertical velocity, density, temperature, and perturbation pressure, respectively, the turning-region equations are as follows:

$$\frac{\partial}{\partial r}(r\rho u) + \frac{\partial}{\partial y}(r\rho v) = 0 , \tag{1a}$$

$$\rho\left(u\frac{\partial u}{\partial r} + v\frac{\partial u}{\partial y}\right) = -\frac{\partial P}{\partial r} + M_1\left(\frac{1}{r}\frac{\partial}{\partial r}\left(r\frac{\partial u}{\partial r}\right) - \frac{u}{r^2}\right) , \tag{1b}$$

$$\frac{\partial P}{\partial y} + A\rho = 0 , \tag{1c}$$

$$\rho\left(u\frac{\partial T}{\partial r} + v\frac{\partial T}{\partial y}\right) = q(r, y) - \sigma(T^4 - 1) + K_1\left(\frac{1}{r}\frac{\partial}{\partial r}\left(r\frac{\partial T}{\partial r}\right)\right) , \tag{1d}$$

$$\rho T = 1 , \tag{1e}$$

where the dimensionless parameters are

$$A = \frac{gH}{U^2} ,$$

$$U = \frac{\gamma - 1}{\gamma}\left(\frac{R}{H}\right)\left(\frac{QH}{P_a}\right) ,$$

$$\sigma = 4\pi\hat{\sigma}T_a^4\left(\frac{k^*H}{QH}\right) , \tag{2}$$

and

$$M_1 = \frac{\mathcal{E}_1/\rho_a}{UR} ,$$

$$K_1 = \frac{k_1/c_p\rho_a}{UR} . \tag{3}$$

Here, R and H denote fire radius and maximum flame height; Q the scale and q(r, y) the spatial distribution for the rate of volumetric heat addition; and P_a, ρ_a, and T_a ground-level atmospheric pressure, density, and temperature in the far field, respectively. Further, $\hat{\sigma}$ is Stefan's constant, k^* is the reciprocal of the graybody radiation mean free path (assumed constant), and $\mathcal{E}_1$ and k_1 are dimensional eddy coefficients for turbulent momentum and heat transfer.[†]

We consider the dependence of model predictions on the size parameters R and H, the burning rate parameters QH[††] and q(r, y), the radiation mean free path k^{*-1}, and the dimensionless eddy coefficients M_1 and K_1. The terms $\mathcal{E}_1/\rho_a$ and $k_1/c_p\rho_a$ remain constant, except when variations with M_1 and K_1 are specifically studied.

BASELINE ANALYSIS

As a baseline case, we consider an axisymmetric fire with the following parameters:

$$R = 10 \quad km , \tag{4a}$$

$$H = 100 \quad m , \tag{4b}$$

$$QH = 5.7 \times 10^4 \quad cal/m^2\text{-sec} , \tag{4c}$$

[†]As in Part I, g is the acceleration due to gravity, γ the specific heat ratio, and U the radial velocity scale. The vertical velocity is scaled with (H/R)U, temperature and density with T_a and ρ_a, and perturbation pressure with δP_a, where $\delta = U^2/(P_a/\rho_a)$.

[††]QH is used as a parameter instead of Q because areal heat release rates are encountered much more frequently than volumetric rates in the large-fire literature.

$$q(r, y) = \begin{cases} 1.6 & \text{for} \quad 0 \le y \le 0.25 \\ 1.6 \left(\frac{4}{3}(1 - y)\right) & \text{for} \quad 0.25 \le y \le 1.0 \, , \\ 0 & \text{for} \quad y \ge 1.0 \end{cases} \tag{4d}$$

$$M_1 = K_1 = 0.2 \, , \tag{4e}$$

$$k^{*^{-1}} = 20 \quad m \, . \tag{4f}$$

The heat release rate in this case is the same as that in our simulation in Part I of the 1943 Hamburg firestorm, and is characteristic of the rates estimated in Sec. III for a variety of U.S. cities. The parameter QH is the nominal specific scale rate suggested by DCPA [1973]. The form of q(r, y) represents maximum heating in and around the fuel zone and a decrease in heating with increased altitude. All other parameter choices used in Eqs. (4) are of the same order as those used in the model city analysis.

From Eqs. (2) and (4), the radial velocity scale for the baseline case is

$$U = 67.2 \quad m/sec \, , \tag{5}$$

and

$$A = 0.217 \, ,$$

$$\sigma = 0.110 \, . \tag{6}$$

The temperatures, pressures, and velocities predicted for this case are summarized in the vector, contour, and profile plots of Figs. 1 through 5. The flow field is illustrated in Fig. 1. Temperature and pressure contours are plotted in Figs. 2 and 3, respectively. The temperature attains a maximum in the fire center at the top of the maximum heating zone ($y = 0.25$). It then decreases rapidly with increased altitude, the flow becoming weakly buoyant above three

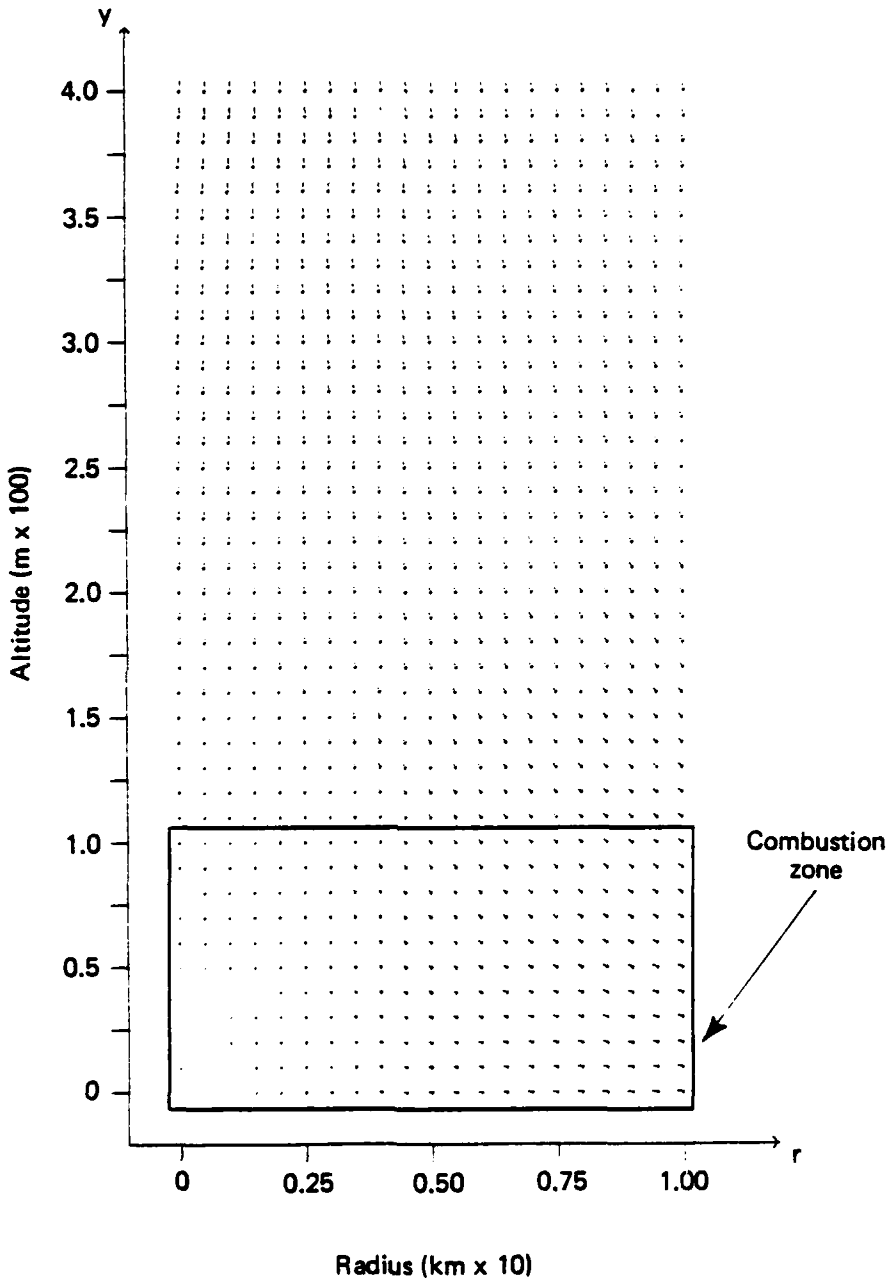

Fig. 1--Velocity field for baseline fire

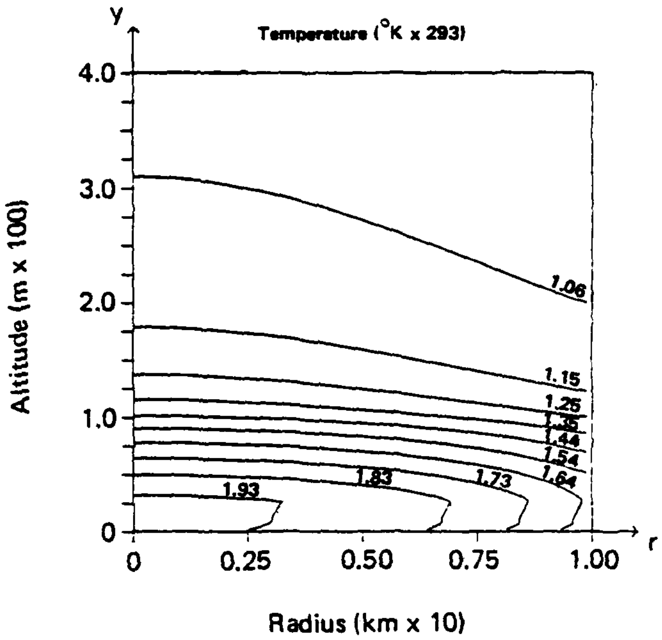

Fig. 2--Temperature contours for baseline fire

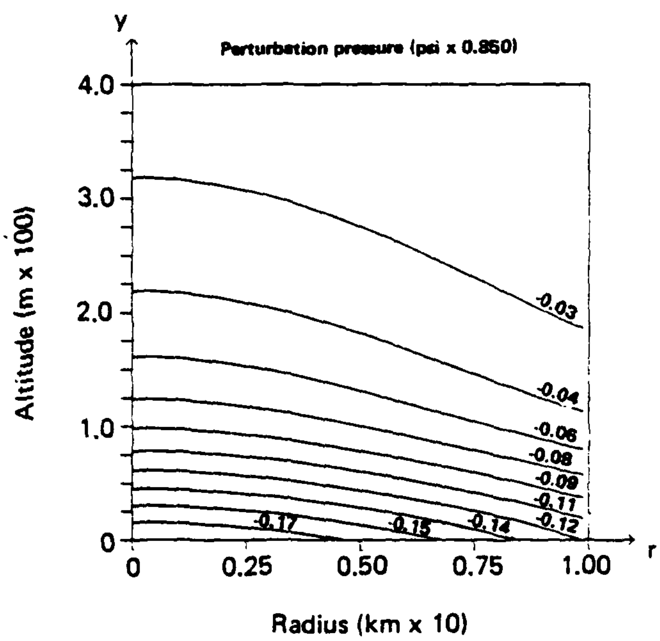

Note: Perturbation pressure is δP_0 (P + Ay); see footnote † on p. 6.

Fig. 3--Pressure contours for baseline fire

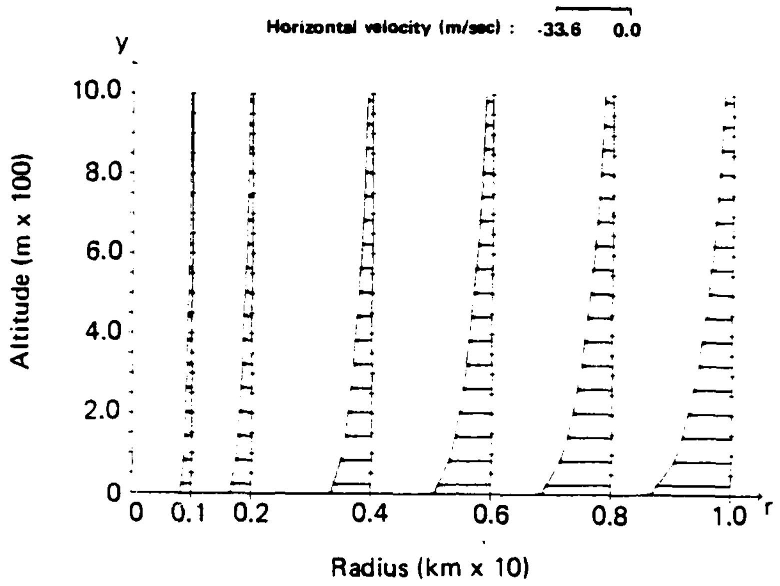

Fig. 4--Radial velocity profiles for baseline fire

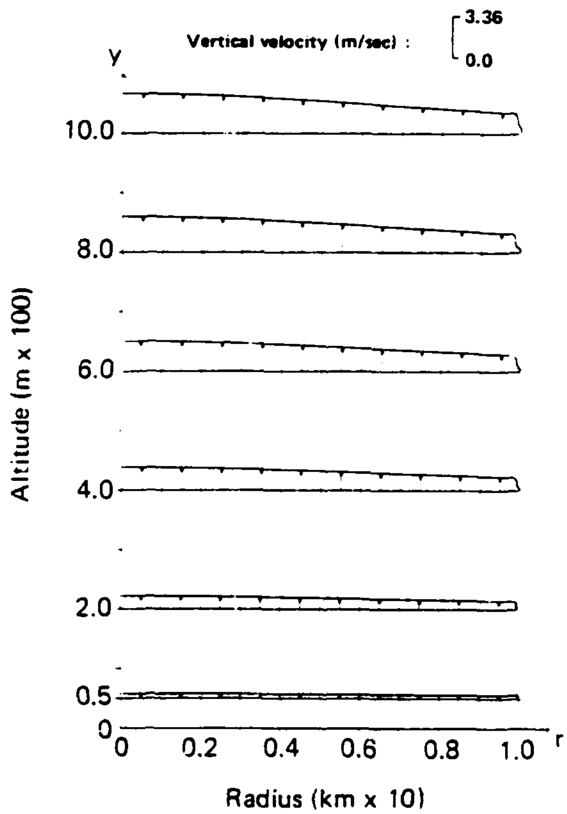

Fig. 5--Vertical velocity profiles for baseline fire

flame heights. As expected, the pressure drop is maximum at ground level. Profiles of the horizontal inflow induced by the pressure drop are presented in Fig. 4, and those of the resulting upflow in Fig. 5. The maximum inflow occurs on the ground at the fire periphery. The upflow profiles are nearly "top-hat."

In most parameter excursions, the hydrothermodynamic predictions are qualitatively the same as those for the baseline case. The results are summarized below.

DEPENDENCE ON FIRE SIZE AND BURNING RATE SCALE

We consider first the dependence of the large-fire environment on R, H, and QH--the parameters that collectively describe the fire. For nuclear-weapon-ignited fires, the effective value of R will depend on the number and yields of bursts, ambient atmospheric conditions, various characteristics of the preblast urban area (e.g., flammability of exposed combustibles, susceptibility of structures to secondary fires), and a variety of lesser factors [Johnson and Larson, 1982]). Parameters QH and H will depend on the type and distribution of combustibles in the postblast environment, as detailed in Sec. III.

Tables 1 through 3 summarize the variations that we consider in fire size and burning rate, and the corresponding changes in model parameters that follow from Eqs. (2) and (3). In most excursions, the variations are of the type in Table 2, where the parameter under study is simply doubled or halved. The additional variations in Tables 1 and 3 are considered in order to refine the excursions that we believe to be of greatest intrinsic interest--i.e., those defining the dependence of fire winds and temperatures on fire radius (weapon coverage) and intensity (concentration of combustibles).

Figures 6 through 11 summarize the results of the fire size and burning rate excursions. The dependence of fire winds and temperatures on fire size and intensity is plotted in Figs. 6 through 8. As expected, the maximum induced velocity u_{max} and the maximum temperature T_{max} both increase with either radius or intensity. The increases are nearly linear for relatively small radii and heating rates,

Table 1

PARAMETER DEPENDENCE ON FIRE RADIUS

R (km)	U (m/sec)	A	σ	M_1, K_1
2.5	16.8	3.4720	0.110	3.200
5.0	33.6	0.8680	0.110	0.800
10.0	67.2	0.2170	0.110	0.200
15.0	100.8	0.0964	0.110	0.089
20.0	134.4	0.0534	0.110	0.050

Table 2

PARAMETER DEPENDENCE ON FIRE HEIGHT

H (m)	U (m/sec)	A	σ	M_1, K_1
50	134.4	0.0272	0.055	0.4
100	67.2	0.2170	0.110	0.2
200	33.6	1.7360	0.220	0.1

Table 3

PARAMETER DEPENDENCE ON BURNING RATE SCALE

QH (kcal/m^2-sec)	U (m/sec)	A	σ	M_1, K_1
14.35	16.8	3.4720	0.4400	0.80
28.70	33.6	0.8680	0.2200	0.40
57.40	67.2	0.2170	0.1100	0.20
86.10	100.8	0.0964	0.0825	0.15
114.80	134.4	0.0534	0.0550	0.10

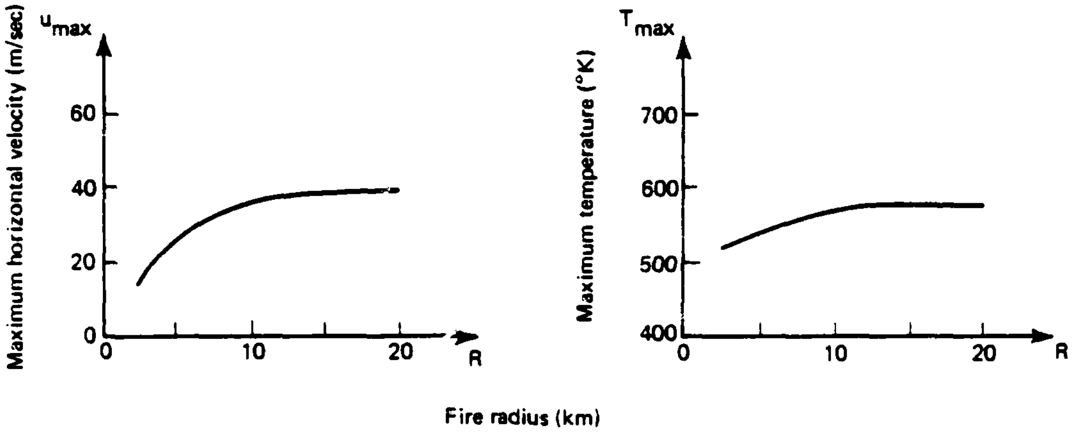

Fig. 6--Dependence of maximum radial velocity and temperature on fire radius

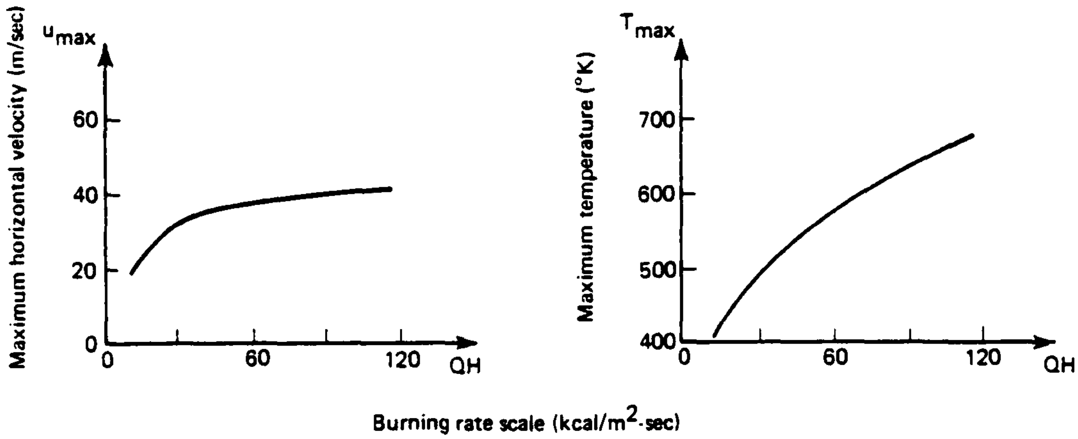

Fig. 7--Dependence of maximum radial velocity and temperature on burning rate scale

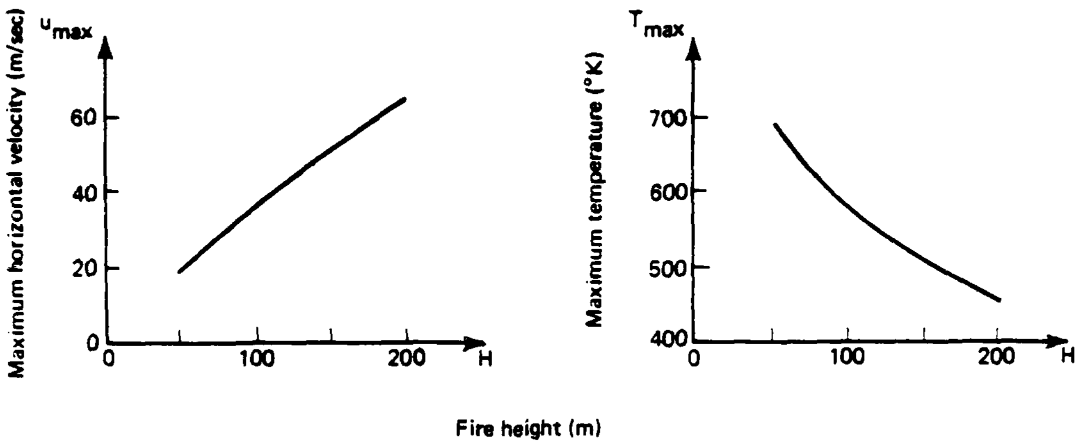

Fig. 8--Dependence of maximum radial velocity and temperature on fire height

but tail off markedly for fires of much greater size and intensity. In fact, u_{max} and T_{max} appear to asymptote toward finite values as R or QH $\rightarrow \infty$. Surprisingly, the apparent asymptotic values of u_{max} as either R or QH $\rightarrow \infty$ are almost identical. T_{max}, however, exhibits a stronger dependence on QH than on R.

Figure 8 describes the variation of u_{max} and T_{max} with fire height. As H increases, u_{max} increases but T_{max} decreases. Such behavior is presumably explained as follows. With QH fixed, Q decreases when H increases. Temperature decreases correspondingly, because of the shorter characteristic residence times of fluid particles in the heating zone. Lower temperatures might be expected to decrease velocities as well. However, a smaller fraction of the constant total heat release QH is radiated away at lower temperatures, so higher kinetic energies can be supported.

The results in Fig. 8 must be interpreted with some care. Whenever H is varied, QH may be varied as well. For example, when buildings have the same construction and contents, both H and QH should

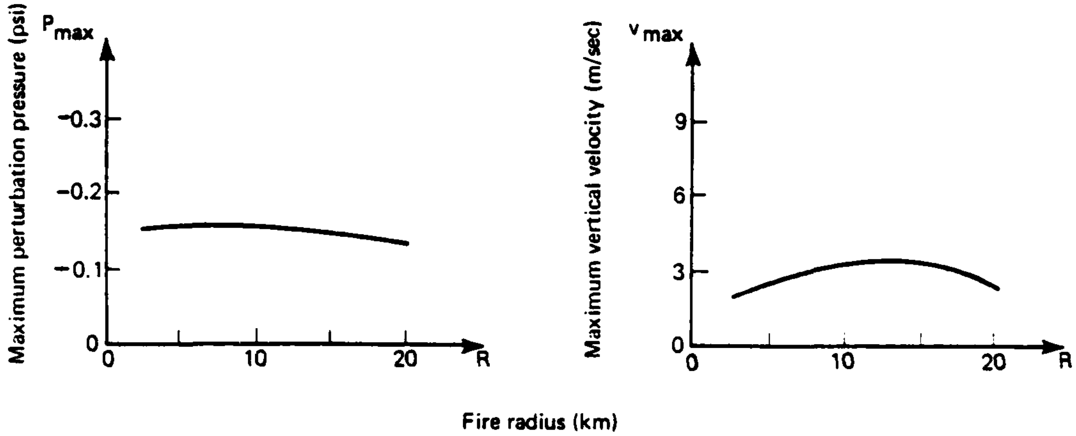

Fig. 9--Dependence of maximum perturbation pressure and vertical velocity on fire radius

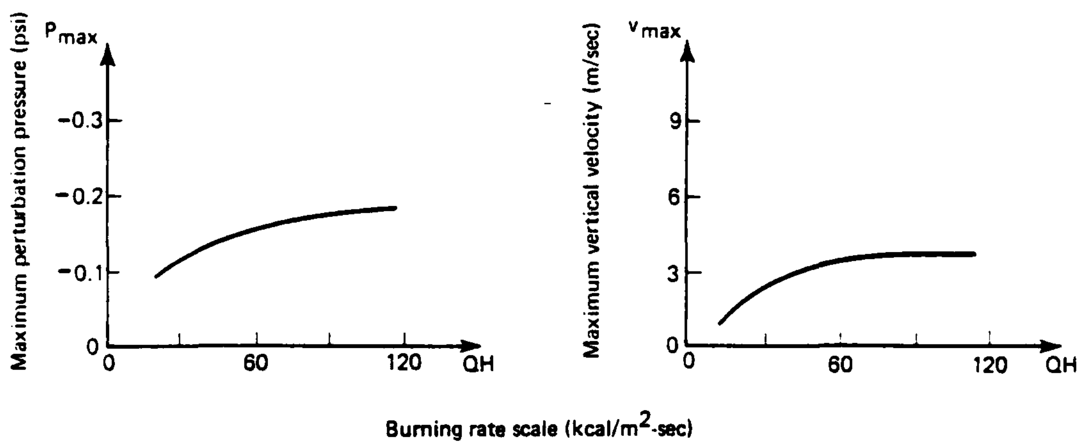

Fig. 10--Dependence of maximum perturbation pressure and vertical velocity on burning rate scale

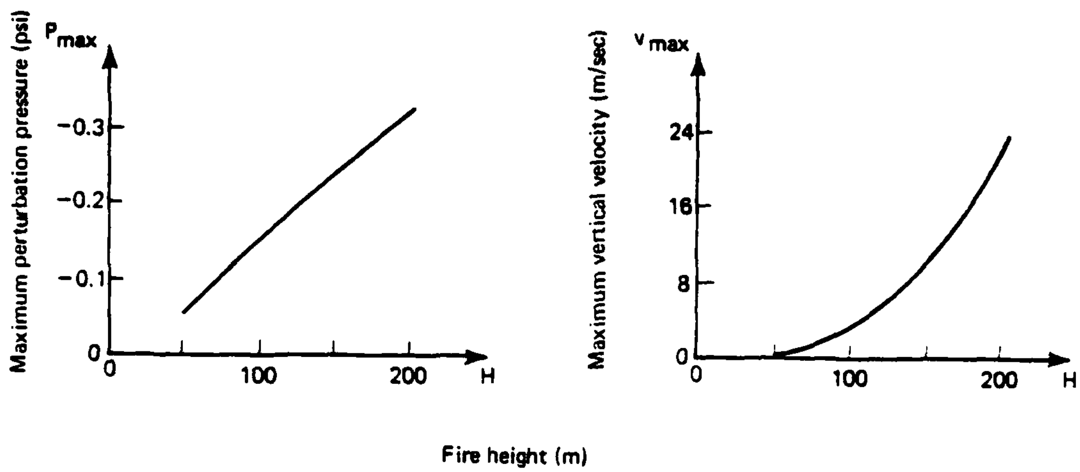

Fig. 11--Dependence of maximum perturbation pressure and vertical velocity on fire height

increase with the number of stories. In such cases, the results in Fig. 7 may be more applicable.

Figures 9 through 11 plot the dependence of maximum pressure drop P_{max} and vertical velocity v_{max} on R, QH, and H. As expected, vertical velocities generally increase with radial velocities. Greater pressure gradients foster greater radial velocities, and are less strongly correlated with temperature variations than Eq. (1c) suggests.

DEPENDENCE ON BURNING RATE SPATIAL DISTRIBUTION

We now briefly explore the effects of different spatial dependences of the heat release rate q(r, y). We consider several sinusoidal and annular variations in radial dependence, but just one in vertical dependence. Further variations are considered in the model city analysis in Sec. III.

Table 4 summarizes the variations in q(r, y) and the resulting hydrothermodynamic changes. As expected, a relatively high-frequency

Table 4

VELOCITY, TEMPERATURE, AND PERTURBATION PRESSURE MAXIMA FOR VARIOUS BURNING RATES

Type of Fire	$\left(\frac{q(r,\ y)}{\{q(r,\ y)\}_{baseline}}\right)$	u_{max} (m/sec)	T_{max} (°K)	P_{max} (psi)	v_{max} (m/sec)
Baseline	1.0	37.2	570	0.156	3.26
Sinusoidal					
Low-frequency	$1.0 - \cos 4\pi r$	38.1	588	0.160	3.50
High-frequency	$1.0 - \cos 20\pi r$	37.2	573	0.157	3.28
Annular	$\begin{Bmatrix} 0.0 \text{ for } 0 \le r < 0.5 \\ 1.0 \text{ for } 0.5 \le r \le 1 \end{Bmatrix}$	33.9	515	0.119	2.46

radial variation on the baseline heat-release distribution has little effect. Surprisingly, however, a fairly low-frequency radial variation also produces trivial changes in velocity, temperature, and perturbation pressure. Those results suggest that the large-fire environment may be more sensitive to the basic scale for heat release than to the specific spatial distribution of the heat release rate (see Fig. 7).

That conclusion is further supported by a comparison of the results in Table 4 for the annular fire with those for the circular baseline fire. The ground area covered by the annular fire--and hence its total heat release--is 25 percent less than that of the baseline fire. The corresponding drop in maximum temperature difference from ambient (i.e., in $T_{max} - T_a$) is just slightly less--20 percent. The drop in u_{max} is significantly less--only 9 percent. Such behavior suggests that the maximum winds and temperatures generated by nuclear-weapon-ignited urban fires may be relatively insensitive to changes in the geometry and loading of the blast-damaged region, provided of course that the blast does not nearly extinguish the fire.

Figures 12 and 13 compare the temperature and flow fields of the baseline and annular fires. Since the fire is located only in the annulus, the highest temperatures occur near the inner edge of the fire annulus (r = 0.5), rather than on the symmetry axis. The resulting

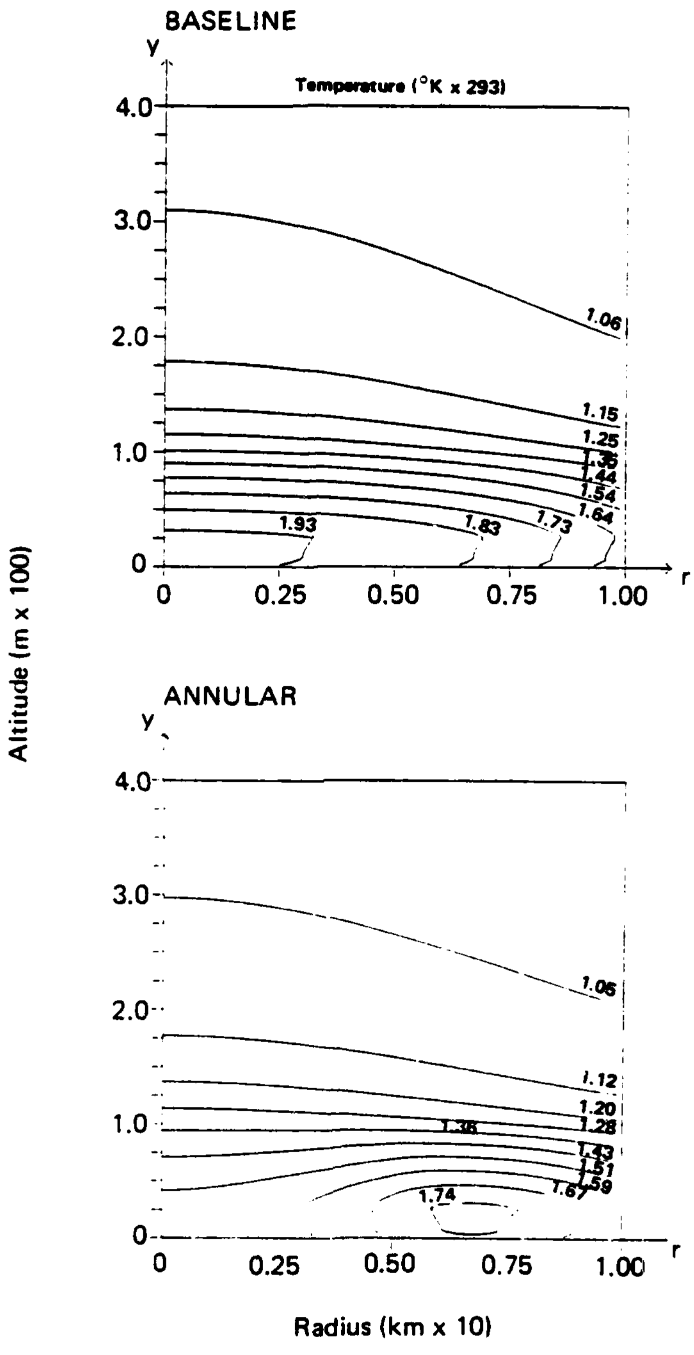

Fig. 12--Temperature contours of baseline and annular fires

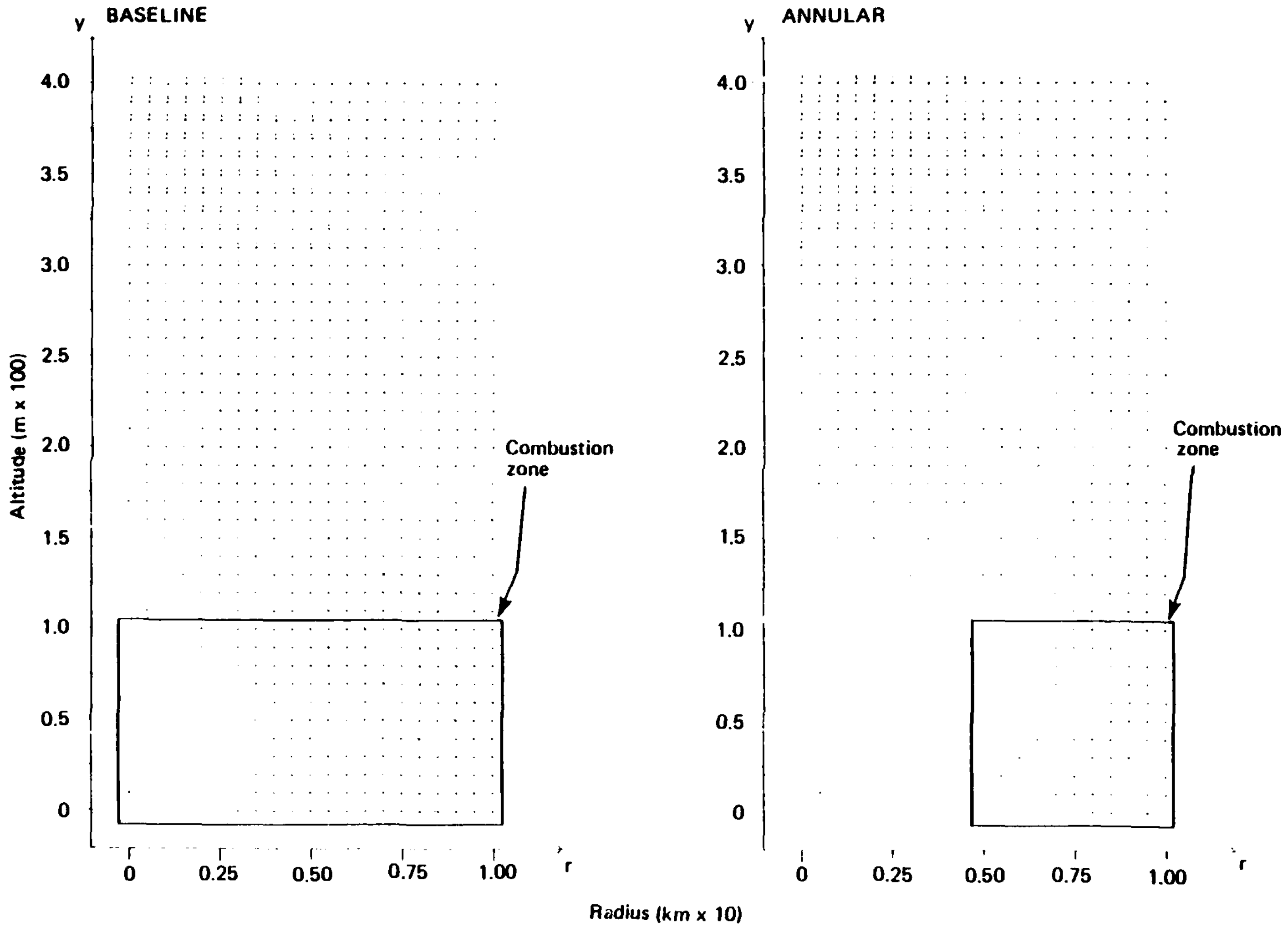

Fig. 13--Flow fields of baseline and annular fires

temperature field is thus qualitatively different from that of the baseline fire. Further, as Fig. 13 shows, winds in the annular fire do not blow toward the fire from both edges of the annulus. Rather, they blow inward (toward the symmetry axis) and upward at all points, as do those in the baseline fire. By means of heat convection and branding, annular fires might therefore be expected to spread inward.

Similarly, a cluster of separated large fires, such as could result from multiple nuclear bursts over a large city, might coalesce and engulf much of the intervening region. The patterns of airflow and fire spread envisioned for such situations are sketched in Figs. 14 and 15. The cluster of fires represented in Fig. 14 nearly forms an annulus, as indicated by the dashed circles. The fire-wind flow

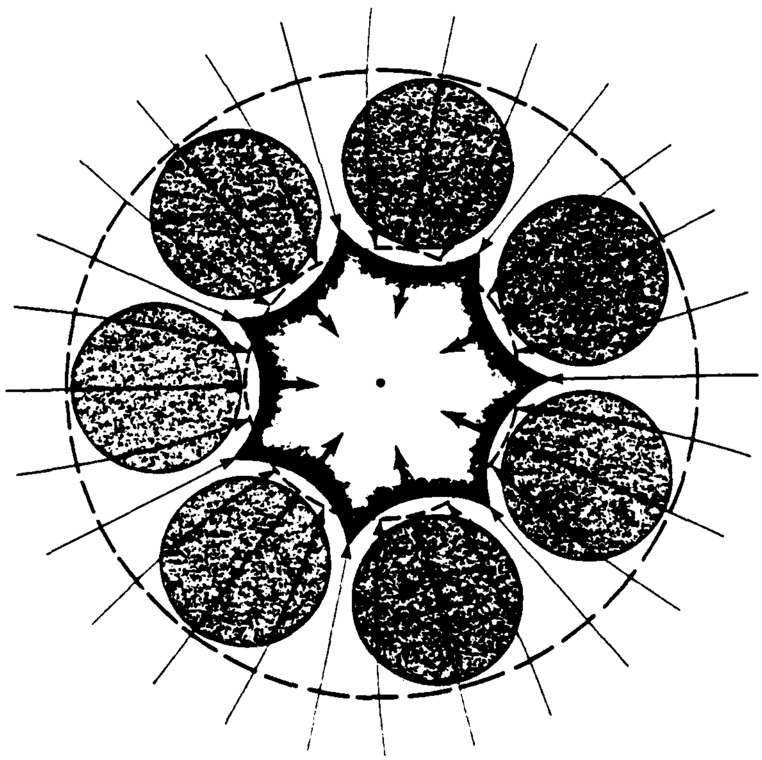

Fig. 14--Radial airflow and fire spread patterns suggested for annular cluster of large area fires

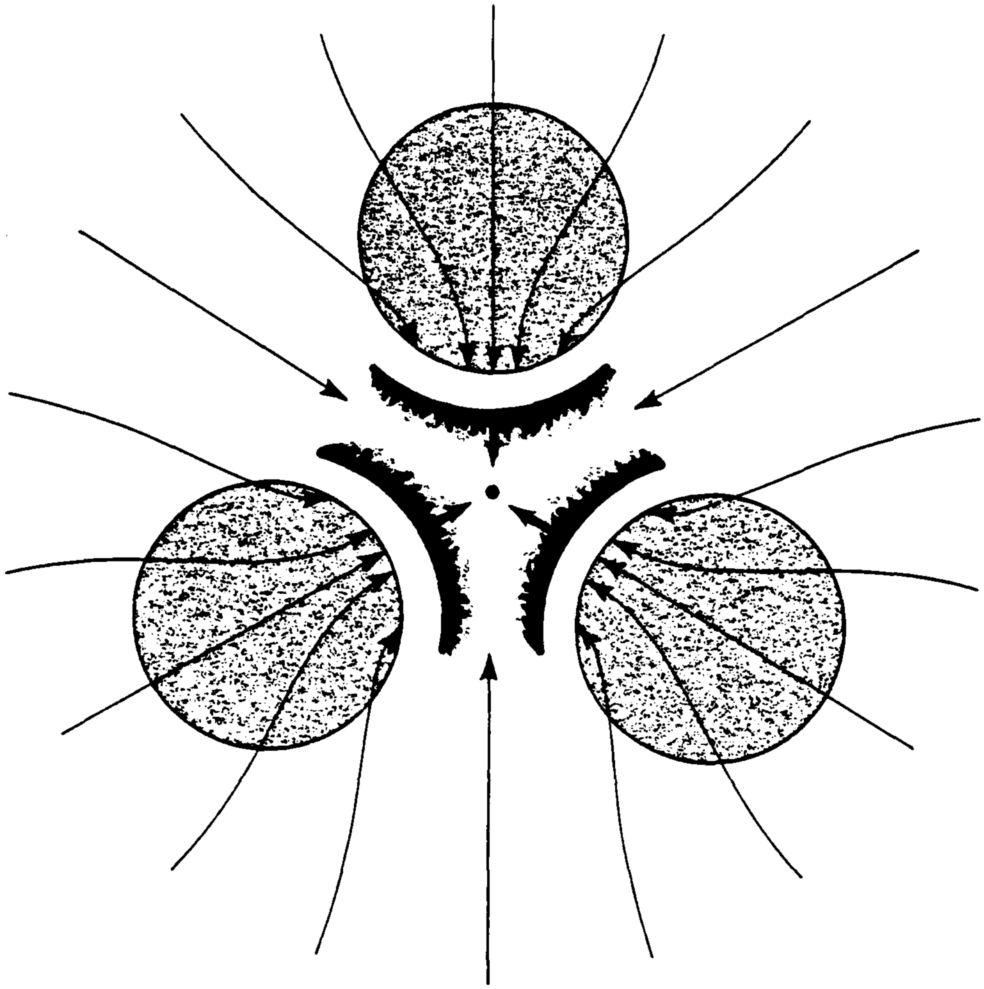

Fig. 15--Radial airflow and fire spread patterns suggested for cluster of three large area fires

should thus be nearly axisymmetric and of the type illustrated in Fig. 13. Correspondingly, the fire should spread inward, and may ultimately cover much of the area inside the inner dashed curve. As shown in Fig. 15, the flow and spread patterns for asymmetric clusters should be less axisymmetric, but still basically inward. Such hypotheses could presumably be verified by extensive, three-dimensional numerical computations.

We now consider a variation of heat release rate with altitude. Specifically, we compare the results for the baseline [q(r, y) defined by Eq. (4)] with those for the more uniform case where q is independent of y--and hence constant. That comparison, summarized in Table 5, reflects the results illustrated in Figs. 8 and 11. For less concentrated heat releases, temperatures are lower, but pressure drops and velocities are greater.

Table 5

VELOCITY, TEMPERATURE, AND PERTURBATION PRESSURE MAXIMA
FOR BASELINE AND UNIFORM FIRES

Type of Fire	q(r, y)	u_{max} (m/sec)	T_{max} (°K)	P_{max} (psi)	v_{max} (m/sec)
Baseline	$\begin{cases} 1.6 & \text{for } 0 \le y \le 0.25 \\ 1.6\left(\frac{4}{3}(1-y)\right) & \text{for } 0.25 \le y \le 1 \\ 0 & \text{for } y \ge 1 \end{cases}$	37.2	570	0.156	3.26
Uniform	1.0	50.9	497	0.231	7.19

DEPENDENCE ON TURBULENCE AND RADIATION

Finally, we consider the variation of the large-fire environment with the eddy coefficients M_1, K_1 and the graybody radiation parameter k^*. The results are summarized in Figs. 16 through 23.

The dependence of fire winds and temperatures on eddy coefficients is demonstrated by Figs. 16, 17, and 18. As expected, the maximum radial velocity decreases with an increase in the eddy coefficient for momentum transfer (Fig. 16). Correspondingly, the maximum temperature increases. An increase in the eddy coefficient for heat transfer might also decrease temperatures, and hence increase velocities. In Fig. 17, such variations are shown to occur, but so weakly that both T_{max} and u_{max} must be considered almost independent of K_1. When M_1 and K_1 are varied together, as in Fig. 18, the results are thus similar to those with only M_1 varied (cf. Fig. 16).

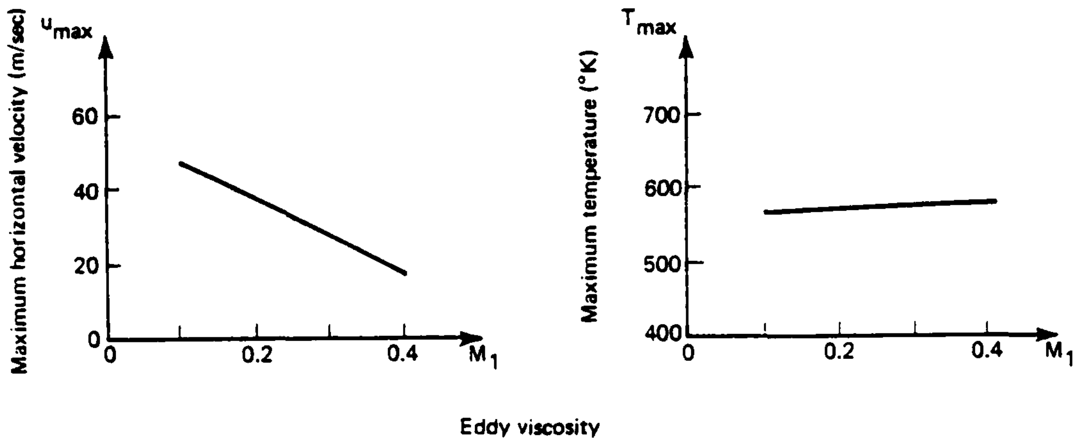

Fig. 16--Dependence of maximum radial velocity and temperature on eddy coefficient for momentum transfer

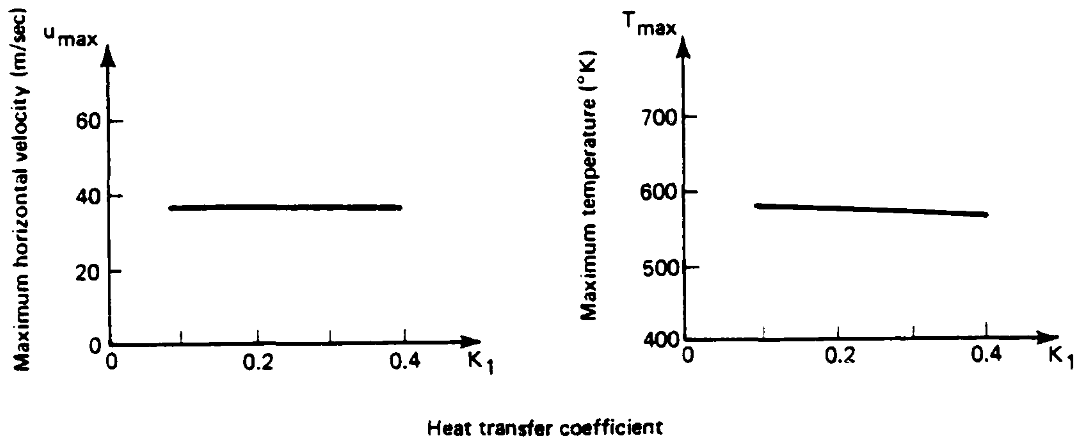

Fig. 17--Dependence of maximum radial velocity and temperature on eddy coefficient for heat transfer

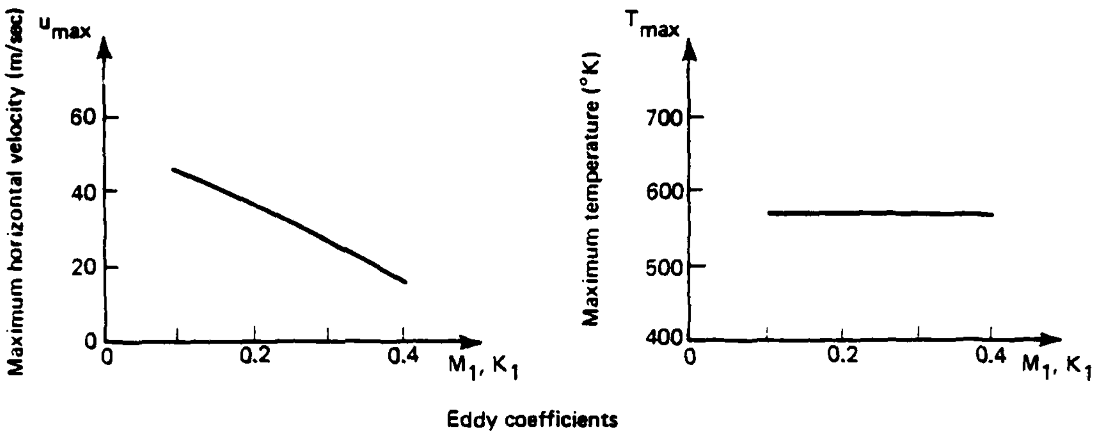

Fig. 18--Dependence of maximum radial velocity and temperature on eddy coefficients

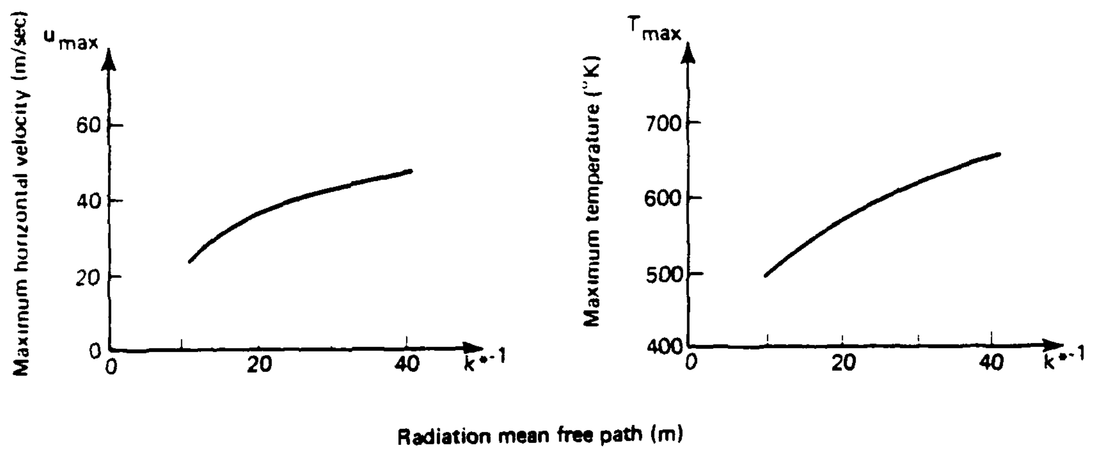

Fig. 19--Dependence of maximum radial velocity and temperature on radiation mean free path

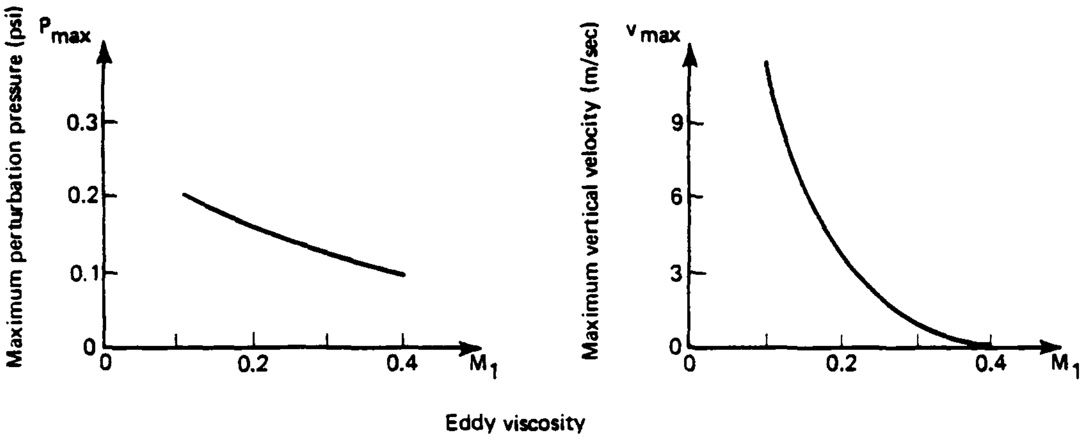

Fig. 20--Dependence of maximum perturbation pressure and vertical velocity on eddy coefficient for momentum transfer

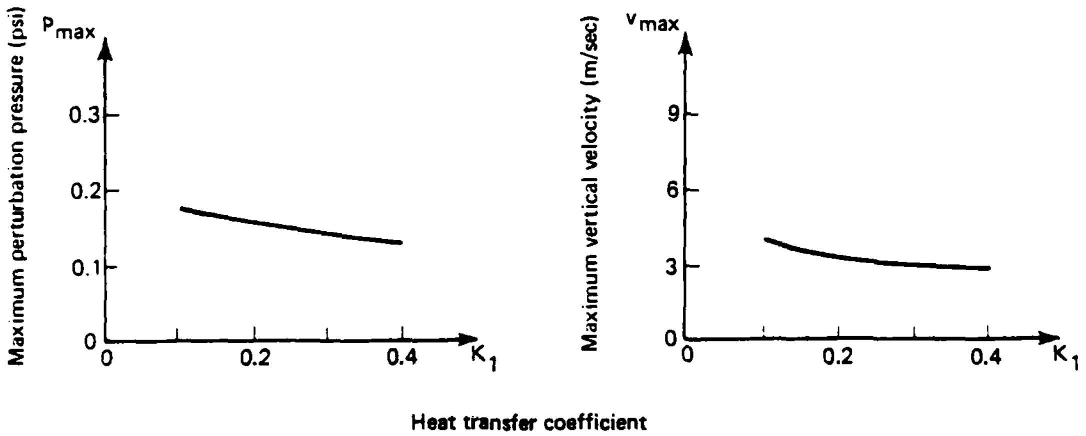

Fig. 21--Dependence of maximum perturbation pressure and vertical velocity on eddy coefficient for heat transfer

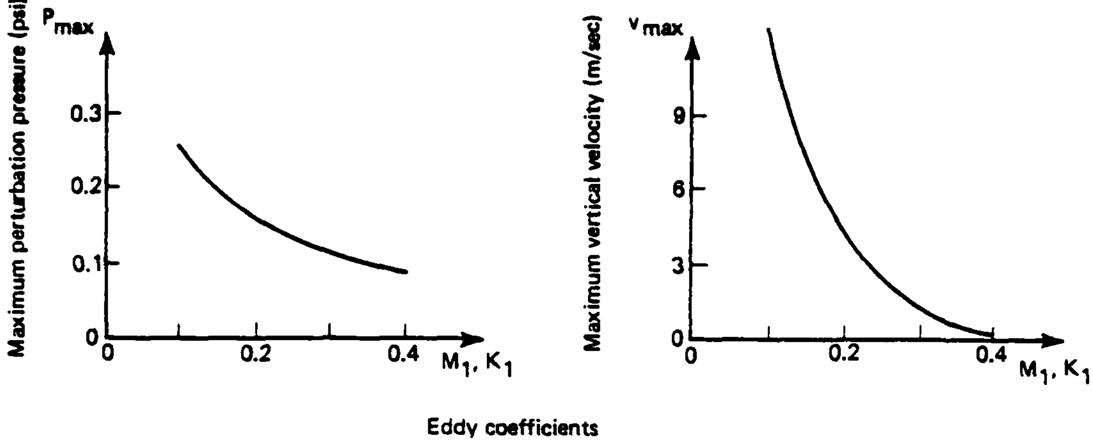

Fig. 22--Dependence of maximum perturbation pressure and vertical velocity on eddy coefficients

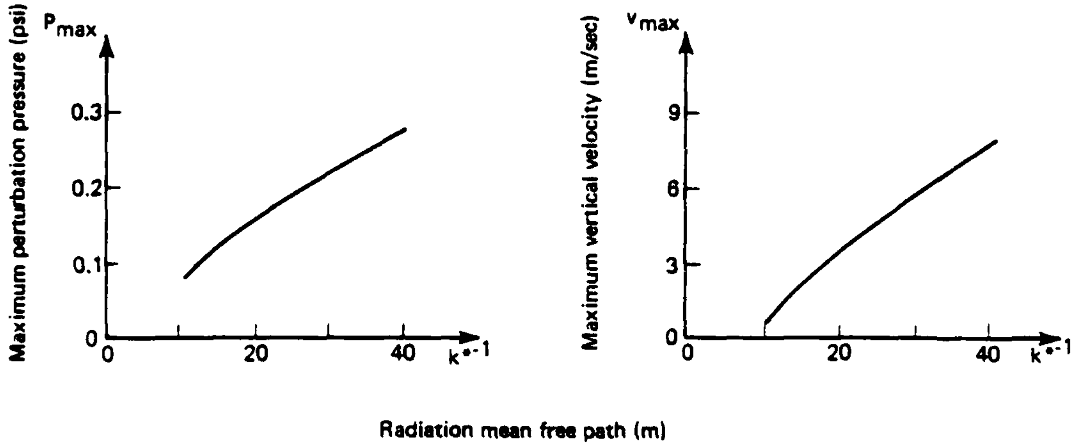

Fig. 23--Dependence of maximum perturbation pressure and vertical velocity on radiation mean free path

Figure 19 indicates the dependence of fire winds and temperatures on the radiation parameter k^*. Both winds and temperatures increase with k^{*-1}--as expected, since the effective scale for radiative energy loss σ is proportional to k^* [see Eqs. (1) and (2)].

The dependence of pressure drops and vertical velocities on M_1, K_1, and k^* is shown by Figs. 20 through 23. As in previous comparisons (Figs. 6 through 11 and 16 through 19), variations in those parameters are strongly correlated with variations in radial velocity.

III. MODEL CITY ANALYSIS

Using the turning-region analysis of Part I, we obtain predictions of the large-fire environment for three model U.S. cities. City W is lightly built-up, and intended to represent new, sprawling cities. City E is heavily built-up, and intended to represent old, congested cities. City M is of intermediate building density. For each city, two cases are considered: a baseline fire and one modified by blast. In all cases, however, the fire radius is taken to be 12 km--believed to be about the size of the fire that would result from a 1 Mt near-surface nuclear burst [Johnson and Larson, 1982].

DEFINITION

Few metropolitan areas are axisymmetric. Nevertheless, most cities have a main business district with high-rise office and apartment buildings, surrounded by lower density tracts. Our model cities reflect that situation. Each has three regions: a tall central city; a residential/industrial belt of intermediate height around the central city; and a low, primarily residential outer belt. We refer to those regions as the central city, inner belt, and outer belt, respectively.

Table 6 summarizes the geometry of the model cities, including both the horizontal extent of each city region, the corresponding vertical extent N_s (average number of stories), and the building density f_{Bu}. We assume that the top and bottom stories are each 4 m high and all other stories are 3 m high.† The values for building density f_{Bu} in each model city region are comparable to those in the DCPA manual, and thus considered representative of U.S. cities [DCPA, 1973]. The values are all less than 0.45, which approximates the densely packed Hamburg districts devastated in the firestorm of 1943 (see Part I).

---

†The average heights of the outer-belt buildings in cities W and E are taken to be 6 and 10 m, respectively.

Table 6

SIZE AND DENSITY OF MODEL CITY REGIONS

Region	City W	City M	City E
Radial Dimension (km)			
Central city	0-1	0-1	0-2
Inner belt	1-3	1-4	2-6
Outer belt[a]	3-12	4-12	6-12
Average Number of Stories, N_s			
Central city	8	12	16
Inner belt	3	4	6
Outer belt	1.5	2	2.5
Building Density, f_{Bu}[b]			
Central city	0.30	0.35	0.40
Inner belt	0.25	0.30	0.35
Outer belt	0.15	0.20	0.25

[a]Radius of outer belt may extend beyond 12 km, but the fire does not.

[b]Calculated as the ratio of land area covered by buildings to total land area.

The corresponding geometry of the baseline model-city fire simulations is summarized in Figs. 24 through 26. In each figure, the shaded area represents the fuel zone (defined by Table 6) and the hatched area represents the remainder of the combustion zone. The total height of the combustion zone in the outer belt is assumed to be five times the fuel zone height.[†] Since turbulence will break the flame envelope and tend to keep flame heights uniform [Thomas, 1963], the ratio of combustion zone height to fuel zone height in the central city is taken as only half as much; the combustion zone height in the inner belt is assumed to be the average of the other two.

[†]As noted in Part I, a combustion-zone-height to fuel-zone-height ratio of about five was observed for the largest Flambeau fires and the 1943 Hamburg firestorm.

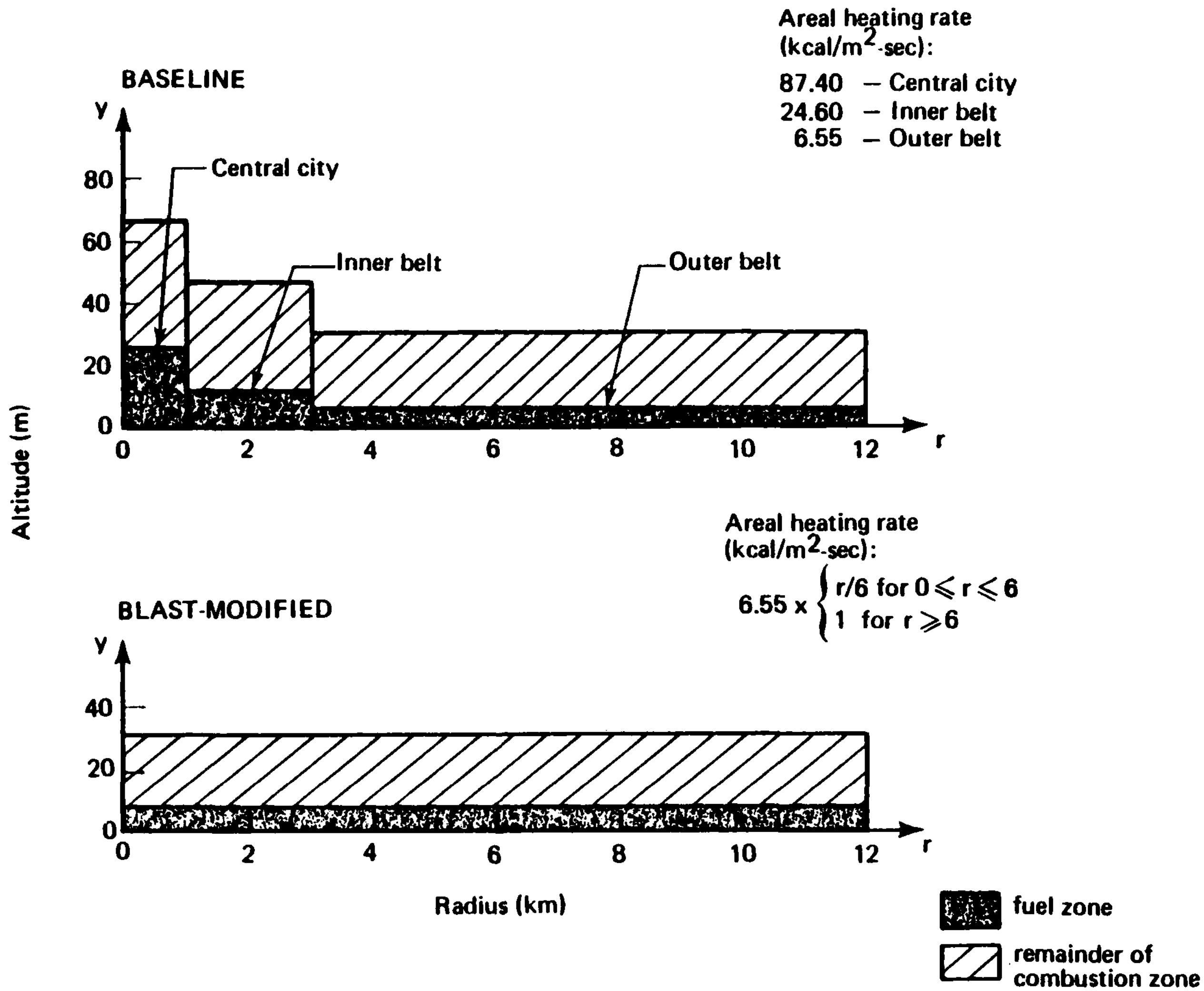

Fig. 24--Fire schematic for baseline and blast-modified city W

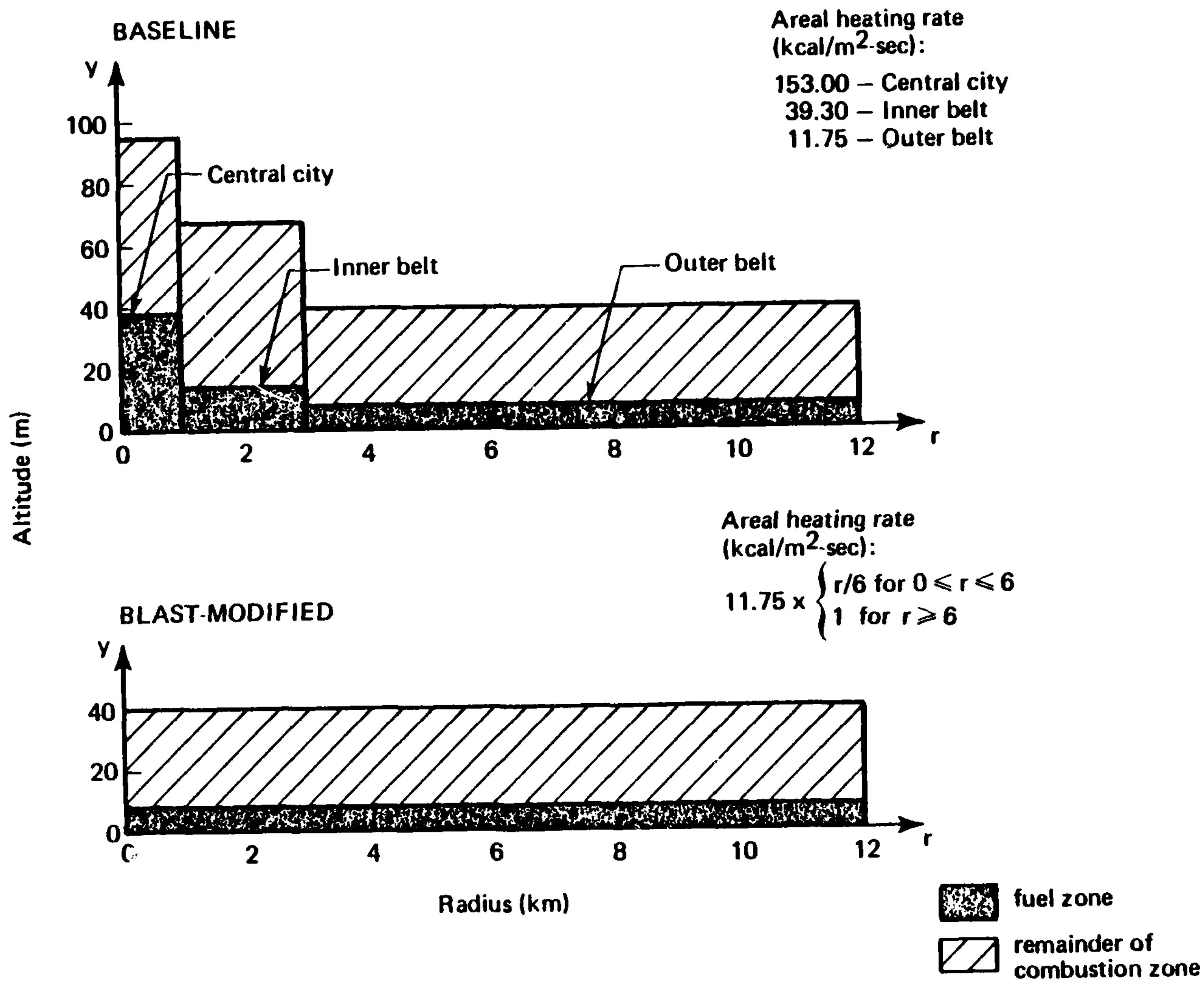

Fig. 25--Fire schematic for baseline and blast-modified city M

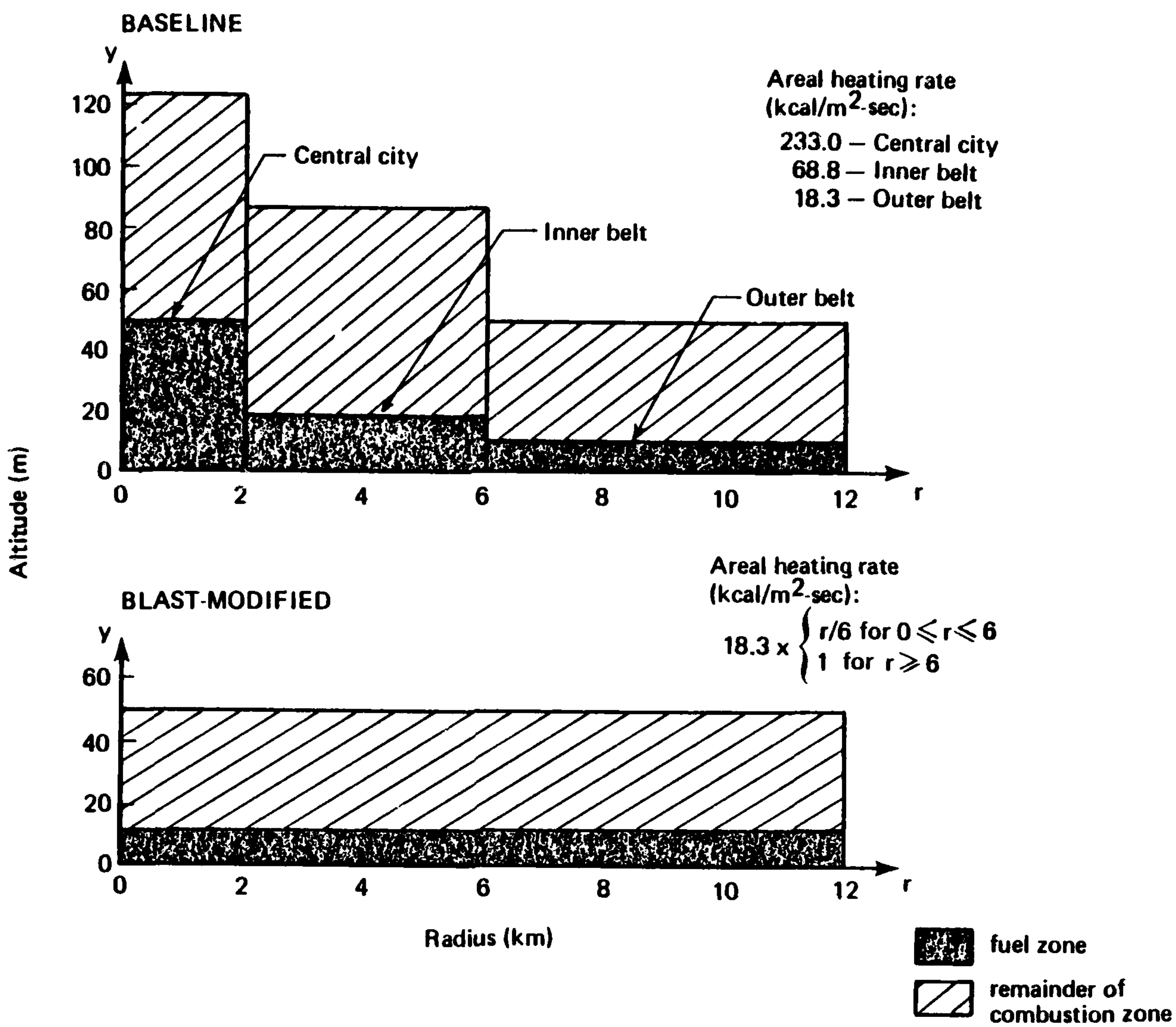

Fig. 26--Fire schematic for baseline and blast-modified city E

The baseline areal heating rates (see Figs. 24 through 26) for the central city, inner belt, and outer belt are estimated as follows. The average fuel loading per story L_s in each city region is defined in Table 7. The corresponding average total areal fuel loading L_T is then computed from

$$L_T = L_s \times N_s \times f_{Bu} , \tag{7}$$

with values for N_s and f_{Bu} taken from Table 6. The resulting total-loading estimates are also listed in Table 7. The central cities and outer belts are somewhat taller and shorter, respectively, than were those in the devastated Hamburg districts, and have higher and lower total loadings. The inner belts are defined to be on the order of the

Table 7

FUEL LOADING IN MODEL CITY REGIONS

Region	City W	City M	City E
Average Fuel Loading per Story, L_s[a] *(lb/ft^2-story)*			
Central city	20	20	20
Inner belt	18	18	18
Outer belt	16	16	16
Total Areal Fuel Loading, L_T *(lb/ft^2)*			
Central city	48.0	84.0	128.0
Inner belt	13.5	21.6	37.8
Outer belt	3.6	6.4	10.0

[a]Based on DCPA [1973] estimates, which take into account both the structures and their contents.

Hamburg districts, but less built-up. Similarly, the inner-belt loadings tend to be somewhat less than the 32 lb/ft^2 estimated for Hamburg [DCPA, 1973].

Finally, in each model city region, the fire is assumed to consume 90 percent of the available fuel in 3 hr. The areal heating rate Q_A is thus computed from

$$Q_A = L_T \times \left(\frac{90\%}{3\ \text{hr}}\right) \times E_B \ , \tag{8}$$

with L_T taken from Table 7 and E_B, the average heat released per unit weight of combustibles, taken as [DCPA, 1973]

$$E_B = 8000\ \text{Btu/lb} \ . \tag{9}$$

For the blast-modified fire simulations represented in Figs. 24 through 26, the weapon burst is assumed to occur over the city center, leveling many buildings in the central city and inner belt. A centered, low-level burst of a 1 Mt weapon ould produce such an effect, with blast damage extending out to radii on the order of 6 km (and fire to around 12 km) [Johnson and Larson, 1982]. The height of the fuel zone is thus simply assumed constant and equal to its outer-belt value in the baseline case. The total height of the combustion zone is chosen similarly.

The blast-modified areal heating rates are not considered independent of radius, however. In each case, the combustibles of the central city and inner belt would be spread radially to some degree by the blast, and piled up in a debris field. Since some combustibles in that zone may be buried under layers of nonflammable materials (e.g., concrete, brick, metal), the areal heating rate is not expected to be correspondingly higher, and may in fact be relatively small. We consider such a situation in each simulation. It is assumed that the areal heating rate is zero at the fire center, increases linearly with radius over the debris zone, and equals its baseline outer-belt value for radii greater than 6 km.

In each model city simulation, the required data set consists of the geometric parameters R and H, the heating rate parameters QH and q(r, y), the radiation coefficient σ, and the turbulence coefficients M_1 and K_1. Once R, H, and QH are chosen, the parameter A in Eqs. (1) is determined along with the radial velocity scale U from Eqs. (2).

In all cases, the fire radius R is taken to be 12 km. However, since the combustion zone height is not constant in the baseline cases, there are no natural choices for H. The values for H listed in Table 8

Table 8

PARAMETERS IN MODEL CITY SIMULATIONS

Parameter	City W	City M	City E
Fundamental Parameters			
R (km)	12	12	12
H (m)	40	60	100
QH (kcal/m^2-sec)	9.50	14.25	23.75
Auxiliary Parameters			
U (m/sec)	33.6	33.6	33.6
A	0.347	0.521	0.868
σ	0.264	0.264	0.264
M_1, K_1	0.125	0.125	0.125

are arbitrarily selected as characteristic of the baseline geometry in Figs. 24 through 26. The values of the heating rate scale QH in Table 8 are chosen likewise.

Table 8 also lists the corresponding values of U and A, calculated using Eqs. (2).† From Eqs. (2) and (3), σ depends on H, QH, and the radiation mean free path k^{*-1}; and M_1 depends on R, U, and the dimensional eddy viscosity $\mathcal{E}_1/\rho_a$. As in our earlier simulation

†The value of the dimensionless perturbation pressure scale δ is 1.44×10^{-2} for all cases.

(Part I), we take $k^{*^{-1}} = 20$ m, $\mathcal{E}_1/\rho_a = 5.04 \times 10^4\ m^2$/sec, and $M_1 = K_1$. The values we use for σ, M_1, and K_1 [from Eqs. (2) and (3)] are also listed in Table 8.

Finally, we use the heating rate distributions q(r, y) defined in Figs. 27 through 29. The heating rate is taken to be constant in the fuel zone of each baseline city region, and to decrease linearly with altitude over the remainder of the combustion zone, approaching zero at the top of that zone. Subject to the choices of QH in Table 8, the fuel zone values of q(r, y) are selected so that the resulting areal heating rates

$$\int_0^\infty QH\ q(r, y)\ dy$$

are equivalent to those in Figs. 24 through 26. The blast-modified forms of q(r, y) are developed likewise.

SIMULATION RESULTS

The results of the model city simulations are summarized by Table 9, which compares predicted baseline and blast-modified velocity, temperature, and pressure maxima. As expected, the predictions for the baseline simulations are all larger than those for the blast-modified simulations. The differences are great for the temperature, pressure, and vertical velocity maxima, but small for the radial velocity maxima (10 percent or less). Therefore, the winds and wind damage resulting from nuclear-weapon-ignited fires may be relatively insensitive to the degree of blast disruption of the fuel bed.

In any case, the predictions in Table 9 indicate that the winds generated by a large urban fire will in themselves constitute a major threat. Although most of the velocities in the table are less than hurricane force (more than 30 m/sec), it should be noted that those values represent *means*. Near street level, where fire winds will be channeled between buildings, wind speeds of hurricane force should

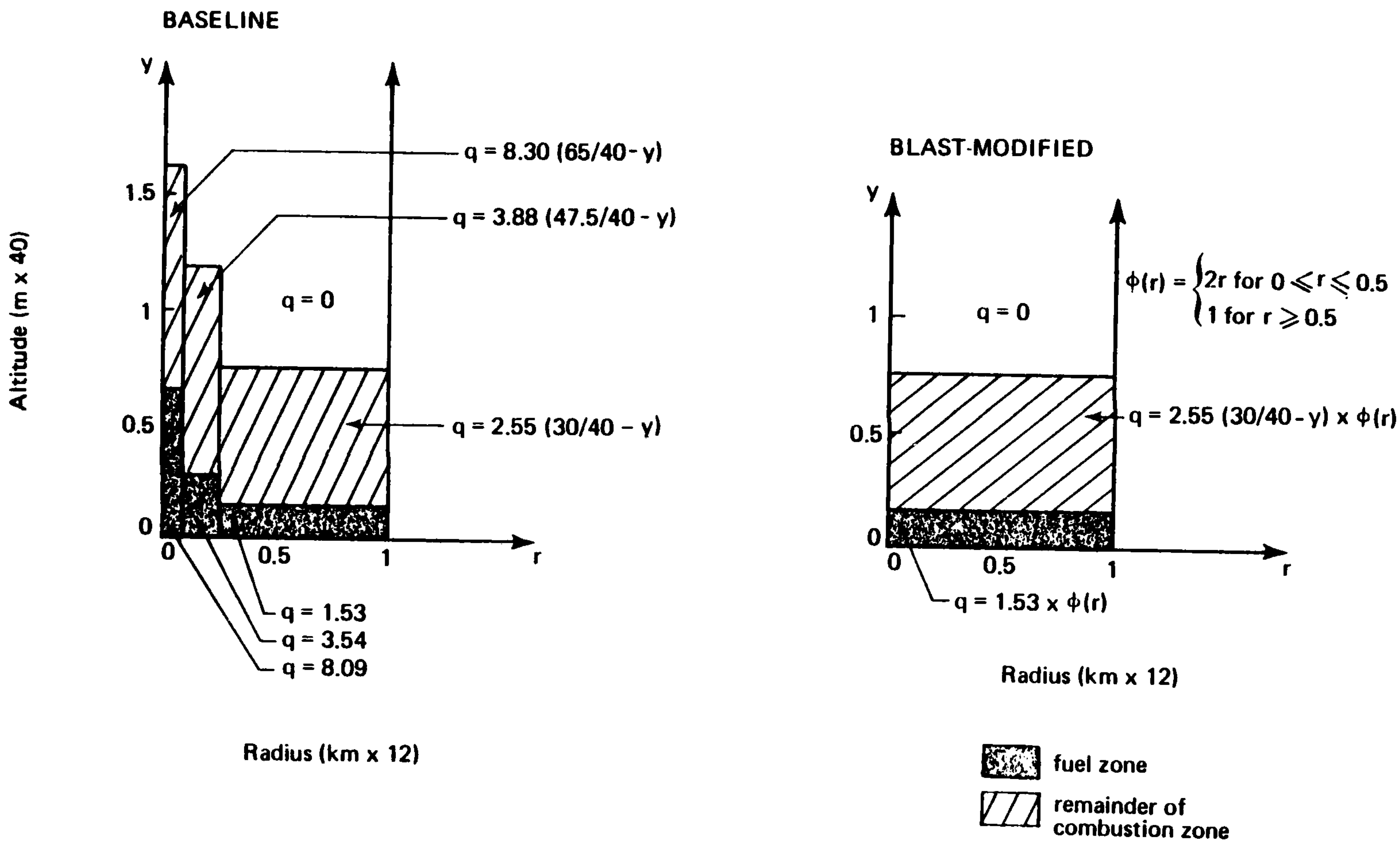

Fig. 27--Baseline and blast-modified heating rate spatial distributions for city W

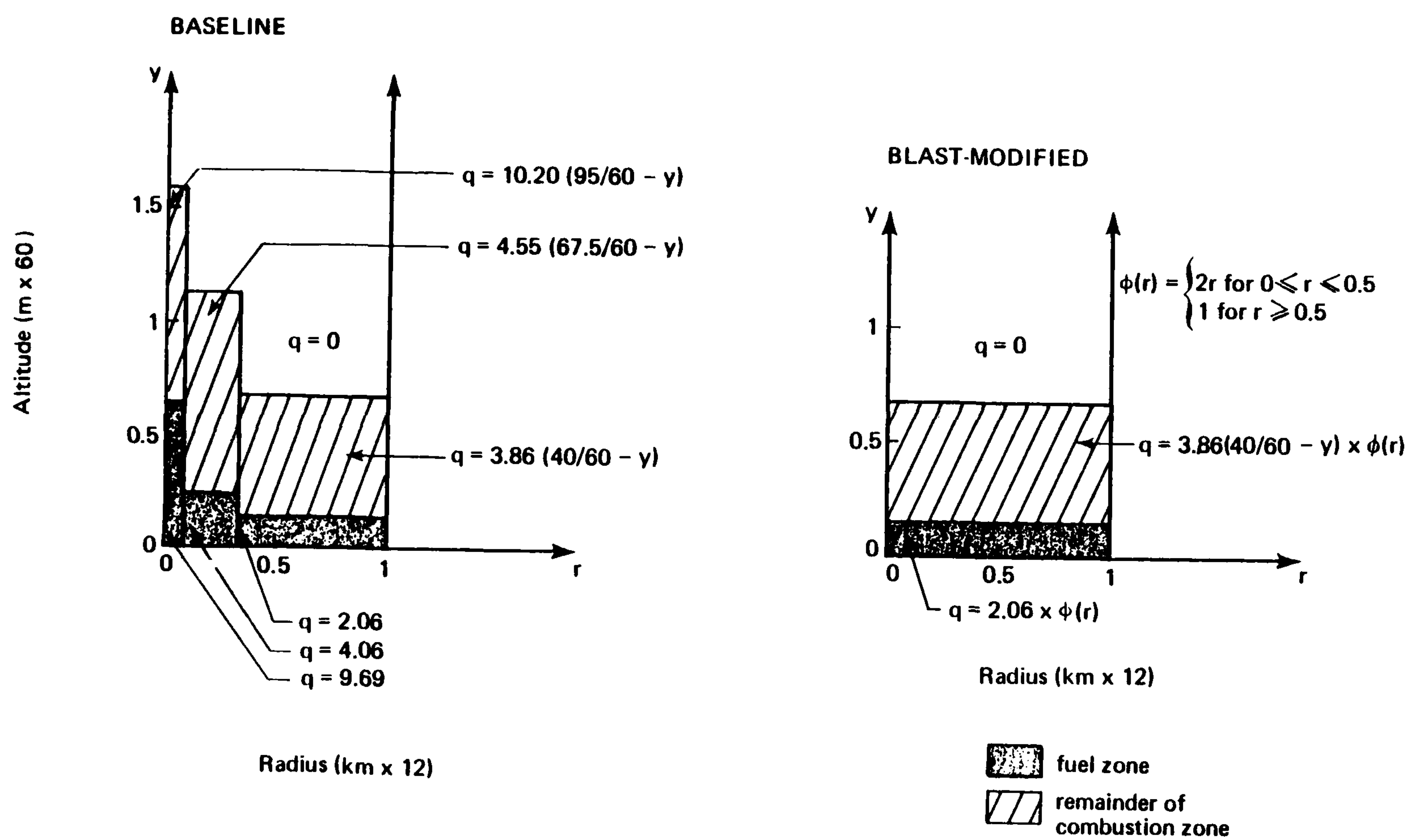

Fig. 28--Baseline and blast-modified heating rate spatial distributions for city M

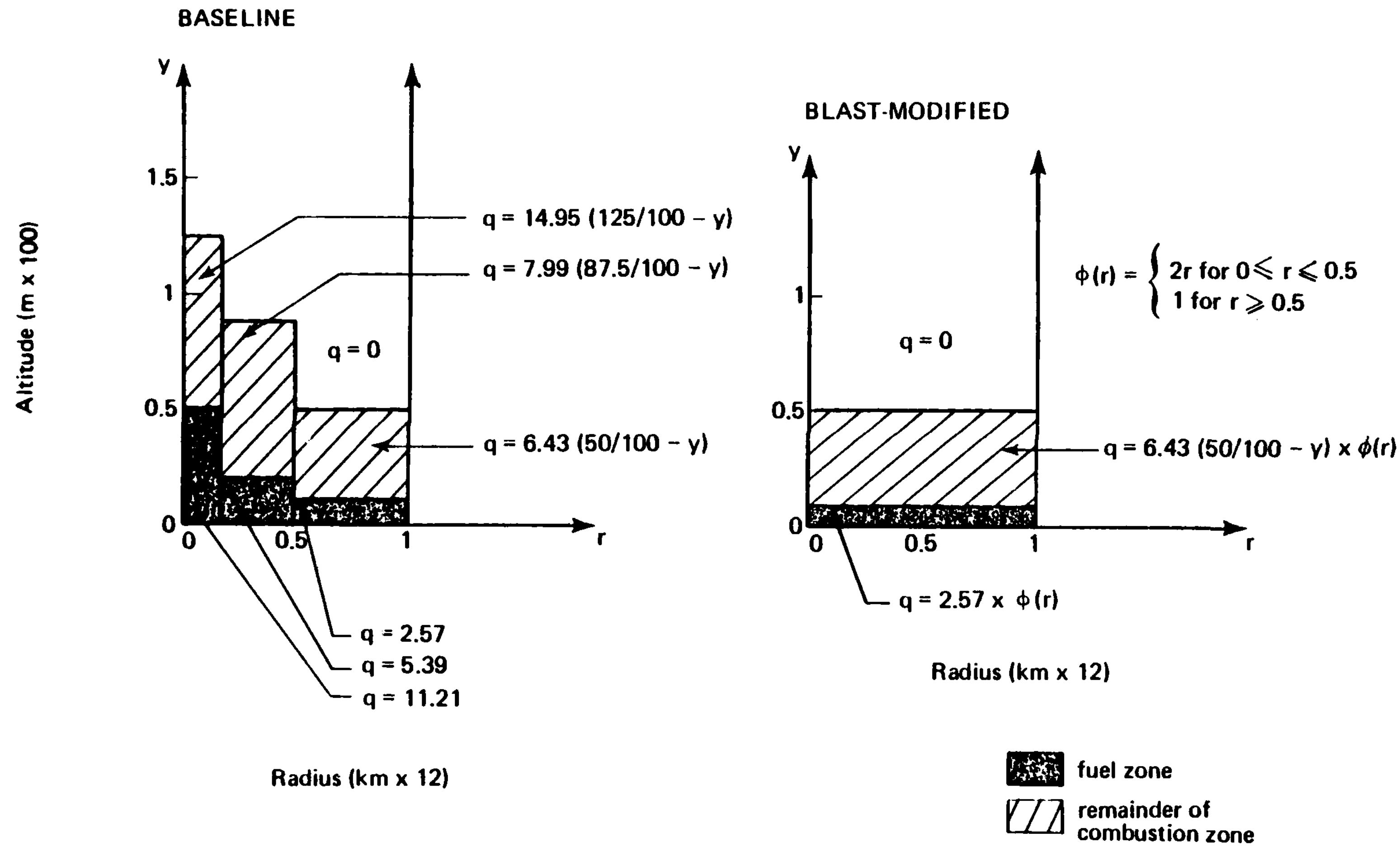

Fig. 29--Baseline and blast-modified heating rate spatial distributions for city E

Table 9

VELOCITY, TEMPERATURE, AND PERTURBATION PRESSURE MAXIMA IN MODEL CITY SIMULATIONS

	City		
Simulation	W	M	E
Maximum Radial Velocity, u_{max} (m/sec)			
Baseline	20.2	26.3	39.0
Blast-Modified	17.9	23.9	28.5
Maximum Temperature, T_{max} (°K)			
Baseline	577	619	704
Blast-Modified	455	485	510
Maximum Perturbation Pressure, P_{max} (psi)			
Baseline	0.056	0.113	0.271
Blast-Modified	0.011	0.044	0.076
Maximum Vertical Velocity, v_{max} (m/sec)			
Baseline	0.89	3.12	12.48
Blast-Modified	0.37	1.56	4.32

be considered typical. The winds may be even greater than those encountered in the Hamburg firestorm of 1943 (see Part I).

Also as expected, the velocity, temperature, and pressure predictions in Table 9 are all greatest for city E (the tallest and densest) and least for city W (the shortest and sparsest). For a given fire, therefore, the threat will be most severe for the most congested cities. In general, however, the shorter cities sprawl out over greater areas than do taller ones of comparable population, and are thus capable of supporting more widespread fires. Multiple weapon bursts can greatly increase the fire severity in such cities.

In the remainder of this subsection, we describe the results of the model city simulations in more detail. The vector plot in Fig. 30 is representative of the flow fields obtained in the simulations. The flow in each case is everywhere inward (toward the symmetry axis) and upward, with the horizontal velocity typically maximum on the symmetry axis in the upper portion of the turning region. Figures 31 through 34 present, respectively, the temperature and pressure contours and radial and vertical velocity profiles for baseline and blast-modified simulations for city W. Similar sets of plots for cities M and E are presented in Figs. 35 through 38, and 39 through 42, respectively.

As expected (cf. Fig. 12), the baseline and blast-modified temperature contours in Fig. 31 are quite different. In the baseline case, the heat release is greatest at the center of the fire (see Fig. 27) and the temperature is maximum on the symmetry axis. At any fixed altitude, the variation of temperature with radius is roughly Gaussian. However, in the blast-modified case, the temperature maximum does not occur on the symmetry axis. Rather, since the heat release is greatly diminished and actually least in the fire center (Fig. 27), the temperature is maximum about halfway between the center and the periphery. Additionally, the temperature is uniformly reduced in the blast-modified case.

Figures 32 through 34 show little qualitative difference between the baseline and blast-modified pressures and velocities. The contour plots in Fig. 32 exhibit the same behavior, the pressure drop decreasing with an increase in either radius or altitude. Likewise, the profile plots in both Figs. 33 and 34 are qualitatively the same. The radial velocity is maximum at ground level on the periphery and the vertical velocity is maximum on the symmetry axis in the upper part of the turning region. At any specified altitude, the variation of vertical velocity with radius is again roughly Gaussian. Of course, as expected, certain quantitative differences are evident: pressure drops and velocities are all less in the blast-modified case than in the baseline case. However, the radial velocity differences are relatively small.

The comparisons in both Figs. 35 through 38 and Figs. 39 through 42 are similar to those in Figs. 31 through 34. The primary difference

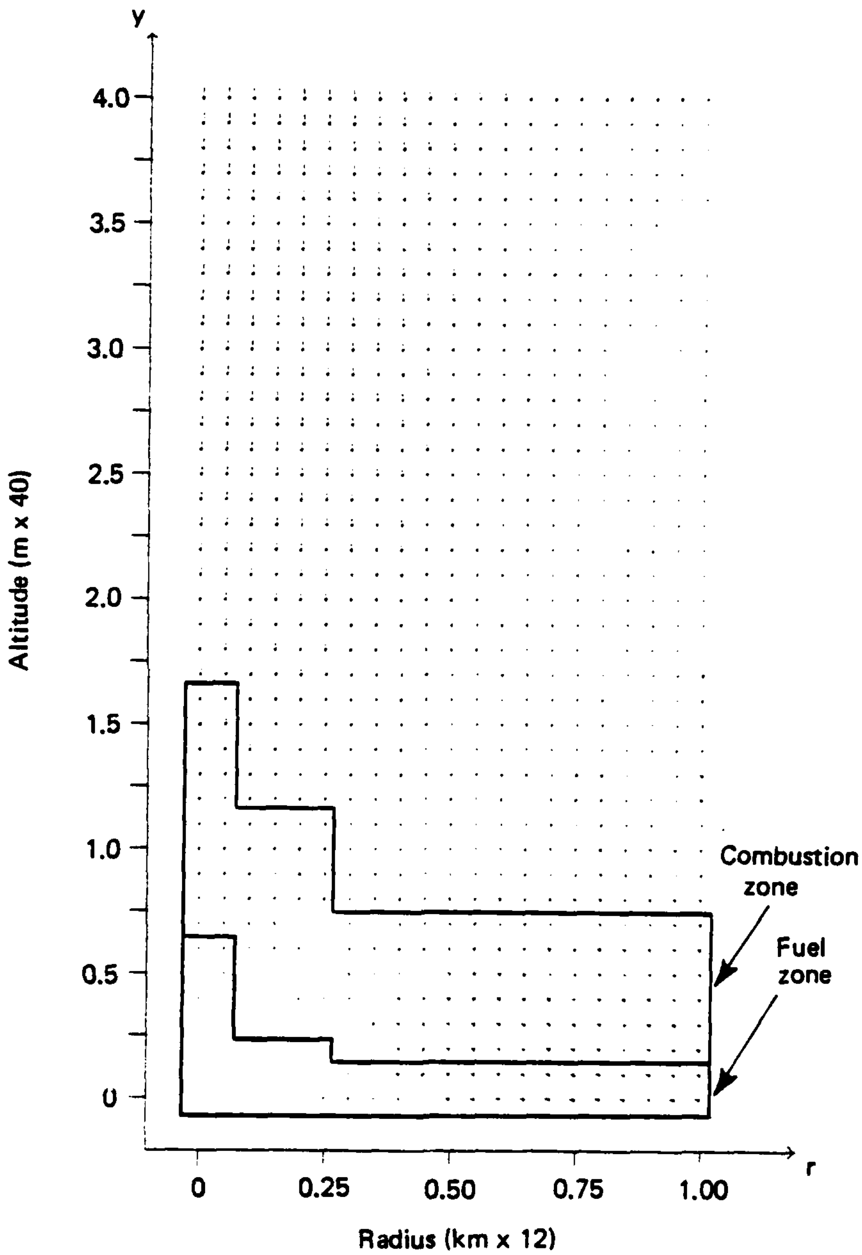

Source: From calculation for baseline city W.

Fig. 30--Typical velocity field in model city simulations

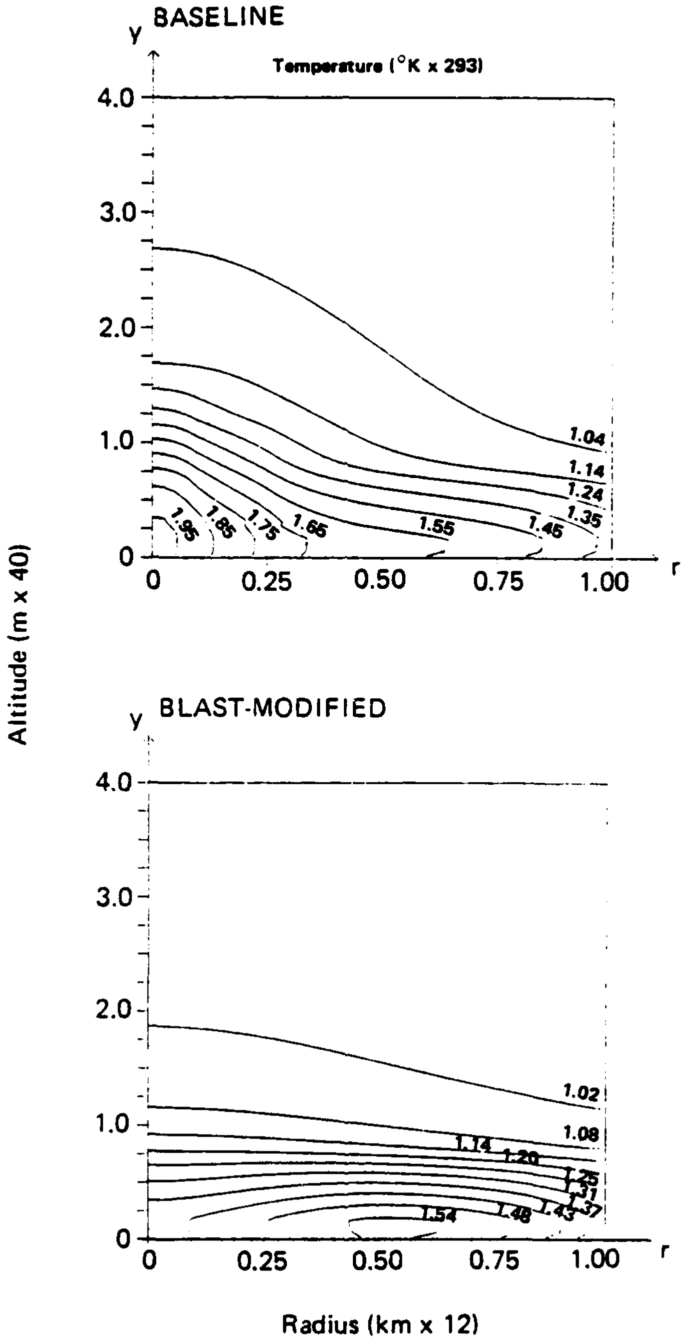

Fig. 31--Baseline and blast-modified temperature contours for city W

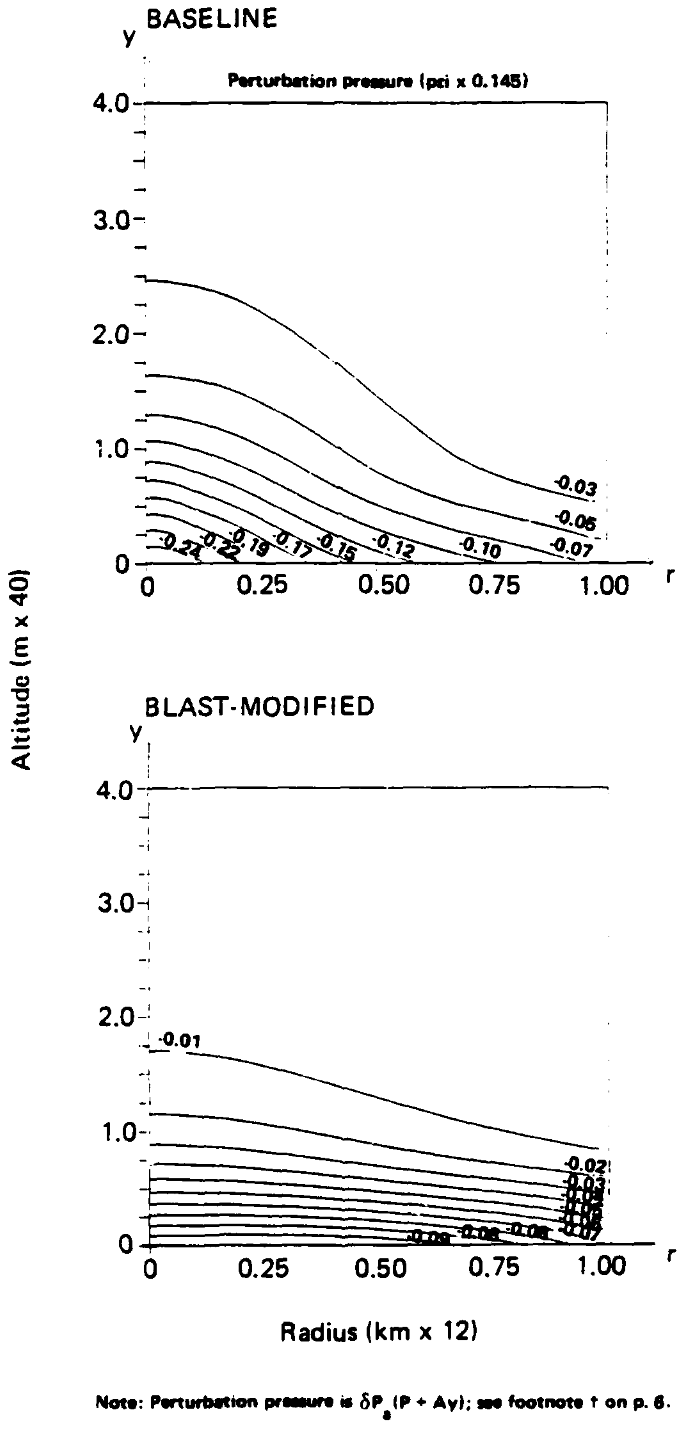

Fig. 32--Baseline and blast-modified pressure contours for city W

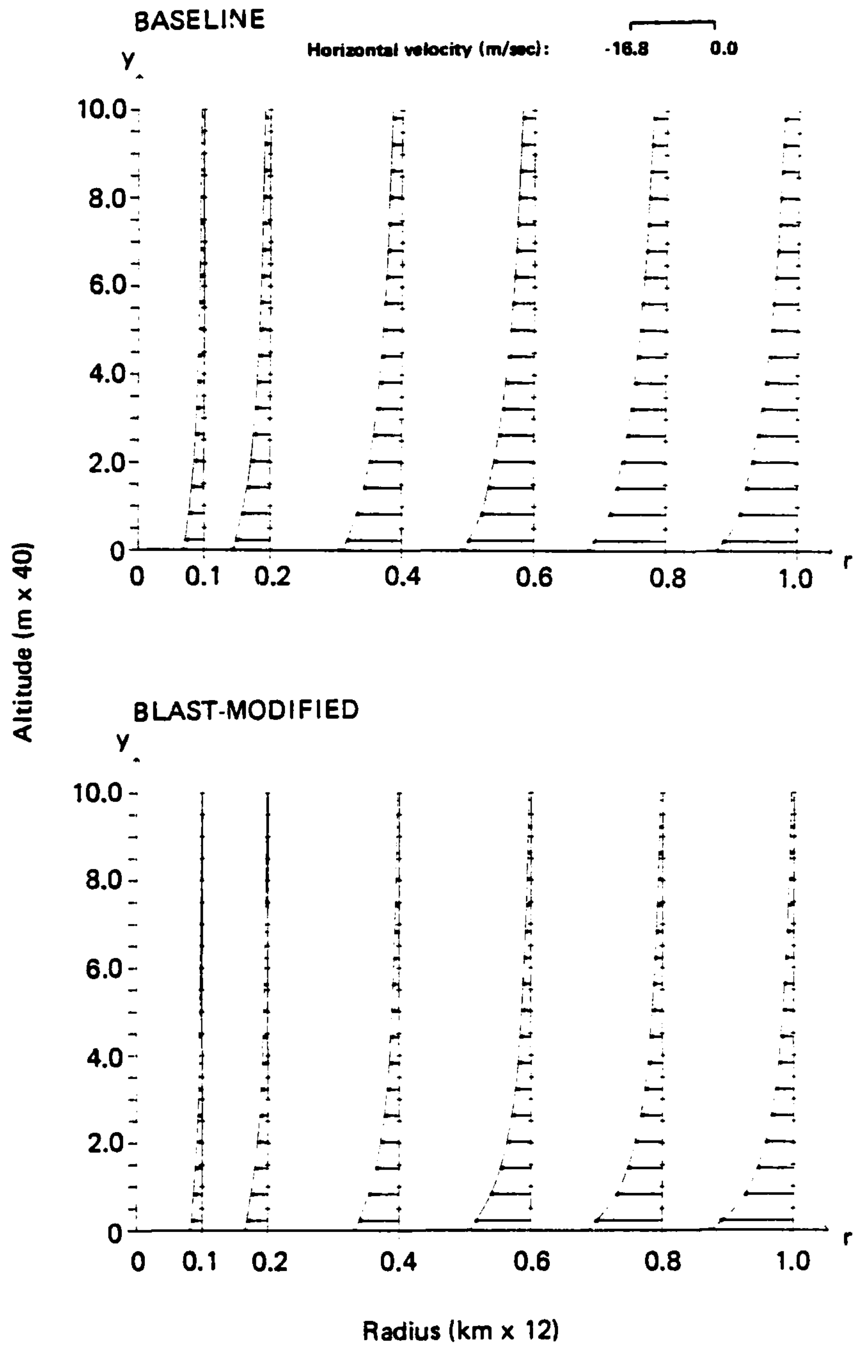

Fig. 33--Baseline and blast-modified radial velocity profiles for city W

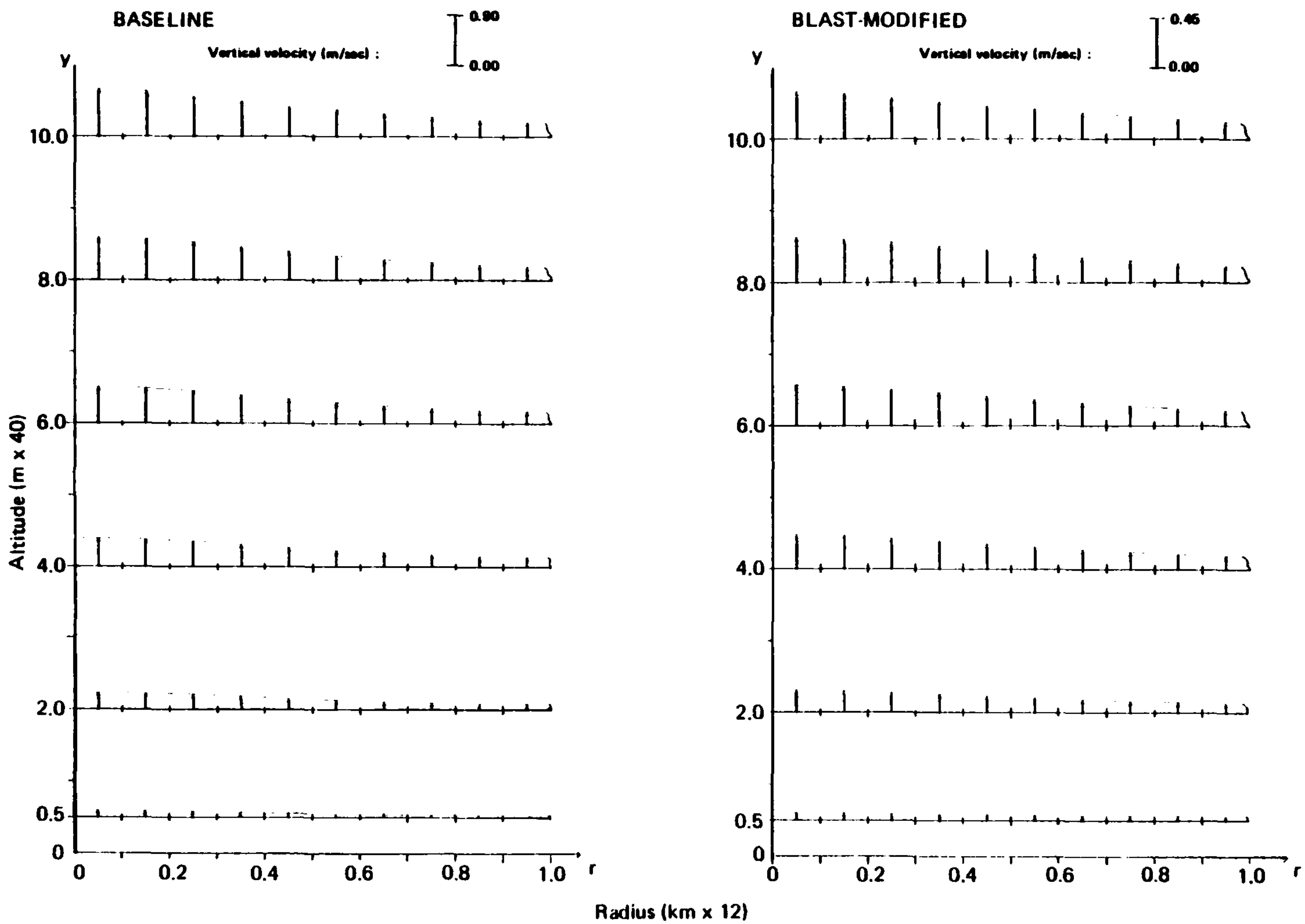

Fig. 34--Baseline and blast-modified vertical velocity profiles for city W

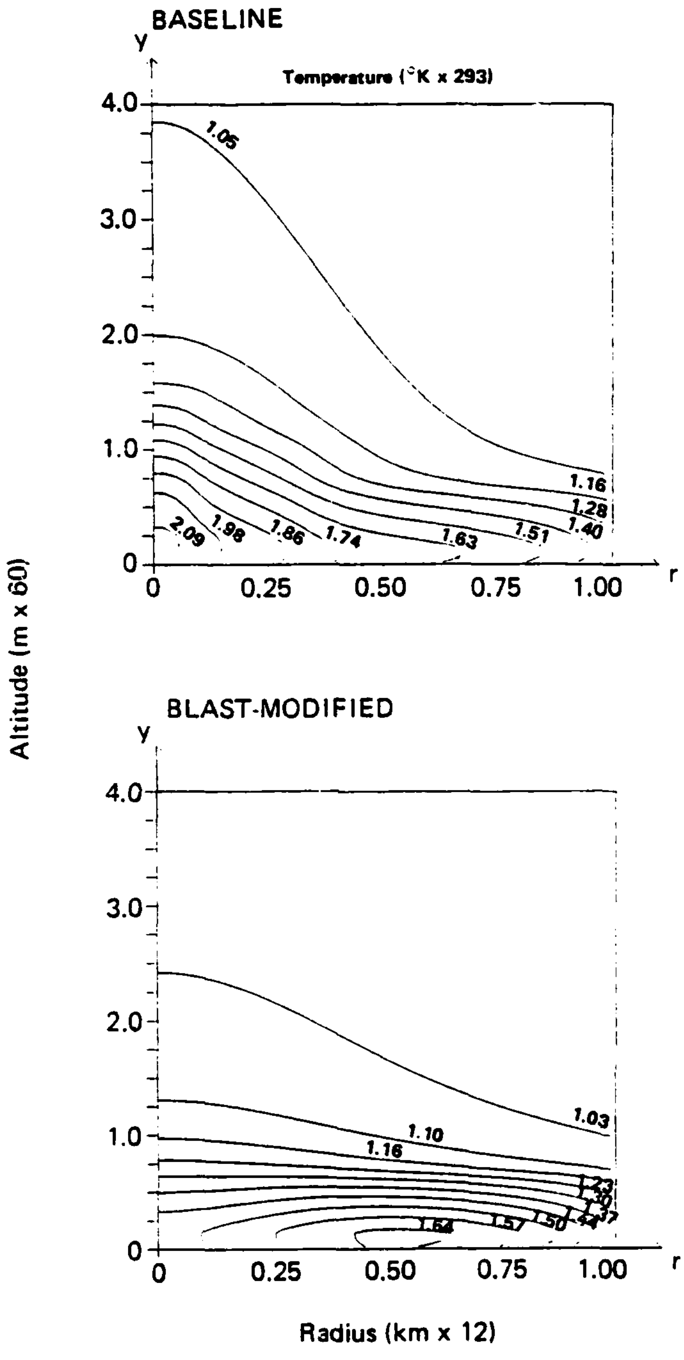

Fig. 35--Baseline and blast-modified temperature contours for city M

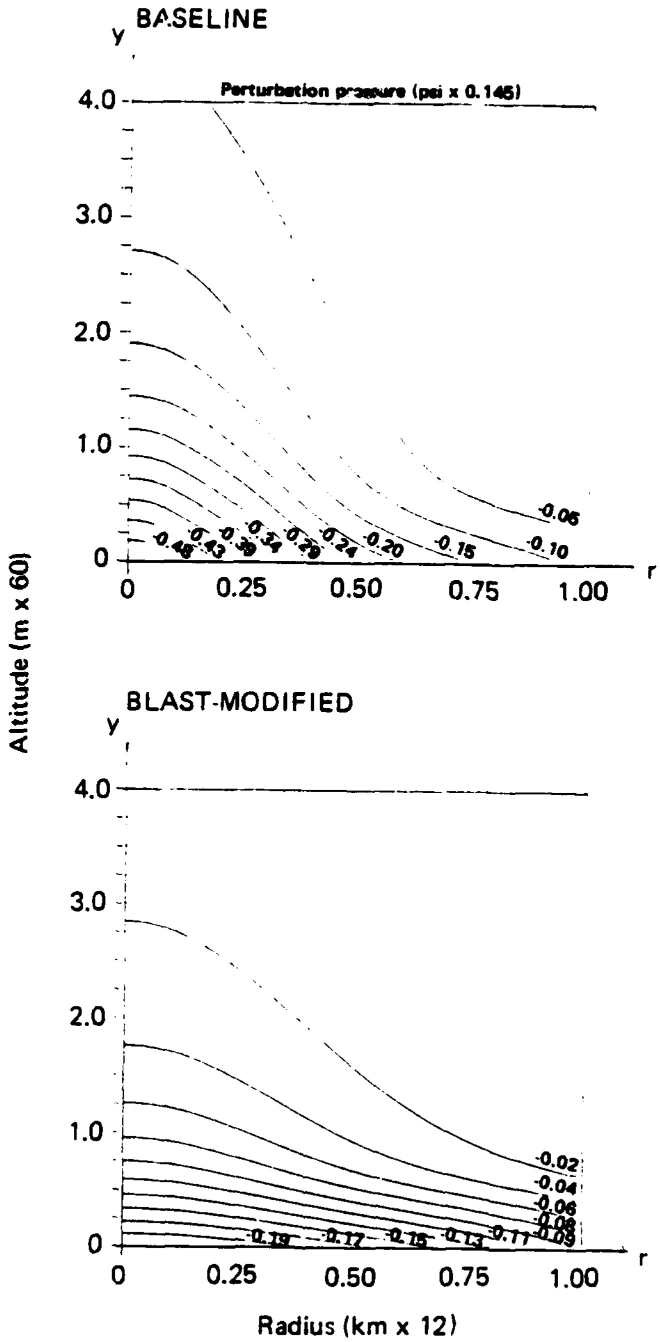

Note: Perturbation pressure is $\delta P_s(P + Ay)$; see footnote † on p. 6.

Fig. 36--Baseline and blast-modified pressure contours for city M

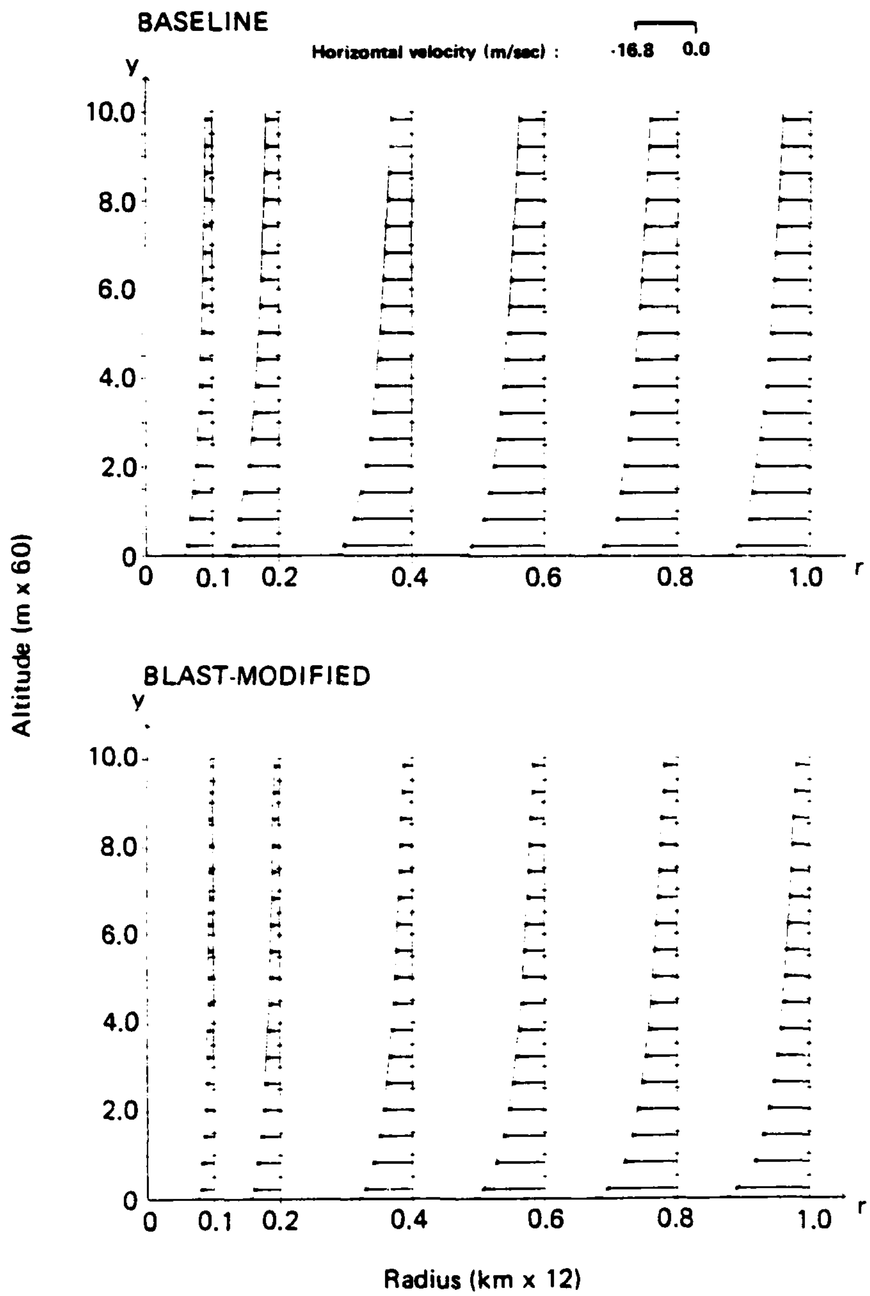

Fig. 37--Baseline and blast-modified radial velocity profiles for city M

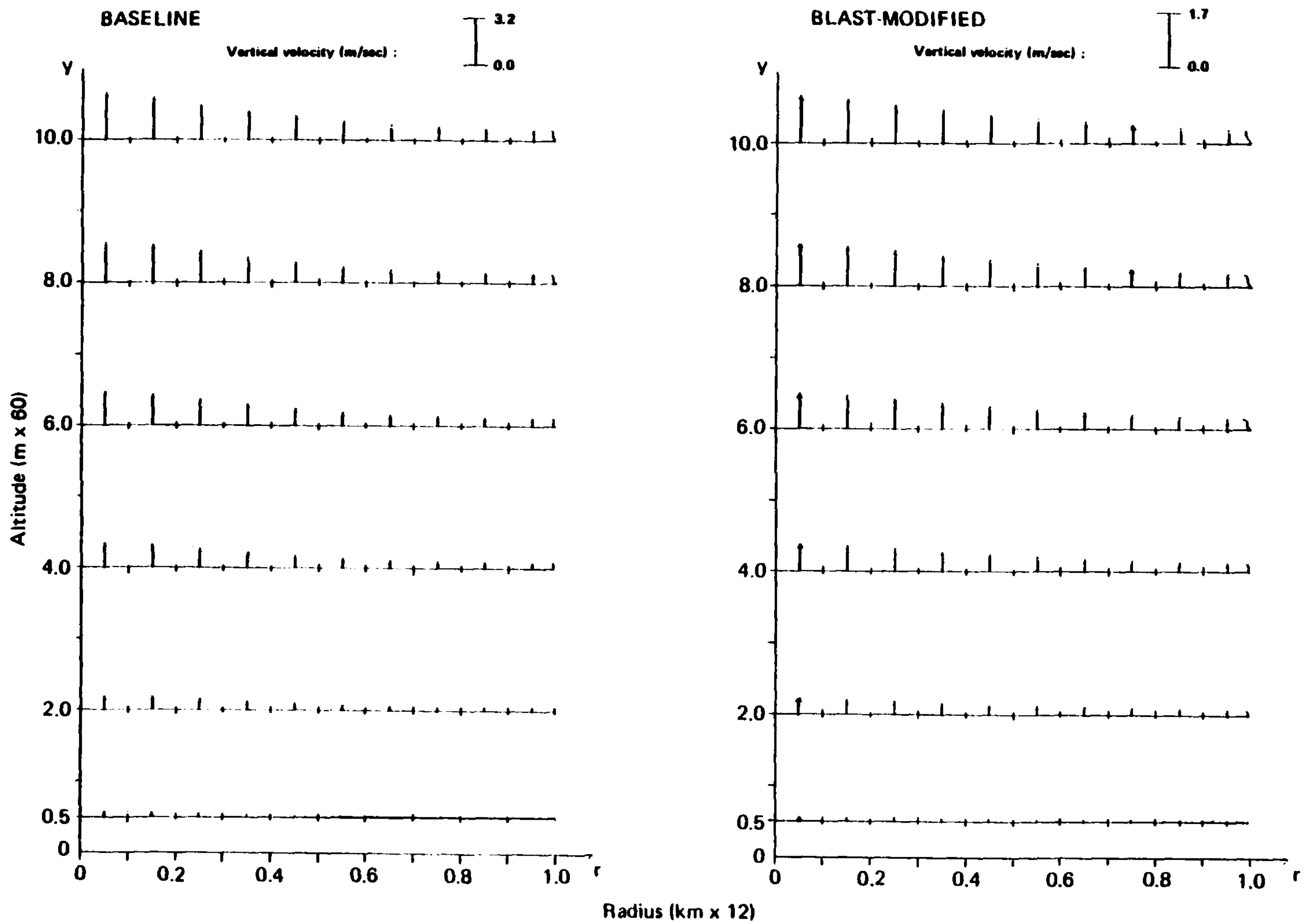

Fig. 38--Baseline and blast-modified vertical velocity profiles for city M

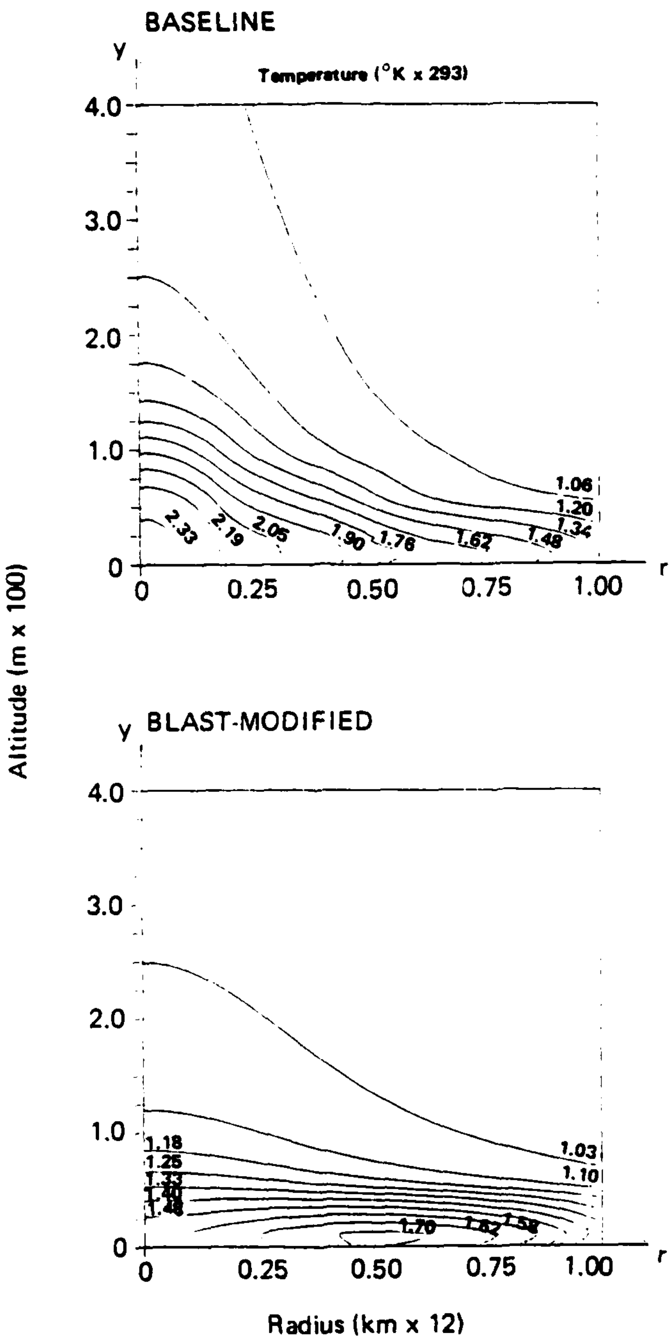

Fig. 39--Baseline and blast-modified temperature contours for city E

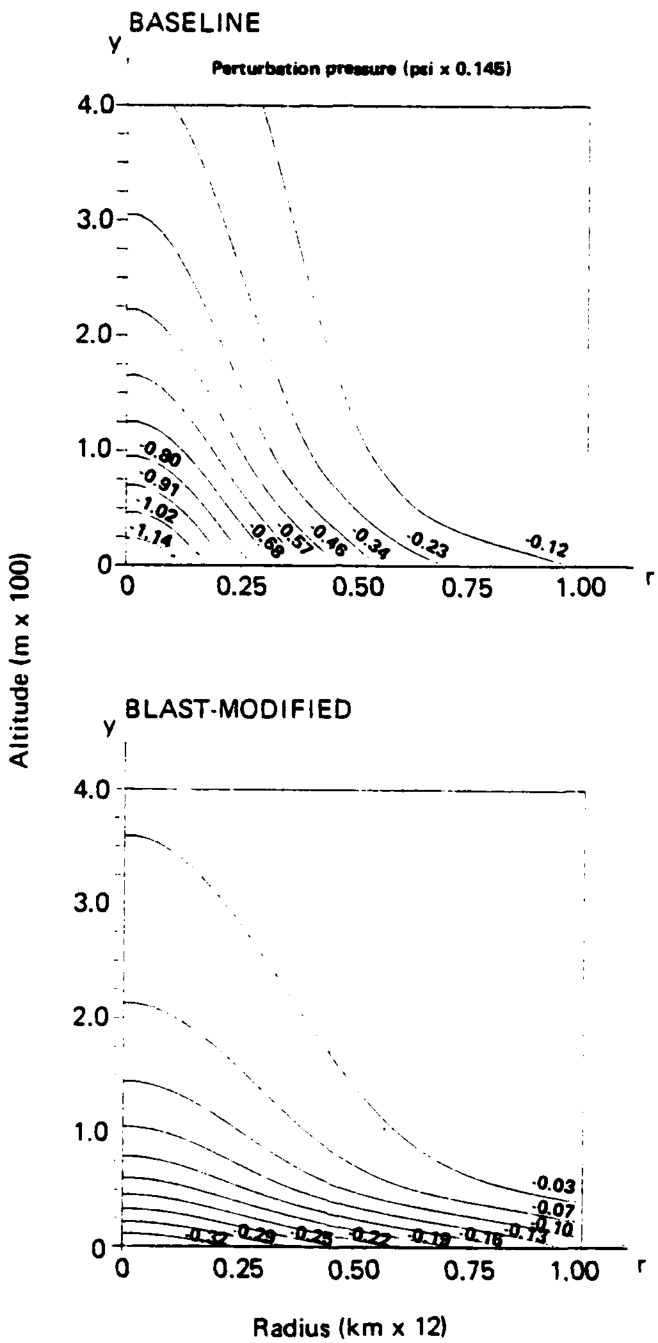

Note: Perturbation pressure is $\delta P_a(P + Ay)$; see footnote † on p. 6.

Fig. 40--Baseline and blast-modified pressure contours for city E

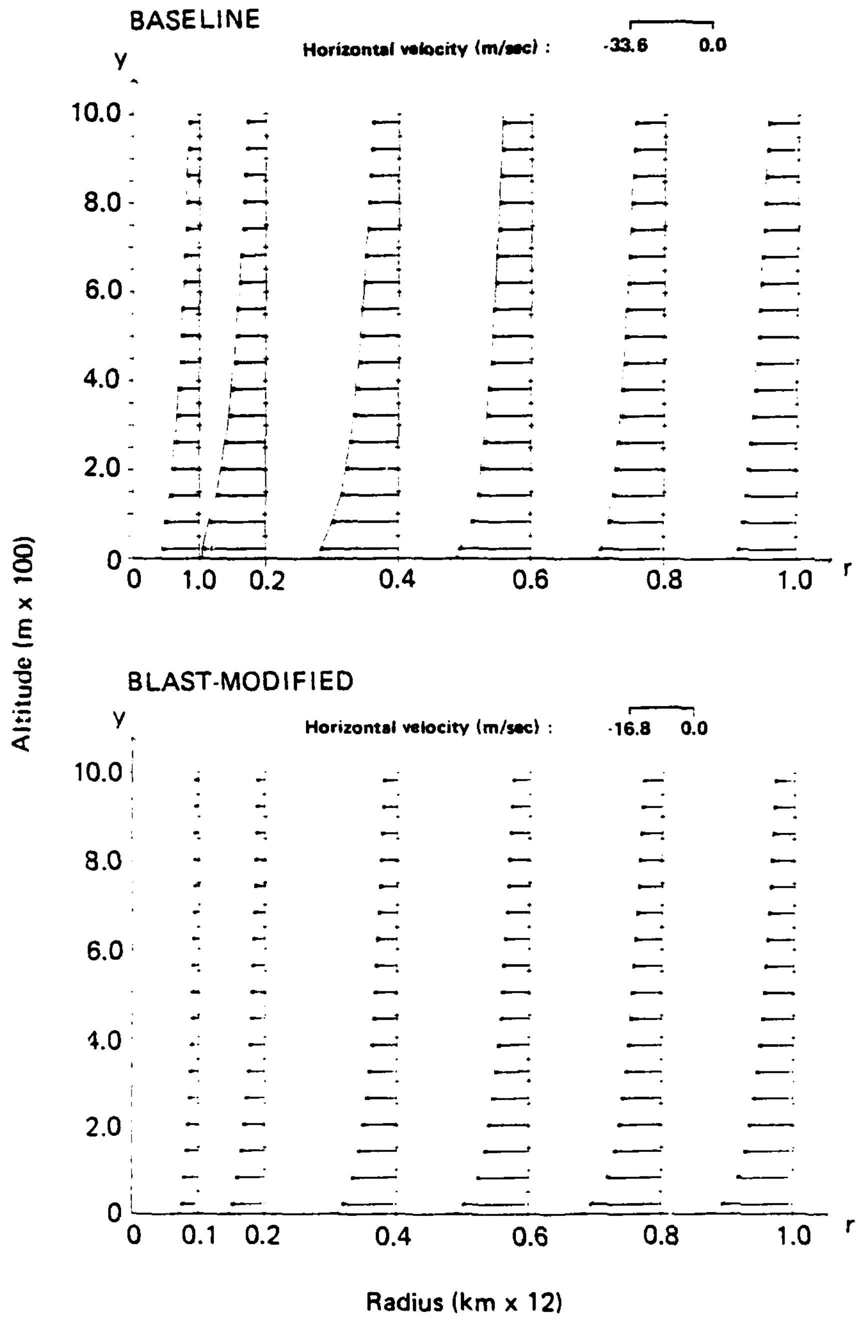

Fig. 41--Baseline and blast-modified radial velocity profiles for city E

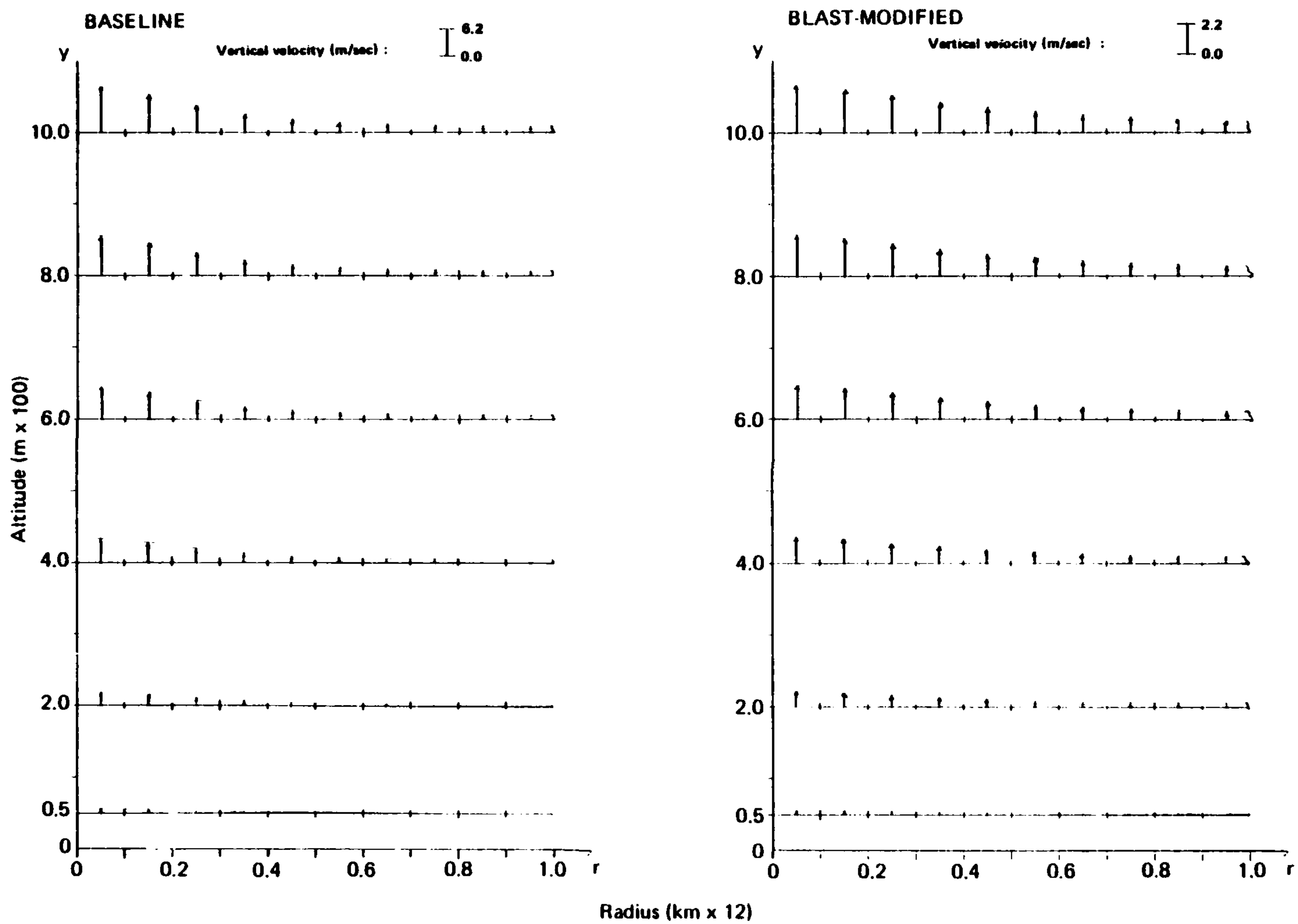

Fig. 42--Baseline and blast-modified vertical velocity profiles for city E

in the results presented in the corresponding plots is that temperatures, pressure drops, and velocities all increase with total loading, and are least for city W and greatest for city E. Further, as shown in Fig. 41, the baseline radial velocity for city E is not maximum at the fire periphery, as in the other cases (cf. Figs. 33 and 37), but rather about halfway between the periphery and the center. That difference presumably reflects the greater radial extent of the taller central-city and inner-belt regions in this case than in the others (cf. Figs. 27 through 29).

IV. SAMPLE TIME-DEPENDENT SIMULATION

This section extends the quasi-steady turning-region analysis of Part I to obtain time-dependent predictions. The multiple-fuel-bed Flambeau fire [Countryman, 1969; Palmer, 1981] treated in Part I is used as a sample case.

Figure 43 presents a typical time-history of the areal heat release in the largest Flambeau fires. During the period encompassing most of the burning (5 to 55 min after the fire starts), variations in the mean heat release rate occur on a time scale of many minutes. At any given point during that period, a steady-state analysis like that in Part I (Sec. IV) is justified as long as dynamic transients occur on a much shorter time scale of, say, a minute or less. As we now show, that criterion is satisfied at all times between 5 and 45 min. A time-dependent simulation is constructed by performing steady-state calculations at several points in that interval.

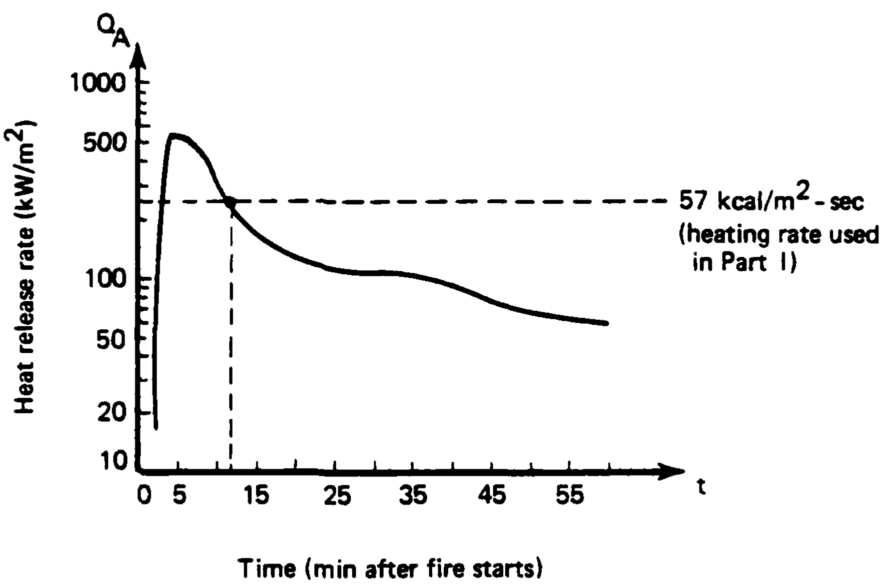

Source: Adapted from Fig. 3 of Palmer [1981]. Reprinted with permission from *Atmospheric Environment*, Vol. 15, Thomas Y. Palmer, "Large Fire Winds, Gases and Smoke," 1981, Pergamon Press, Ltd.

Fig. 43--Areal heat release time-history for Flambeau fire 760-12

In the steady-state Flambeau simulation, we used R = 250 m, H = 20 m, QH $\sim$ 50 kcal/m^2-sec, and hence had U $\sim$ 8 m/sec [see Eqs. (2)]. For that case, the time scale R/U on which dynamic transients occurred was approximately 30 sec, satisfying the criterion for the flow to be quasi-steady. In the new, time-dependent analysis, we similarly use

$$\begin{aligned} R &= 250 \quad m , \\ H &= 20 \quad m , \end{aligned} \tag{10}$$

but vary QH with time as shown in Fig. 43. At any given time, the criterion for the flow to be quasi-steady is that QH $\gtrsim$ 25 kcal/m^2-sec. From Fig. 43, it is certainly satisfied for periods between 5 and 45 min, and possibly up to 55 min as well.

In the following simulation, we calculate quasi-steady flows at points 5 min apart. The specific values of QH used at those points are summarized in Table 10. As in the steady-state simulation of Part I, we also use

$$q(r, y) = \begin{cases} 1.6 & \text{for} \quad 0 \le y \le 0.25 \\ 1.6 \left(\frac{4}{3} (1 - y)\right) & \text{for} \quad 0.25 \le y \le 1.0 , \\ 0 & \text{for} \quad y \ge 1.0 \end{cases}$$

$$k^{*-1} = 20 \quad m ,$$

$$\frac{\mathcal{E}_1}{\rho_a} = \frac{k_1}{c_p \rho_a} = 8410 \quad m^2/sec \tag{11}$$

at each point. Thus, from Eqs. (2) and (3),

$$U = 8.41 \times F \quad m/sec ,$$

$$A = \frac{2.77}{F^2} ,$$

$$\sigma = \frac{0.022}{F} ,$$

$$M_1 = K_1 = \frac{4.0}{F} , \qquad (12)$$

where

$$F = \frac{QH}{57\ kcal/m^2\text{-sec}} \qquad (13)$$

and, from p. 6, $\delta = 9.04 \times 10^{-14} \times F^2$.

Figures 44 through 47 summarize the results of the time-dependent Flambeau simulation. The predicted variations with time of the temperature, pressure, and velocity fields are shown for the heat release described in Fig. 43. The solid curves represent the results of the quasi-steady analysis, which is considered appropriate for the period approximately 5 to 55 min after the fire starts.

Table 10

HEAT RELEASE SCALES USED IN TIME-DEPENDENT FLAMBEAU SIMULATION

Time (min)	QH ($kcal/m^2$-sec)
5	134
10	84
15	53
20	38
25	31
30	24
35	20
40	18
45	18
50	14
55	10

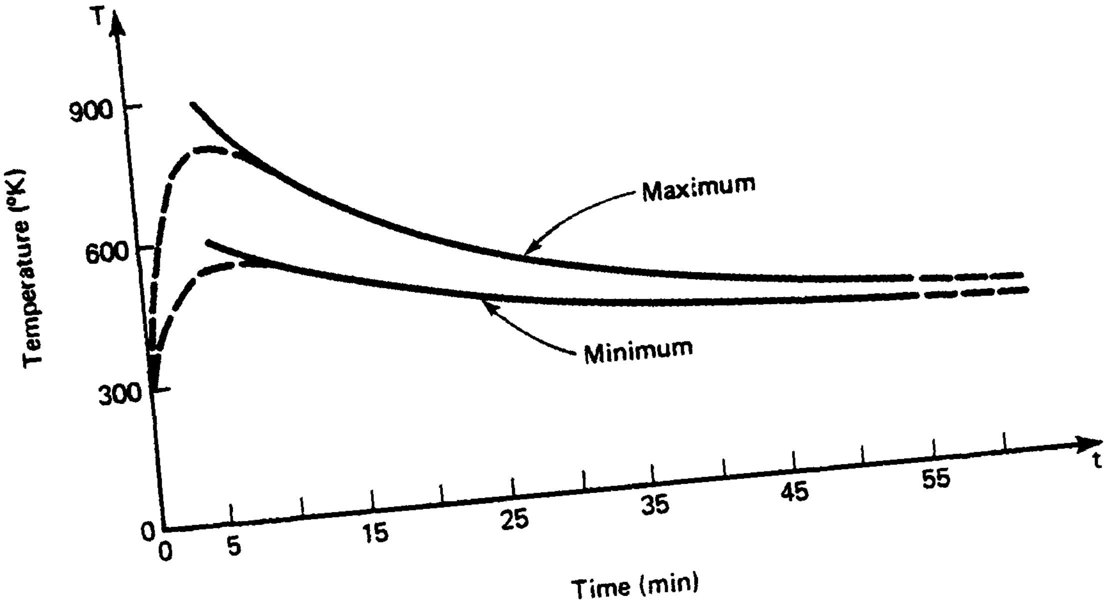

Fig. 44--Time-history of maximum and minimum combustion zone temperatures for sample Flambeau fire

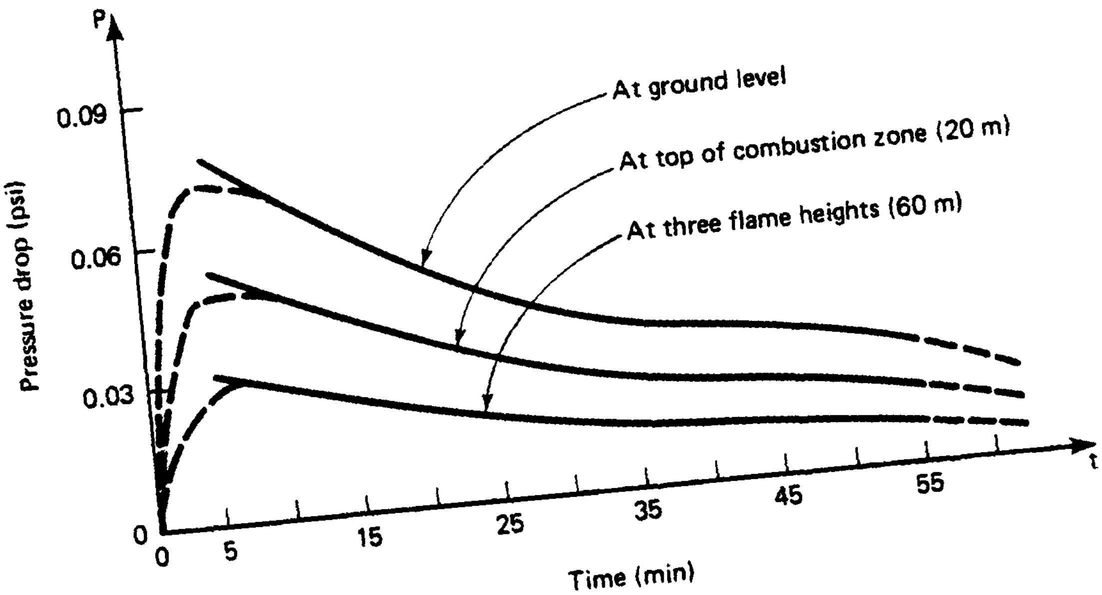

Fig. 45--Time-history of peripheral pressure drop for sample flambeau fire

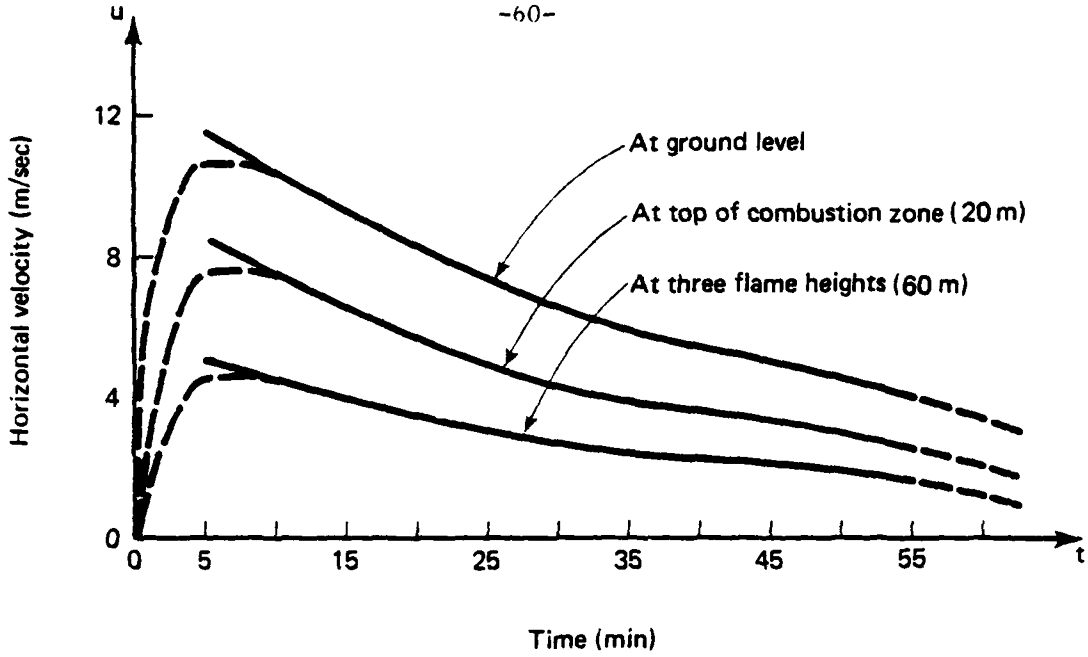

Fig. 46--Time-history of induced peripheral fire wind (radial velocity) for sample Flambeau fire

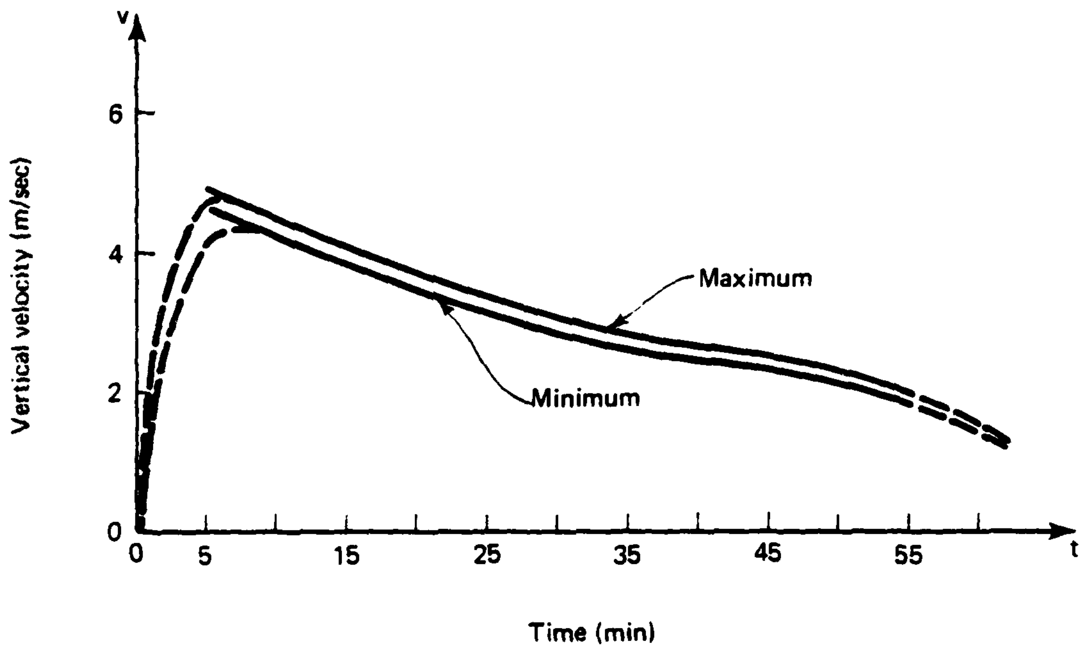

Fig. 47--Time-history of emerging column flow (vertical velocity at top of turning region) for sample Flambeau fire

During the first 5 min of burning, when the individual fires are coalescing to form a large-fire system, the heat release rate (Fig. 43) is changing on a time scale that is fairly fast compared with that for convection. The same is also true during the final phase of fire activity, i.e., the period later than 1 hr or so when the large fire begins to disintegrate and burn out. For those two periods, the quasi-steady analysis is thus inappropriate, and the dashed curves in Figs. 44 through 47 illustrate the expected results of a more rigorous analysis.

Figure 44 describes the predicted variation of the temperature field with time in the burning zone. The contours shown in Fig. 48 are representative of the temperature field at any given time. Maximum temperatures occur in the center of the fire just above the top of the fuel zone (height ≈ 4 m). Minimum temperatures occur on the periphery at the top of the burning region. As expected, the time-histories of those temperatures resemble the heat release time-history shown in Fig. 43. Temperatures are everywhere greatest about 5 min after the fire starts, when the heat release is greatest, and then decrease with time.

The corresponding pressure and velocity time-histories shown in Figs. 45 through 47 follow the same pattern. As illustrated in Figs. 49 and 50, pressure gradients and radial velocities at any given time are maximum at the fire periphery. At all times, they are greatest at ground level and decrease with altitude. Finally, Fig. 47 characterizes the variation with time of the vertical velocity emerging at the top of the computational region (10 flame heights, 200 m). As illustrated in Fig. 51, velocity profiles at that height are almost top-hat at all times. Maximum and minimum velocities, which occur above the fire center and on the periphery, respectively, are thus always quite similar.

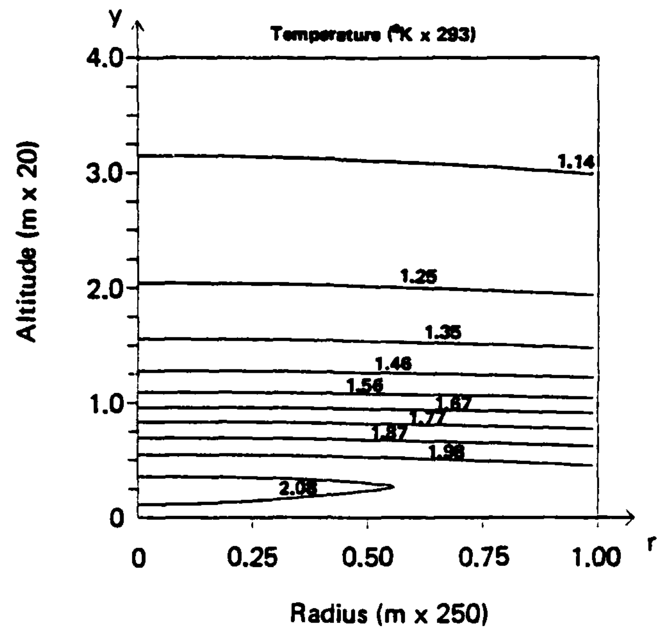

Fig. 48--Temperature contours after 15 min for sample Flambeau fire

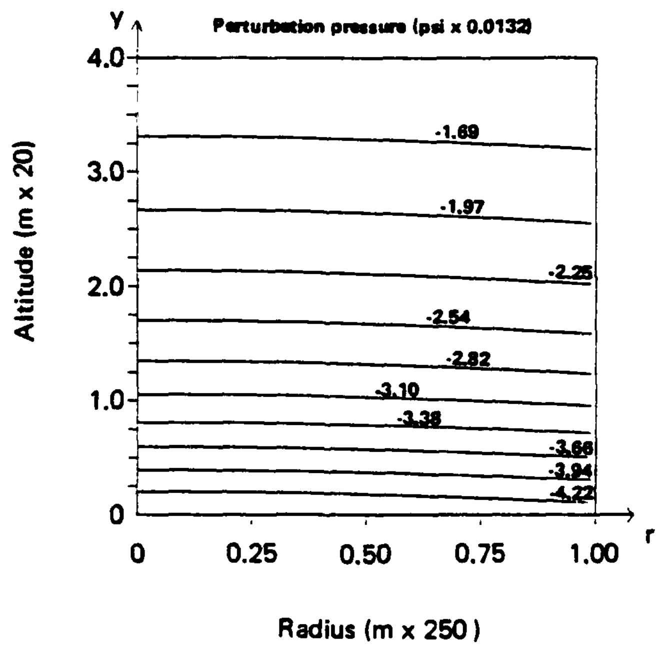

Note: Perturbation pressure is δP_a $(P + Ay)$; see footnote † on p. 6.

Fig. 49--Pressure contours after 15 min for sample Flambeau fire

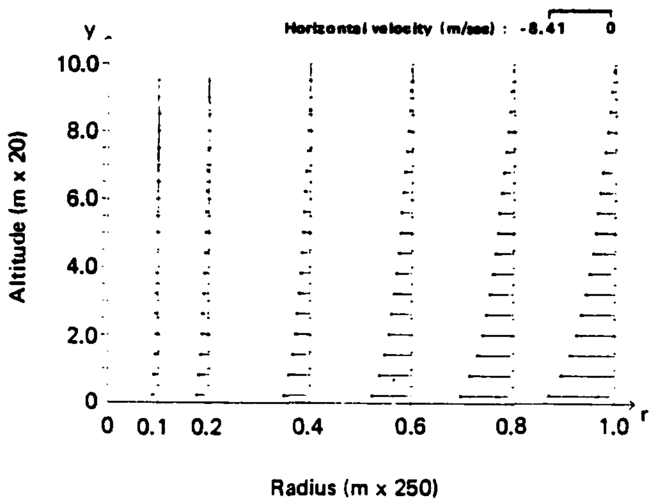

Fig. 50--Radial velocity profiles after 15 min for sample Flambeau fire

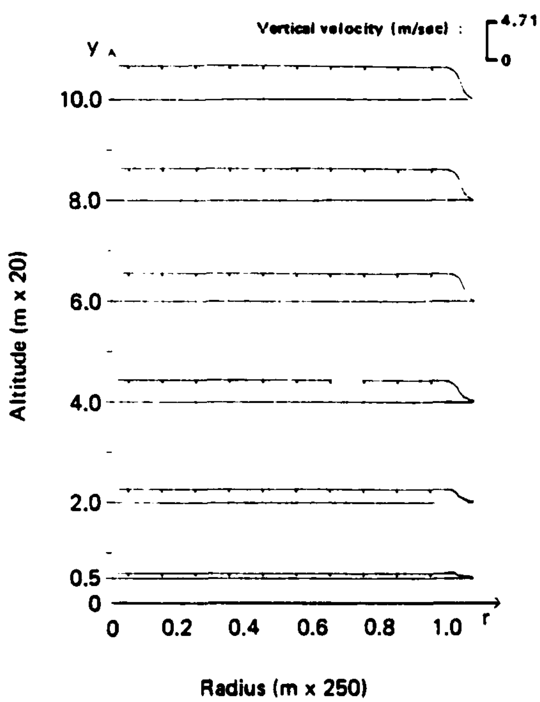

Fig. 51--Vertical velocity profiles after 15 min for sample Flambeau fire

V. DISCUSSION

In presenting calculations of the urban fire environment that may result from a nuclear weapon burst, our aim has been to describe the macroscopic features of a large area fire through analysis of the interactions that produce high temperatures and fire winds. Our approach has been to develop a model based on first principles. In contrast to asymptotic theories that extrapolate the properties of a free-convection plume, we consider the fire region directly. Despite our use of several simplifications and empiricisms, we expect that the theory yields a fine resolution of the hydrothermodynamics of a large area fire.

The analysis considers a quasi-steady axisymmetric fire in an urban area. A spatially dependent volume-heat-release function is used to describe the energy input from fires in a blast-disturbed urban fuel bed. Though the function can be defined to reflect varying fuel loads and distributions of burning, the results presented are based on sectionally uniform heating rates.

The formulation of the boundary value problem is unique in that analytic jump conditions are derived for the fire-column boundary. Such a formulation obviates the need for extensive far-field calculations and allows demonstration of the dependence of induced fire winds on the fire area and heat release rate. Improvements to the model could include the use of multiparameter models to describe the structure of local turbulence and hot-gas/smoke radiation (in place of the simple one-parameter formulations used here) as well as a heat release function dependent on the local thermodynamic and flow conditions.

The effects of the model parameters were explored in a sensitivity study. Varying fire areas, heat distributions and release rates, mixing coefficients, and radiation lengths were investigated. Qualitatively similar flows were observed for all parameter ranges, despite significant quantitative differences. The fire-induced velocities increased with both heat release and fire area. For small values, the velocity increased almost linearly. For larger values of either fire area or heat release rate, the induced velocities increased more slowly. Presumably, the magnitudes are limited by compressibility effects through a slowing production of buoyancy.

Variations in the degree of turbulent mixing produced substantial changes in the velocity fields. As expected, large mixing coefficients tend to reduce the velocities at the fire periphery; smaller values produce higher velocities. In general, the mixing coefficients should reflect both the apparent surface roughness (urban structure) and the fire-generated turbulence. The present analysis used constant eddy diffusivities.

Fuel distributions and heat release rates were developed to explore the effects of varying city constructions and fuel densities on the fire environment in three model urban areas. Though the models provide only a simple representation of a city cross section, the results indicate the importance of modeling a particular fuel bed. More refined distributions based on city surveys could be used.

A fire radius of 12 km is assumed for each model urban area, since megaton-yield explosions would cause area fires of that magnitude. Each model area is characterized by a high-density city center, a lower density annulus representing a mixed residential/industrial construction, and an outer belt of low-density residential tracts. The heat release function reflected the sectionally variable fuel densities and loadings.

Computed results for each fire illustrate the dependence of the fire winds and temperature levels on the urban geography. The most severe fires occur in the higher density cities, though even the lower density constructions support high temperatures and velocities. Application of those results to definition of shelter hardness (thermal) would imply different criteria for each city.

An additional set of numerical experiments considered each model area with a reduced level of burning in the center region. A slow-burning debris field created by extensive blast damage may foster such a heat release distribution. In general, peak velocities were only slightly reduced, though temperature changes were substantial. Temperature levels in the central region were markedly reduced from those in the full-burning outer annulus. It is reasonable to expect that the fire winds would fan the slow-burning central area, creating a more severe environment.

The analysis and results presented here describe the environment of a large area fire at fixed times. Past experience indicates that such fires develop, peak, and ebb over a period of several hours. The methods developed here can be used successively to estimate the environment at different times in the fire evolution. The high velocities and temperatures predicted would encourage a rapid internal fire spread, which may considerably hasten burnout of the city. Improved estimates would result from use of a responsive heat release function that depends on the local gas dynamic state. A time-dependent calculation that includes the high-resolution analysis presented here could provide a complete map of the evolution and ebb of urban fires. Synthesis of the present analysis with a large hydro-code may provide a numerically efficient model for calculating the mesoscale flow field of a large area fire.

Appendix

PREDICTION-ALGORITHM DOCUMENTATION

This appendix documents the computer algorithm used to generate the predictions and other results presented in Secs. II through IV. The algorithm yields numerical solutions to the turning-region boundary value problem derived in Part I.

The turning-region problem is defined by the following balances:

$$\frac{\partial}{\partial r}(r\rho u) + \frac{\partial}{\partial y}(r\rho v) = 0 \ ,$$

$$\rho\left(u\frac{\partial u}{\partial r} + v\frac{\partial u}{\partial y}\right) = -\frac{\partial P}{\partial r} + M_1\left(\frac{1}{r}\frac{\partial}{\partial r}\left(r\frac{\partial u}{\partial r}\right) - \frac{u}{r^2}\right) \ ,$$

$$\frac{\partial P}{\partial y} + A\rho = 0 \ ,$$

$$\rho\left(u\frac{\partial T}{\partial r} + v\frac{\partial T}{\partial y}\right) = q(r, y) - \sigma(T^4 - 1) + K_1\left(\frac{1}{r}\frac{\partial}{\partial r}\left(r\frac{\partial T}{\partial r}\right)\right) \ ,$$

$$\rho T = 1 \ , \qquad \text{(A.1)}$$

subject to

$$v = 0 \qquad \text{on } y = 0 \ , \qquad \text{(A.2a)}$$

$$u = \frac{\partial T}{\partial r} = 0 \qquad \text{on } r = 0 \ , \qquad \text{(A.2b)}$$

$$P + Ay_{max} = 0 \qquad \text{on } y = y_{max} \ , \qquad \text{(A.2c)}$$

$$M_1\frac{\partial u}{\partial r} = \left(\frac{u}{T}\right)^2(T - 1) + (P + Ay) \ , \qquad K_1\frac{\partial T}{\partial r} = \frac{u}{T}(T - 1)$$

$$\text{on } r = 1 \ . \qquad \text{(A.2d)}$$

The flow chart in Fig. A.1 summarizes the solution algorithm. As indicated in the figure (and discussed in Part I, pp. 16-17), the algorithm uses an iterative "shooting" method [Keller, 1968] to solve the overall boundary value problem. Each shoot employs a nonlinear Crank-Nicolson finite difference scheme.

INPUTS AND OUTPUTS

The following is an ordered list of the FORTRAN inputs required for automated algorithm usage:

a. System parameters:

A	A
SIGMA	σ
XNUIN	M_1
XKIN	K_1

b. Mesh descriptors:

YMAX	y_{max}
M	Number of finite difference cells in the radial direction.†
N	Number of finite difference cells in the vertical direction.†

c. Iteration parameters:

ETLINE	Maximum absolute error allowed in solving discretized Crank-Nicolson equations on any line of constant y.
ETOLP	Maximum absolute error allowed in P on $y = y_{max}$.
MAXITL	Maximum number of Newton iterations allowed in solving discretized equations on any line of constant y.
MAXITP	Maximum number of complete-shoot iterations allowed in solving the complete boundary value problem.

---

†In the present coding, cell widths are taken to be uniform, the common width being denoted by Δr. For $0 \leq y \leq 5$, cell heights Δy are also taken to be Δr; for $5 \leq y \leq y_{max}$, they are taken to be $2\,\Delta r$.

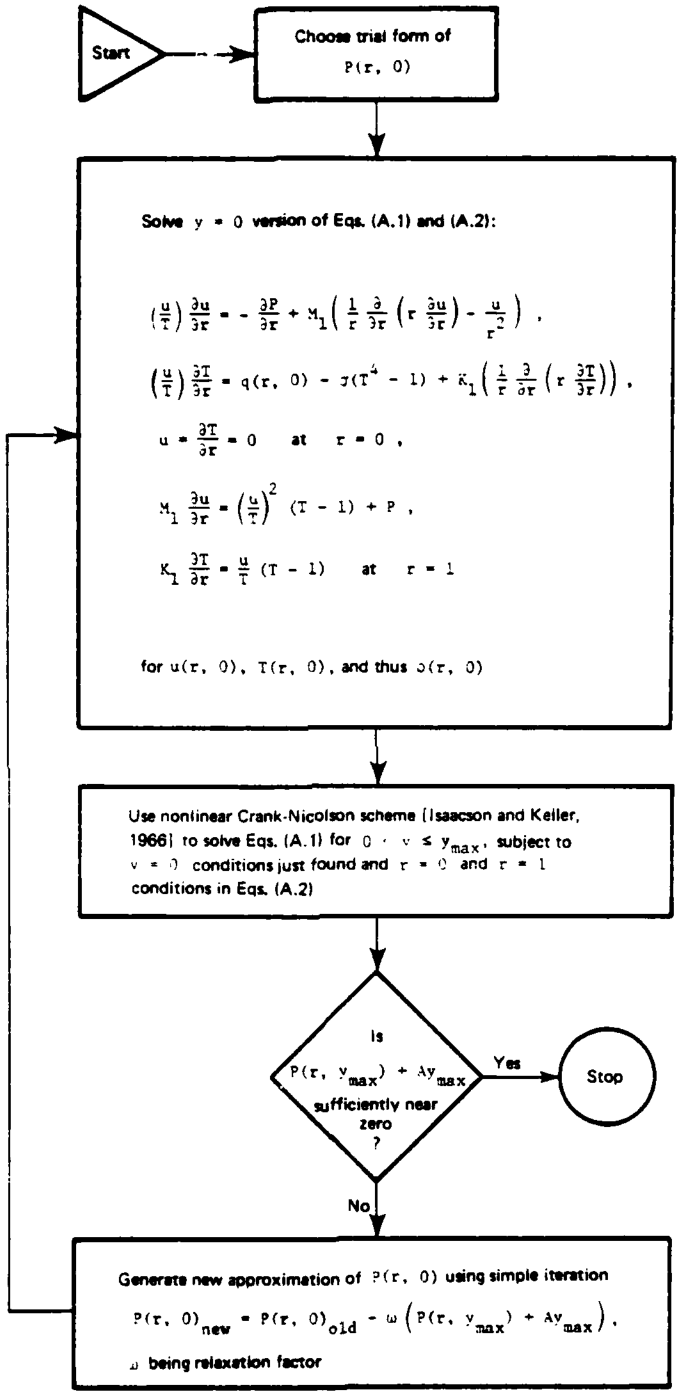

Fig. A.1--Flow chart of prediction algorithm for turning-region boundary value problem

d. Program control parameters:

ALPHA	$(Qq)_{max}$, maximum value of Qq in present coding.
BETA, BLOSS	Parameters available for either system description or program control. (These parameters are currently unused, so they are set equal to zero.)
IGUESS	Parameter that controls the initial choices of first-shoot values along y = 0. IGUESS = 1: Discretized versions of P(r, 0), T(r, 0), and u(r, 0) must be supplied as inputs. IGUESS = 2: "Standard" initial choices are made automatically. IGUESS = 3: Discretized versions of P(r, 0), T(r, 0), and u(r, 0) from the last algorithm run are used automatically.

The "standard" initial guesses in the present coding represent the ground-level pressure, temperature, and radial velocity profiles predicted in Part I (pp. 13-16) for the case of a weakly heated flow:

$$P(r, 0) = -(Qq)_{max}\left(\frac{A}{4\sigma}\right) ,$$

$$T(r, 0) = 1.0 + (Qq)_{max}\left(\frac{1}{4\sigma}\right) ,$$

$$u(r, 0) = -(Qq)_{max}\left(\frac{A}{4\sigma M_1}\right) r . \qquad (A.3)$$

Finally, the functional form of q(r, y) must be prescribed. Currently, it is given in the form used in our analysis:

$$q(r, y) = \begin{Bmatrix} (Qq)_{max} & \text{for } 0 \le y \le 0.25 \\ (Qq)_{max}\left(\frac{4}{3} \quad (1 - y)\right) & \text{for } 0.25 \le y \le 1.0 \\ 0 & \text{for } y \ge 1.0 \end{Bmatrix} . \quad (A.4)$$

Changes require reprogramming in subroutine BCFUNC. As a user option, the dissipation coefficients M_1 and K_1 may also be made to depend on r and y through reprogramming, also in BCFUNC. Currently, those coefficients are simply taken as constants.

A sample input data stream is

A = 0.217 , SIGMA = 0.110 , XNUIN = XKIN = 0.200 ;

YMAX = 10 , M = 40 , N = 300 ;

ETLINE = 0.0003 , ETOLP = 0.001 , MAXITL = 30 , MAXITP = 9 ;

ALPHA = 1.6 , BETA = 0.0 , BLOSS = 0.0 , IGUESS = 3 . (A.5)

The corresponding output is listed in Table A.1. All output data are automatically dumped onto a disk file and used in constructing the vector, contour, and profile plots presented in Secs. II through IV.

PROGRAM FLOW

Figure A.1 outlines the overall flow of the computer algorithm. Inputs, outputs, and the basic shooting iteration are controlled by the main program. Figure A.2 presents a flow chart of that program. In subroutine BCFUNC, functional forms that may be varied [e.g., q(r, y)] are specified; and in subroutine SPRINT, final output data are printed. Subroutine MSWEEP performs most of the computations--i.e., those providing a one-shoot finite difference solution to Eqs. (A.1) for given data along y = 0, r = 0, and r = 1. The flow of that subroutine is shown in Figs. A.4 and A.5 below (pp. 80-81); the underlying numerical analysis is detailed in the accompanying

Table A.1

SAMPLE CODE OUTPUT

```
FIRES: SOLUTION OF COMBUSTION LAYER BOUNDARY VALUE PROBLEM

SYSTEM PARAMETERS:   A =   0.217  SIGMA =   0.110  NU =   0.200  K =   0.200

MESH:   M =   40  DR =   0.025  N =  300   DY =   0.025

ITERATION PARAMETERS:   FTLINE = 0.000300  MAXITL =   30  FTOLP = 0.3(1000   MAXITP =    9

INLET PARAMETERS:   ALPHA =   1.600  BETA =   0.000  HLOSS =   0.000


FOR J =    1  (Y =   0.000):
```

I	R	U	V	T	RHO	P	PR	NU*URR	K*TRR	Q(T)
1	0.000	0.000	0.000	1.938	0.516	-0.183	0.000	0.000	0.000	0.158
2	0.025	-0.019	0.000	1.938	0.516	-0.183	0.000	0.000	0.000	0.158
3	0.050	-0.038	0.000	1.938	0.516	-0.183	0.000	0.000	0.000	0.158
4	0.075	-0.057	0.000	1.938	0.516	-0.183	0.020	0.000	-0.320	0.158
5	0.100	-0.076	0.000	1.937	0.516	-0.182	0.020	0.000	0.000	0.161
6	0.125	-0.095	0.000	1.936	0.517	-0.182	0.000	0.320	-0.320	0.165
7	0.150	-0.113	0.000	1.934	0.517	-0.182	0.020	-0.320	0.320	0.171
8	0.175	-0.132	0.000	1.933	0.517	-0.181	0.040	0.320	-0.320	0.174
9	0.200	-0.150	0.000	1.931	0.518	-0.180	0.040	0.000	-0.320	0.181
10	0.225	-0.168	0.000	1.928	0.519	-0.179	0.020	0.000	0.320	0.190
11	0.250	-0.186	0.000	1.926	0.519	-0.179	0.020	0.000	-0.320	0.196
12	0.275	-0.204	0.000	1.923	0.520	-0.178	0.040	0.320	0.000	0.206
13	0.300	-0.221	0.000	1.920	0.521	-0.177	0.060	0.000	-0.320	0.215
14	0.325	-0.238	0.000	1.916	0.522	-0.175	0.060	0.000	0.320	0.228
15	0.350	-0.255	0.000	1.913	0.523	-0.174	0.040	0.000	-0.640	0.237
16	0.375	-0.272	0.000	1.908	0.524	-0.173	0.040	0.320	0.320	0.252
17	0.400	-0.288	0.000	1.904	0.525	-0.172	0.060	0.000	-0.320	0.264
18	0.425	-0.304	0.000	1.899	0.527	-0.170	0.060	0.320	-0.320	0.279
19	0.450	-0.319	0.000	1.893	0.528	-0.169	0.060	0.000	0.000	0.297
20	0.475	-0.334	0.000	1.887	0.530	-0.167	0.080	0.000	-0.320	0.315
21	0.500	-0.349	0.000	1.880	0.532	-0.165	0.060	0.320	0.000	0.336
22	0.525	-0.363	0.000	1.873	0.534	-0.164	0.060	0.000	0.000	0.356
23	0.550	-0.377	0.000	1.866	0.536	-0.162	0.080	0.320	-0.640	0.376
24	0.575	-0.390	0.000	1.857	0.539	-0.160	0.080	-0.320	0.000	0.402
25	0.600	-0.404	0.000	1.848	0.541	-0.158	0.080	0.640	0.000	0.427
26	0.625	-0.416	0.000	1.839	0.544	-0.156	0.080	0.000	-0.640	0.452
27	0.650	-0.428	0.000	1.828	0.547	-0.154	0.080	0.000	0.000	0.482
28	0.675	-0.440	0.000	1.817	0.550	-0.152	0.080	0.000	-0.320	0.511
29	0.700	-0.452	0.000	1.805	0.554	-0.150	0.080	0.640	-0.320	0.542
30	0.725	-0.462	0.000	1.792	0.558	-0.148	0.080	-0.320	0.000	0.576
31	0.750	-0.473	0.000	1.779	0.562	-0.146	0.080	0.320	-0.640	0.608
32	0.775	-0.483	0.000	1.764	0.567	-0.144	0.100	0.000	-0.320	0.645
33	0.800	-0.493	0.000	1.748	0.572	-0.141	0.100	0.320	0.000	0.683
34	0.825	-0.502	0.000	1.732	0.577	-0.139	0.080	0.320	-0.640	0.720
35	0.850	-0.510	0.000	1.714	0.583	-0.137	0.100	-0.320	-0.320	0.761
36	0.875	-0.519	0.000	1.695	0.590	-0.134	0.120	0.320	-0.320	0.802
37	0.900	-0.527	0.000	1.675	0.597	-0.131	0.100	0.320	-0.640	0.844
38	0.925	-0.534	0.000	1.653	0.605	-0.129	0.100	0.000	-0.320	0.889
39	0.950	-0.541	0.000	1.630	0.613	-0.126	0.120	0.000	-0.320	0.933
40	0.975	-0.548	0.000	1.606	0.623	-0.123	0.120	0.320	-0.320	0.978
41	1.000	-0.554	0.000	1.581	0.633	-0.120	0.120	0.320	-0.320	1.023

⋮

Table A.1--Continued

. . .

FOR J = 2 .(Y = 0.025):

I	R	U	V	T	RHO	P	PR	NU*URR	K*TRR	Q(T)
1	0.000	0.000	0.036	1.941	0.515	-0.180	0.000	0.000	0.000	0.154
2	0.025	-0.017	0.036	1.941	0.515	-0.180	0.000	0.014	-0.099	0.154
3	0.050	-0.033	0.036	1.940	0.515	-0.180	0.000	0.014	-0.079	0.155
4	0.075	-0.050	0.036	1.940	0.516	-0.180	0.020	0.045	-0.078	0.156
5	0.100	-0.067	0.035	1.939	0.516	-0.179	0.020	0.041	-0.078	0.159
6	0.125	-0.083	0.035	1.938	0.516	-0.179	0.000	0.015	-0.080	0.162
7	0.150	-0.099	0.035	1.936	0.516	-0.179	0.020	0.045	-0.082	0.167
8	0.175	-0.116	0.035	1.935	0.517	-0.178	0.040	0.069	-0.085	0.172
9	0.200	-0.131	0.035	1.933	0.517	-0.177	0.040	0.067	-0.089	0.178
10	0.225	-0.147	0.035	1.931	0.518	-0.176	0.020	0.043	-0.092	0.185
11	0.250	-0.163	0.034	1.929	0.518	-0.176	0.020	0.046	-0.096	0.192
12	0.275	-0.178	0.034	1.926	0.519	-0.175	0.040	0.070	-0.101	0.201
13	0.300	-0.194	0.034	1.923	0.520	-0.174	0.060	0.092	-0.106	0.211
14	0.325	-0.209	0.034	1.920	0.521	-0.172	0.060	0.090	-0.112	0.221
15	0.350	-0.223	0.033	1.916	0.522	-0.171	0.040	0.067	-0.119	0.233
16	0.375	-0.238	0.033	1.912	0.523	-0.170	0.040	0.068	-0.125	0.246
17	0.400	-0.252	0.033	1.907	0.524	-0.169	0.060	0.091	-0.133	0.260
18	0.425	-0.266	0.032	1.903	0.526	-0.167	0.060	0.090	-0.141	0.275
19	0.450	-0.280	0.032	1.897	0.527	-0.166	0.060	0.089	-0.150	0.291
20	0.475	-0.293	0.032	1.892	0.529	-0.164	0.080	0.109	-0.159	0.309
21	0.500	-0.306	0.031	1.885	0.530	-0.162	0.060	0.086	-0.170	0.327
22	0.525	-0.319	0.031	1.879	0.532	-0.161	0.060	0.086	-0.180	0.348
23	0.550	-0.332	0.031	1.871	0.534	-0.159	0.080	0.106	-0.191	0.369
24	0.575	-0.344	0.030	1.863	0.537	-0.157	0.079	0.104	-0.204	0.393
25	0.600	-0.356	0.030	1.855	0.539	-0.156	0.079	0.102	-0.216	0.417
26	0.625	-0.368	0.030	1.845	0.542	-0.154	0.079	0.100	-0.229	0.443
27	0.650	-0.379	0.029	1.835	0.545	-0.152	0.079	0.099	-0.243	0.471
28	0.675	-0.390	0.029	1.825	0.548	-0.150	0.079	0.097	-0.258	0.501
29	0.700	-0.400	0.029	1.813	0.552	-0.148	0.079	0.095	-0.273	0.531
30	0.725	-0.411	0.029	1.801	0.555	-0.146	0.079	0.094	-0.287	0.564
31	0.750	-0.421	0.029	1.787	0.559	-0.144	0.079	0.092	-0.305	0.598
32	0.775	-0.431	0.028	1.773	0.564	-0.142	0.099	0.111	-0.320	0.634
33	0.800	-0.440	0.028	1.758	0.569	-0.139	0.099	0.108	-0.337	0.671
34	0.825	-0.449	0.028	1.742	0.574	-0.137	0.079	0.085	-0.353	0.709
35	0.850	-0.458	0.028	1.724	0.580	-0.135	0.099	0.104	-0.370	0.749
36	0.875	-0.467	0.028	1.706	0.586	-0.132	0.119	0.122	-0.386	0.791
37	0.900	-0.475	0.028	1.686	0.593	-0.129	0.098	0.098	-0.402	0.833
38	0.925	-0.482	0.028	1.665	0.601	-0.127	0.098	0.095	-0.417	0.877
39	0.950	-0.490	0.028	1.643	0.609	-0.124	0.118	0.113	-0.431	0.921
40	0.975	-0.497	0.028	1.619	0.618	-0.121	0.118	0.109	-0.445	0.966
41	1.000	-0.504	0.028	1.594	0.627	-0.118	0.118	0.109	-0.445	1.012

. . .

Table A.1--Continued

.
.
.

FOR J = 301 (Y = 10.000):

I	R	U	V	T	RHO	P	PR	NU*URR	K*TRR	Q(T)
1	0.000	0.000	4.835	1.008	0.992	0.000	0.000	0.000	0.000	-0.003
2	0.025	-0.002	4.834	1.008	0.992	0.000	-0.003	-0.002	-0.002	-0.003
3	0.050	-0.005	4.833	1.008	0.992	0.000	-0.007	-0.005	-0.001	-0.003
4	0.075	-0.007	4.815	1.008	0.992	0.000	0.008	0.017	-0.002	-0.003
5	0.100	-0.010	4.785	1.008	0.992	0.001	0.005	0.012	-0.002	-0.003
6	0.125	-0.012	4.771	1.008	0.992	0.000	-0.019	-0.013	-0.001	-0.003
7	0.150	-0.014	4.754	1.008	0.992	0.000	-0.003	0.010	-0.002	-0.003
8	0.175	-0.017	4.712	1.008	0.993	0.000	0.013	0.028	-0.001	-0.003
9	0.200	-0.019	4.657	1.008	0.993	0.000	0.010	0.024	-0.002	-0.003
10	0.225	-0.021	4.617	1.007	0.993	0.001	-0.014	0.000	-0.001	-0.003
11	0.250	-0.023	4.588	1.007	0.993	0.000	-0.017	-0.001	-0.001	-0.003
12	0.275	-0.025	4.547	1.007	0.993	0.000	-0.001	0.019	-0.001	-0.003
13	0.300	-0.028	4.481	1.007	0.993	0.000	0.016	0.037	-0.001	-0.003
14	0.325	-0.030	4.403	1.007	0.993	0.001	0.013	0.033	-0.001	-0.003
15	0.350	-0.031	4.340	1.007	0.993	0.000	-0.010	0.010	-0.001	-0.003
16	0.375	-0.033	4.289	1.007	0.993	0.000	-0.013	0.009	-0.001	-0.003
17	0.400	-0.035	4.226	1.007	0.993	0.000	0.004	0.028	-0.001	-0.003
18	0.425	-0.037	4.153	1.007	0.993	0.000	0.001	0.025	-0.001	-0.003
19	0.450	-0.039	4.080	1.007	0.993	0.000	-0.002	0.023	0.000	-0.003
20	0.475	-0.040	3.997	1.007	0.993	0.000	0.016	0.041	0.000	-0.003
21	0.500	-0.042	3.916	1.007	0.993	0.001	-0.007	0.018	-0.001	-0.003
22	0.525	-0.043	3.848	1.007	0.993	0.000	-0.009	0.016	0.000	-0.003
23	0.550	-0.044	3.770	1.007	0.993	0.000	0.009	0.035	0.000	-0.003
24	0.575	-0.046	3.683	1.007	0.993	0.000	0.006	0.032	0.000	-0.003
25	0.600	-0.047	3.597	1.007	0.993	0.000	0.004	0.029	0.000	-0.003
26	0.625	-0.048	3.515	1.007	0.994	0.000	0.002	0.027	0.000	-0.003
27	0.650	-0.049	3.435	1.006	0.994	0.000	-0.001	0.024	0.001	-0.003
28	0.675	-0.050	3.357	1.006	0.994	0.000	-0.003	0.022	0.000	-0.003
29	0.700	-0.051	3.283	1.006	0.994	0.000	-0.005	0.020	0.001	-0.003
30	0.725	-0.051	3.212	1.006	0.994	0.000	-0.007	0.018	0.000	-0.003
31	0.750	-0.052	3.145	1.006	0.994	0.000	-0.010	0.015	0.001	-0.003
32	0.775	-0.053	3.069	1.006	0.994	0.000	0.008	0.033	0.000	-0.003
33	0.800	-0.053	2.985	1.006	0.994	0.000	0.005	0.030	0.001	-0.003
34	0.825	-0.054	2.917	1.006	0.994	0.000	-0.017	0.006	0.001	-0.003
35	0.850	-0.054	2.854	1.006	0.994	-0.001	0.000	0.024	0.001	-0.003
36	0.875	-0.055	2.772	1.006	0.994	0.006	0.017	0.041	0.001	-0.003
37	0.900	-0.055	2.695	1.006	0.994	0.000	-0.006	0.016	0.000	-0.003
38	0.925	-0.055	2.636	1.006	0.994	0.000	-0.009	0.013	0.002	-0.003
39	0.950	-0.055	2.571	1.006	0.994	0.000	0.007	0.029	0.001	-0.003
40	0.975	-0.055	2.500	1.006	0.994	0.000	0.003	0.025	0.000	-0.003
41	1.000	-0.055	2.436	1.006	0.994	0.000	0.001	0.025	0.000	-0.003

.
.
.

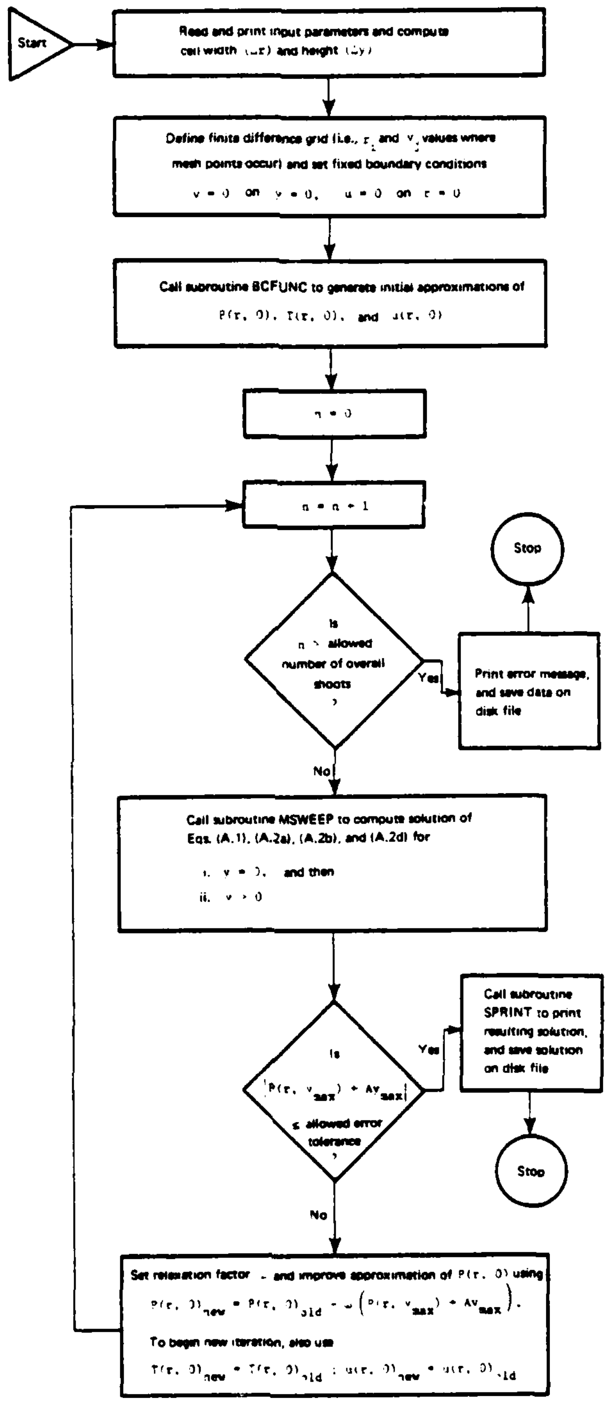

Fig. A.2--Flow chart of main program

text. Complete FORTRAN listings of the main program and all subroutines are presented at the end of this appendix.

FINITE DIFFERENCE ALGORITHM AND SUBROUTINE MSWEEP

The finite difference scheme underlying the computer algorithm is based on the rectangular grid and "stencils" in Fig. A.3. The grid has uniform cell widths ($\Delta r = 1/M$) and piecewise uniform heights ($\Delta y = \Delta r$ for $0 \le y \le 5$, $y = 2\,\Delta r$ for $y > 5$). Mesh points are thus located at (r_i, y_j) points with

$$r_i = (i - 1)\,\Delta r\,, \qquad 1 \le i \le M + 1\,,$$

$$y_j = \left\{\begin{array}{ll} (j - 1)\,\Delta r\,, & 1 \le j \le 5M + 1 \\ 5 + (j - 5M - 1)(2\,\Delta r)\,, & 5M + 2 \le j \le N + 1 \end{array}\right\}. \qquad \text{(A.6)}$$

Dependent variables evaluated at those points are given corresponding (i, j) suffices. For example, $r_1 = 0$ (and not Δr), $y_{N+1} = y_{max}$, and $u_{1,N+1} = u(0, y_{max})$. The accurate approximation of $\{u_{i,j}, v_{i,j}, P_{i,j}, T_{i,j}, \rho_{i,j}\}_{1 \le i \le M+1, 1 \le j \le N+1}$ constitutes a numerical solution of the problem posed by Eqs. (A.1) and (A.2). The stencils in Fig. A.3, explained below (pp. 82-83), indicate the types of differencing used in the algorithm.

Along the $y = 0$ line (where $j = 1$), $v \equiv 0$. As shown in Fig. A.2, a guess at P along that line [actually, the $\{P_{i1}\}_{i=1}^{M+1}$ values] is also made before the MSWEEP subroutine is called. As indicated in the first large block of Fig. A.1, Eqs. (A.1) and (A.2) then reduce along the $y = 0$ line to the following ordinary-differential-equation boundary value problem for u and T alone (with $\rho = 1/T$):

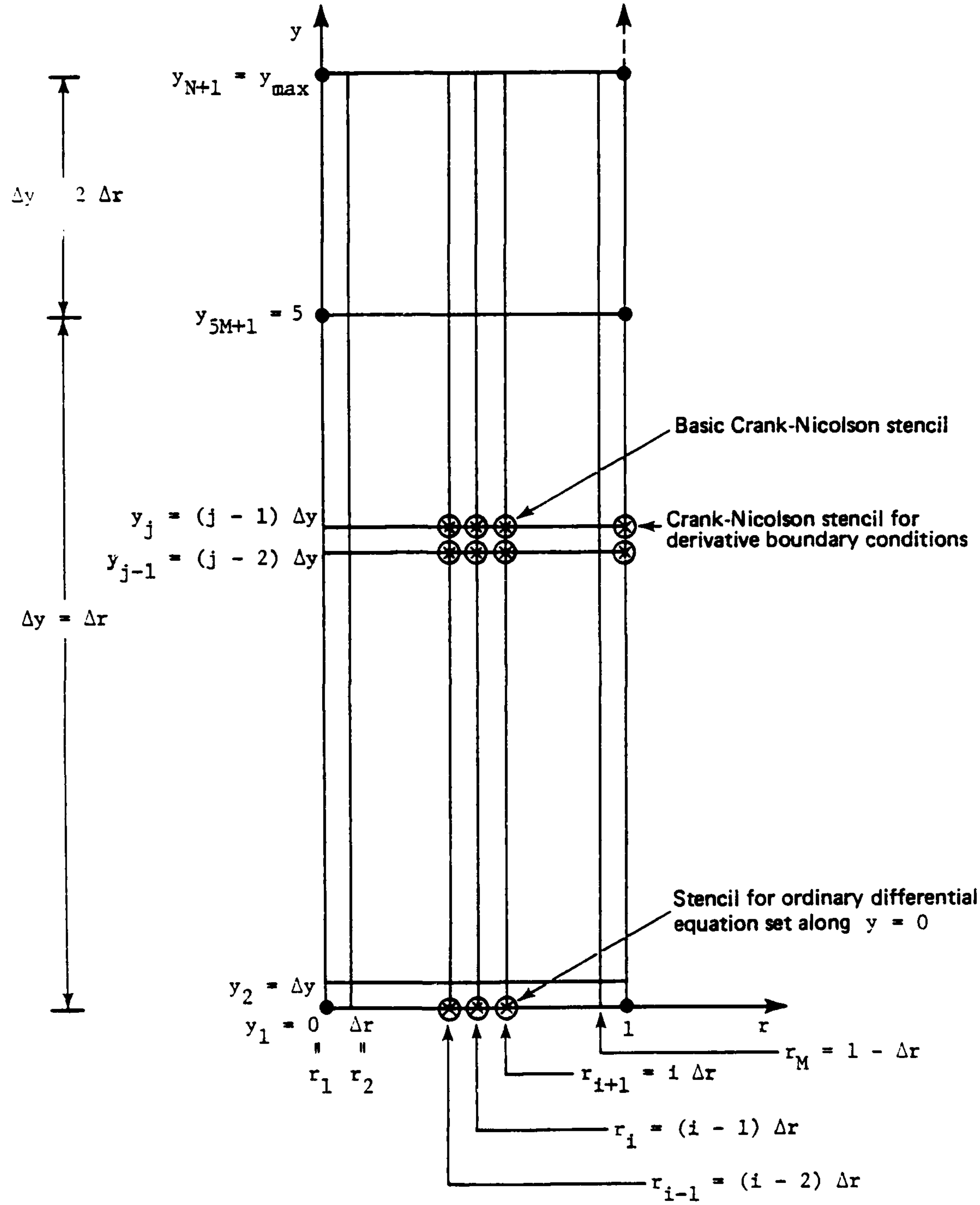

Fig. A.3--Finite difference grid and stencils for numerical solution of turning-region problem

$$\left(\frac{u}{T}\right)\frac{\partial u}{\partial r} = -\frac{\partial P}{\partial r} + M_1\left(\frac{1}{r}\frac{\partial}{\partial r}\left(r\,\frac{\partial u}{\partial r}\right) - \frac{u}{r^2}\right) ,$$

$$\left(\frac{u}{T}\right)\frac{\partial T}{\partial r} = q(r,\ 0) - \sigma(T^4 - 1) + K_1\left(\frac{1}{r}\frac{\partial}{\partial r}\left(r\,\frac{\partial T}{\partial r}\right)\right) ,$$

$$u = \frac{\partial T}{\partial r} = 0 \qquad \text{at } r = 0 ,$$

$$M_1\,\frac{\partial u}{\partial r} = \left(\frac{u}{T}\right)^2 (T - 1) + P , \qquad K_1\,\frac{\partial T}{\partial r} = \frac{u}{T}\,(T - 1)$$

$$\text{at } r = 1 . \qquad \text{(A.7)}$$

The standard finite-difference solution for this problem involves the solution of

$$\vec{F}(\vec{x}) = \vec{0} , \qquad \text{(A.8)}$$

where

$$\vec{x} \equiv \begin{bmatrix} \tilde{x}_1 \\ \tilde{x}_2 \\ \tilde{x}_3 \\ \tilde{x}_4 \\ \cdot \\ \cdot \\ \cdot \\ \tilde{x}_{2M-3} \\ \tilde{x}_{2M-2} \\ \tilde{x}_{2M-1} \\ \tilde{x}_{2M} \end{bmatrix} = \begin{bmatrix} u_{2,1} \\ T_{2,1} \\ u_{3,1} \\ T_{3,1} \\ \cdot \\ \cdot \\ \cdot \\ u_{M,1} \\ T_{M,1} \\ u_{M+1,1} \\ T_{M+1,1} \end{bmatrix} \qquad \text{(A.9)}$$

and the components of $\vec{F}$ are the finite difference equations obtained from the discretization of Eqs. (A.7). The Crank-Nicolson solution of Eqs. (A.1)--subject to Eqs. (A.2b) and (A.2d), and the solution of Eqs. (A.7) [with P(r, 0) given]--also involves the solution of Eq. (A.8) for successive j, j = 2, 3, 4, ..., N, N + 1. In that case, the components of $\vec{F}$ are slightly different from those for j = 1. For each fixed j(≥2), $\vec{x}$ is redefined [cf. Eq. (A.9)] as

$$\vec{x} \equiv \begin{bmatrix} \tilde{x}_1 \\ \tilde{x}_2 \\ \tilde{x}_3 \\ \tilde{x}_4 \\ \cdot \\ \cdot \\ \cdot \\ \tilde{x}_{2M-3} \\ \tilde{x}_{2M-2} \\ \tilde{x}_{2M-1} \\ \tilde{x}_{2M} \end{bmatrix} = \begin{bmatrix} u_{2,j} \\ T_{2,j} \\ u_{3,j} \\ T_{3,j} \\ \cdot \\ \cdot \\ \cdot \\ u_{M,j} \\ T_{M,j} \\ u_{M+1,j} \\ T_{M+1,j} \end{bmatrix} . \qquad (A.10)$$

The overall flow in subroutine MSWEEP is thus as outlined in Fig. A.4, Newton's method (see Fig. A.5) being used in all cases to solve the component equations of Eq. (A.8) because they are nonlinear.

To fully describe subroutine MSWEEP, we must define the following processes:

1. The specific finite-difference schemes used to reduce Eqs. (A.7) to Eq. (A.8) for j = 1 (y = 0), and Eqs. (A.1), (A.2b), and (A.2d) to Eq. (A.8) for j ≥ 2 (y > 0).
2. The corresponding specifications of J (as $\partial\vec{F}/\partial\vec{x}$; see Fig. A.5).
3. The specific Gaussian elimination scheme used to compute $\vec{\delta}$ (as $-J^{-1}\vec{F}$; see Fig. A.5).

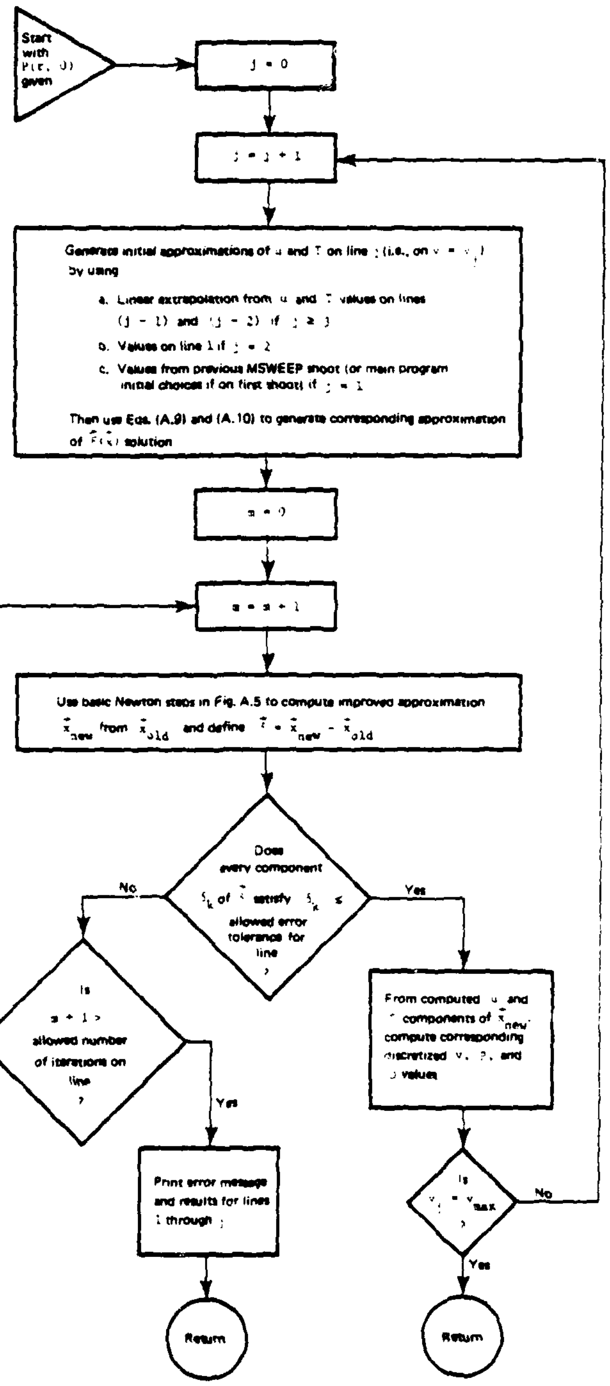

Fig. A.4--Flow chart of subroutine MSWEEP

AD-A125 400 ANALYSIS OF THE LARGE URBAN FIRE ENVIRONMENT PART II PARAMETRIC ANALYSIS A..(U) PACIFIC-SIERRA RESEARCH CORP LOS ANGELES CA D A LARSON ET AL. NOV 82 PSR-1210-PT-2 2/2

UNCLASSIFIED EMW-C-0747 F/G 15/6 NL

END
DATE
FILMED
4 83
DTIC

M-2

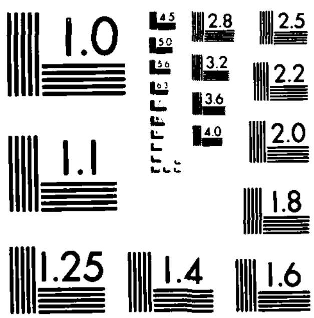

MICROCOPY RESOLUTION TEST CHART
NATIONAL BUREAU OF STANDARDS 1963 A

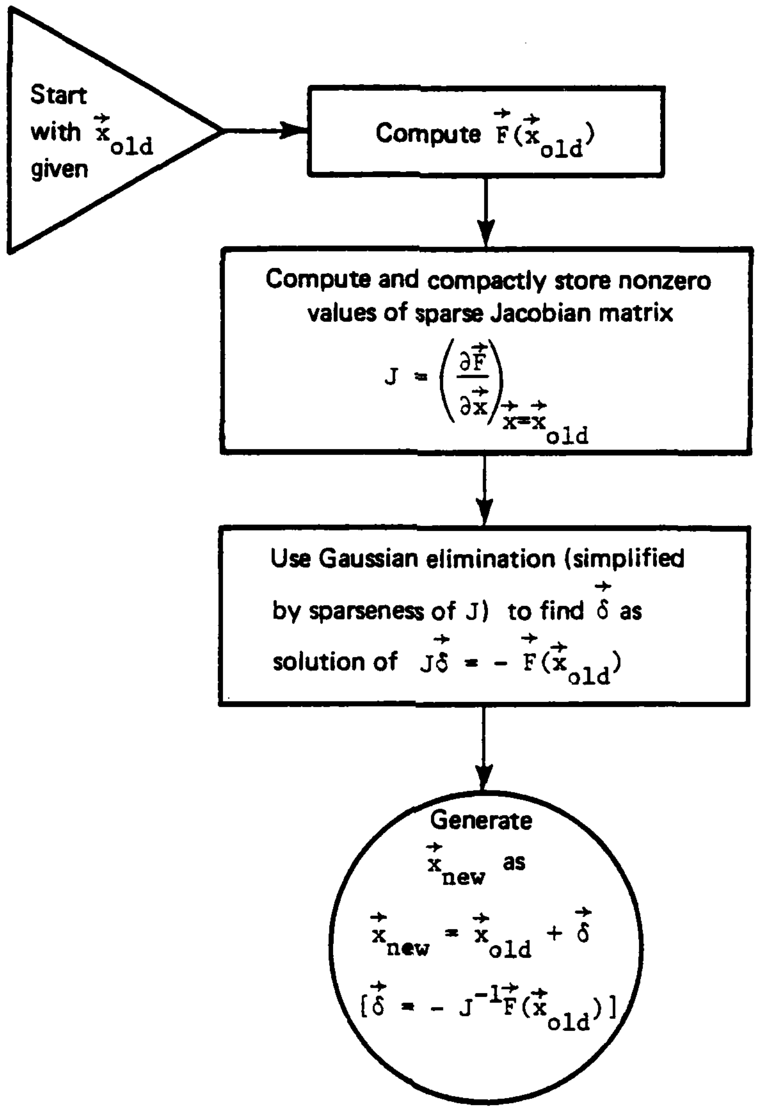

Fig. A.5--Flow chart of Newton steps used in subroutine MSWEEP

For j = 1, the usual discretization for second-order ordinary differential equations is used to reduce Eqs. (A.7) to Eq. (A.8). That is, for any dependent variable w, interior derivatives are replaced by the centered difference approximations

$$\left(\frac{\partial^2 w}{\partial r^2}\right)_{i,1} \to \frac{w_{i+1,1} - 2w_{i,1} + w_{i-1,1}}{(\Delta r)^2} ,$$

$$\left(\frac{\partial w}{\partial r}\right)_{i,1} \to \frac{w_{i+1,1} - w_{i-1,1}}{2\ \Delta r} . \qquad \text{(A.11)}$$

In addition, boundary derivatives are taken as, for example,

$$\left(\frac{\partial w}{\partial r}\right)_{1,1} \to \frac{w_{2,1} - w_{1,1}}{\Delta r} . \qquad \text{(A.12)}$$

Thus, as indicated by the corresponding discretization stencil at the bottom of Fig. A.3, no more than three values of u and T are involved in each component equation in Eq. (A.8) [see Eq. (A.9)]-- and those values are at successive r_i. For each j ≥ 2, the Crank-Nicolson scheme to be defined by Eqs. (A.13) and (A.14) is used to reduce Eqs. (A.1), (A.2b), and (A.2d) to Eq. (A.8). Centered differences are also used, with interior and boundary approximation stencils as shown in Fig. A.3, interior approximations being

$$\left(\frac{\partial^2 w}{\partial r^2}\right)_{i,j} \to \frac{1}{2}\left(\frac{w_{i+1,j} - 2w_{i,j} + w_{i-1,j}}{(\Delta r)^2} + \frac{w_{i+1,j-1} - 2w_{i,j-1} + w_{i-1,j-1}}{(\Delta r)^2}\right) ,$$

$$\left(\frac{\partial w}{\partial r}\right)_{i,j} \to \frac{1}{2}\left(\frac{w_{i+1,j} - w_{i-1,j}}{2\ \Delta r} + \frac{w_{i+1,j-1} - w_{i-1,j-1}}{2\ \Delta r}\right) ,$$

$$\left(\frac{\partial w}{\partial y}\right)_{i,j} \to \left(\frac{w_{i,j} - w_{i,j-1}}{\Delta y}\right) ,$$

$$(w)_{i,j} \to \frac{1}{2} (w_{i,j} + w_{i,j-1}) , \quad \text{(A.13)}$$

and the boundary formulas being of the form

$$\left(\frac{\partial w}{\partial r}\right)_{1,j} \to \frac{1}{2}\left(\frac{w_{2,j} - w_{1,j}}{\Delta r} + \frac{w_{2,j-1} - w_{1,j-1}}{\Delta r}\right) ,$$

$$(w)_{1,j} \to \frac{1}{2} (w_{1,j} + w_{1,j-1}) . \quad \text{(A.14)}$$

As in linear problems [Isaacson and Keller, 1966], the resulting nonlinear scheme has proven to be convergent, stable, and accurate in providing solutions to the turning-region boundary value problem.

In reducing either Eqs. (A.7) or Eqs. (A.1), (A.2b), and (A.2d) to Eq. (A.8) by means of Eqs. (A.11) through (A.14), it proves convenient--both notationally and computationally--to begin by decomposing $\vec{x}$ (for all j) into

$$\vec{u} = \begin{bmatrix} u_{2,j} \\ u_{3,j} \\ \vdots \\ u_{M,j} \\ u_{M+1,j} \end{bmatrix} \quad \text{and} \quad \vec{T} = \begin{bmatrix} T_{2,j} \\ T_{3,j} \\ \vdots \\ T_{M,j} \\ T_{M+1,j} \end{bmatrix} , \quad \text{(A.15)}$$

and arranging the corresponding $\vec{F}(\vec{x})$ as

$$\vec{F} = \begin{bmatrix} G_2 \\ H_2 \\ G_3 \\ H_3 \\ \cdot \\ \cdot \\ \cdot \\ G_M \\ H_M \\ G_{M+1} \\ H_{M+1} \end{bmatrix}, \tag{A.16}$$

where the G_i and H_i represent the components that arise primarily from the discretization of the horizontal momentum and energy equations, respectively, about the grid point (r_i, y_j). The specific forms of the G_i and H_i are derived shortly. As mentioned above (p. 82), centered differencing results in each G_i and H_i involving at most six of the 2M $u_{i,j}$ and $T_{i,j}$. The Jacobian matrix derivatives of

$$\vec{G}(\vec{u}, \vec{T}) = \begin{bmatrix} G_2 \\ G_3 \\ \cdot \\ \cdot \\ \cdot \\ G_M \\ G_{M+1} \end{bmatrix} \quad \text{and} \quad \vec{H}(\vec{u}, \vec{T}) = \begin{bmatrix} H_2 \\ H_3 \\ \cdot \\ \cdot \\ \cdot \\ H_M \\ H_{M+1} \end{bmatrix} \tag{A.17}$$

with respect to $\vec{u}$ and $\vec{T}$ thus have the following sparse, banded forms:

$$\frac{\partial \vec{G}}{\partial \vec{u}} = \begin{bmatrix} \alpha_{11} & \alpha_{12} & & & & & & 0 \\ \alpha_{20} & \alpha_{21} & \alpha_{22} & & & & & \\ & \alpha_{30} & \alpha_{31} & \alpha_{32} & & & & \\ & & \ddots & \ddots & \ddots & & & \\ & & & & \alpha_{M-2,0} & \alpha_{M-2,1} & \alpha_{M-2,2} & \\ & & & & & \alpha_{M-1,0} & \alpha_{M-1,1} & \alpha_{M-1,2} \\ 0 & & & & & & \alpha_{M,0} & \alpha_{M,1} \end{bmatrix},$$

(A.18a)

$$\frac{\partial \vec{G}}{\partial \vec{T}} = \begin{bmatrix} \beta_{11} & \beta_{12} & & & & & & 0 \\ \beta_{20} & \beta_{21} & \beta_{22} & & & & & \\ & \beta_{30} & \beta_{31} & \beta_{32} & & & & \\ & & \ddots & \ddots & \ddots & & & \\ & & & & \beta_{M-2,0} & \beta_{M-2,1} & \beta_{M-2,2} & \\ & & & & & \beta_{M-1,0} & \beta_{M-1,1} & \beta_{M-1,2} \\ 0 & & & & & & \beta_{M,0} & \beta_{M,1} \end{bmatrix},$$

(A.18b)

$$\frac{\partial \vec{H}}{\partial \vec{u}} = \begin{bmatrix} \gamma_{11} & \gamma_{12} & & & & & 0 \\ \gamma_{20} & \gamma_{21} & \gamma_{22} & & & & \\ & \gamma_{30} & \gamma_{31} & \gamma_{32} & & & \\ & & \ddots & \ddots & \ddots & & \\ & & & \gamma_{M-2,0} & \gamma_{M-2,1} & \gamma_{M-2,2} & \\ & & & & \gamma_{M-1,0} & \gamma_{M-1,1} & \gamma_{M-1,2} \\ 0 & & & & & \gamma_{M,0} & \gamma_{M,1} \end{bmatrix}, \tag{A.18c}$$

$$\frac{\partial \vec{H}}{\partial \vec{T}} = \begin{bmatrix} \delta_{11} & \delta_{12} & & & & & 0 \\ \delta_{20} & \delta_{21} & \delta_{22} & & & & \\ & \delta_{30} & \delta_{31} & \delta_{32} & & & \\ & & \ddots & \ddots & \ddots & & \\ & & & \delta_{M-2,0} & \delta_{M-2,1} & \delta_{M-2,2} & \\ & & & & \delta_{M-1,0} & \delta_{M-1,1} & \delta_{M-1,2} \\ 0 & & & & & \delta_{M,0} & \delta_{M,1} \end{bmatrix}. \tag{A.18d}$$

From Eqs. (A.10) and (A.15) through (A.18), the $J = \partial\vec{F}/\partial\vec{x}$ Jacobian is then easily computed from the nonzero elements in the Jacobians of Eqs. (A.18) as

$$
J = \begin{bmatrix}
\alpha_{11} & \beta_{11} & \alpha_{12} & \beta_{12} & & & & & & & & 0 \\
\gamma_{11} & \delta_{11} & \gamma_{12} & \delta_{12} & 0 & & & & & & & \\
\alpha_{20} & \beta_{20} & \alpha_{21} & \beta_{21} & \alpha_{22} & \beta_{22} & & & & & & \\
\gamma_{20} & \delta_{20} & \gamma_{21} & \delta_{21} & \gamma_{22} & \delta_{22} & 0 & & & & & \\
 & 0 & \alpha_{30} & \beta_{30} & \alpha_{31} & \beta_{31} & \alpha_{32} & \beta_{32} & & & & \\
 & & \gamma_{30} & \delta_{30} & \gamma_{31} & \delta_{31} & \gamma_{32} & \delta_{32} & 0 & & & \\
 & & & \ddots & \ddots & \ddots & \ddots & \ddots & \ddots & \ddots & & \\
 & & & & 0 & \alpha_{M-2,0} & \beta_{M-2,0} & \alpha_{M-2,1} & \beta_{M-2,1} & \alpha_{M-2,2} & \beta_{M-2,2} & \\
 & & & & & \gamma_{M-2,0} & \delta_{M-2,0} & \gamma_{M-2,1} & \delta_{M-2,1} & \gamma_{M-2,2} & \delta_{M-2,2} & 0 \\
 & & & & & & 0 & \alpha_{M-1,0} & \beta_{M-1,0} & \alpha_{M-1,1} & \beta_{M-1,1} & \alpha_{M-1,2} \;\; \beta_{M-1,2} \\
 & & & & & & & \gamma_{M-1,0} & \delta_{M-1,0} & \gamma_{M-1,1} & \delta_{M-1,1} & \gamma_{M-1,2} \;\; \delta_{M-1,2} \\
 & & & & & & & & 0 & \alpha_{M,0} & \beta_{M,0} & \alpha_{M,1} \;\; \beta_{M,1} \\
 0 & & & & & & & & & \gamma_{M,0} & \delta_{M,0} & \gamma_{M,1} \;\; \delta_{M,1}
\end{bmatrix}
\quad \text{(A.19)}
$$

DIFFERENCE EQUATIONS AND JACOBIAN ELEMENTS

Specific forms for $\vec{G}$ and $\vec{H}$, and hence for $\vec{F}$ and the various α, β, γ, and δ coefficients in Eqs. (A.18) and (A.19), are derived as follows. Subject to Eqs. (A.11), the first two lines of Eqs. (A.7) are approximated at $r = r_i$, $2 \le i \le M$, by

$$\frac{u_{i,1}}{T_{i,1}}\left(\frac{u_{i+1,1} - u_{i-1,1}}{2\ \Delta r}\right) = -\left(\frac{P_{i+1,1} - P_{i-1,1}}{2\ \Delta r}\right)$$

$$+ M_1\left(\frac{u_{i+1,1} - 2u_{i,1} + u_{i-1,1}}{(\Delta r)^2}\right.$$

$$\left.+ \frac{1}{r_i}\left(\frac{u_{i+1,1} - u_{i-1,1}}{2\ \Delta r}\right) - \frac{u_{i,1}}{r_i^2}\right) ,$$

$$\frac{u_{i,1}}{T_{i,1}}\left(\frac{T_{i+1,1} - T_{i-1,1}}{2\ \Delta r}\right) = q(r_i,\ 0) - \sigma(T_{i,1}^4 - 1)$$

$$+ K_1\left(\frac{T_{i+1,1} - 2T_{i,1} + T_{i-1,1}}{(\Delta r)^2}\right.$$

$$\left.+ \frac{1}{r_i}\left(\frac{T_{i+1,1} - T_{i-1,1}}{2\ \Delta r}\right)\right) . \qquad \text{(A.20)}$$

From Eqs. (A.2b), (A.2d), and (A.12), we then also have

$$u_{1,1} = 0 , \qquad T_{1,1} = T_{2,1} , \qquad \text{(A.21)}$$

and

$$M_1\left(\frac{u_{M+1,1} - u_{M,1}}{\Delta r}\right) = \left(\frac{u_{M+1,1}}{T_{M+1,1}}\right)^2 (T_{M+1,1} - 1) + P_{M+1,1} ,$$

$$K_1\left(\frac{T_{M+1,1} - T_{M,1}}{\Delta r}\right) = \frac{u_{M+1,1}}{T_{M+1,1}} (T_{M+1,1} - 1) . \qquad \text{(A.22)}$$

For $j = 1$, we thus have

$$G_2 = \frac{M_1}{\Delta r}(u_{3,1} - 2u_{2,1}) - \frac{1}{2}\left(\frac{u_{2,1}}{T_{2,1}} - \frac{M_1}{r_2}\right)u_{3,1} - \frac{1}{2}(P_{3,1} - P_{1,1})$$

$$- \left(\frac{M_1}{r_2^2}\right)u_{2,1}\,\Delta r ,$$

$$H_2 = \frac{K_1}{\Delta r}(T_{3,1} - T_{2,1}) - \frac{1}{2}\left(\frac{u_{2,1}}{T_{2,1}} - \frac{K_1}{r_2}\right)(T_{3,1} - T_{2,1})$$

$$+ \left(q(r_2, 0) - \sigma(T_{2,1}^4 - 1)\right)\Delta r ; \qquad (A.23)$$

$$G_i = \frac{M_1}{\Delta r}(u_{i+1,1} - 2u_{i,1} + u_{i-1,1}) - \frac{1}{2}\left(\frac{u_{i,1}}{T_{i,1}} - \frac{M_1}{r_i}\right)(u_{i+1,1} - u_{i-1,1})$$

$$- \frac{1}{2}(P_{i+1,1} - P_{i-1,1}) - M_1\left(\frac{u_{i,1}}{r_i}\right)\frac{\Delta r}{r_i} ,$$

$$H_i = \frac{K_1}{\Delta r}(T_{i+1,1} - 2T_{i,1} + T_{i-1,1}) - \frac{1}{2}\left(\frac{u_{i,1}}{T_{i,1}} - \frac{K_1}{r_i}\right)(T_{i+1,1} - T_{i-1,1})$$

$$+ \left(q(r_i, 0) - \sigma(T_{i,1}^4 - 1)\right)\Delta r \qquad (A.24)$$

for $3 \le i \le M$; and

$$G_{M+1} = \frac{M_1}{\Delta r}(u_{M+1,1} - u_{M,1}) - \left(\frac{u_{M+1,1}}{T_{M+1,1}}\right)^2 (T_{M+1,1} - 1) - P_{M+1,1} ,$$

$$H_{M+1} = \frac{K_1}{\Delta r}(T_{M+1,1} - T_{M,1}) - \frac{u_{M+1,1}}{T_{M+1,1}}(T_{M+1,1} - 1) \ . \quad \text{(A.25)}$$

From Eqs. (A.23) through (A.25), the Jacobian elements in Eqs. (A.18) and (A.19) are then found to be

$$\alpha_{11} = -3\left(\frac{M_1}{\Delta r}\right) - \frac{1}{2}\left(\frac{u_{3,1}}{T_{2,1}}\right) \ ,$$

$$\alpha_{12} = \frac{3}{2}\left(\frac{M_1}{\Delta r}\right) - \frac{1}{2}\left(\frac{u_{2,1}}{T_{2,1}}\right) \ ,$$

$$\beta_{11} = \frac{1}{2}\left(\frac{u_{2,1}u_{3,1}}{T_{2,1}^2}\right) \ ,$$

$$\beta_{12} = 0 \ ,$$

$$\gamma_{11} = -\frac{1}{2}\left(\frac{T_{3,1}}{T_{2,1}} - 1\right) \ ,$$

$$\gamma_{12} = 0 \ ,$$

$$\delta_{11} = -\frac{3}{2}\left(\frac{K_1}{\Delta r}\right) + \frac{1}{2}\left(\frac{u_{2,1}T_{3,1}}{T_{2,1}^2}\right) - 4\sigma T_{2,1}^3 \ (\Delta r) \ ,$$

$$\delta_{12} = \frac{3}{2}\left(\frac{K_1}{\Delta r}\right) - \frac{1}{2}\left(\frac{u_{2,1}}{T_{2,1}}\right) \ ; \quad \text{(A.26)}$$

$$\alpha_{i-1,0} = \frac{M_1}{\Delta r}\left(1 - \frac{\Delta r}{2r_i}\right) + \frac{1}{2}\left(\frac{u_{i,1}}{T_{i,1}}\right) ,$$

$$\alpha_{i-1,1} = -\frac{M_1}{\Delta r}\left(2 + \left(\frac{\Delta r}{r_i}\right)^2\right) - \frac{1}{2}\left(\frac{u_{i+1,1} - u_{i-1,1}}{T_{i,1}}\right) ,$$

$$\alpha_{i-1,2} = \frac{M_1}{\Delta r}\left(1 + \frac{\Delta r}{2r_i}\right) - \frac{1}{2}\left(\frac{u_{i,1}}{T_{i,1}}\right) ,$$

$$\beta_{i-1,0} = 0 ,$$

$$\beta_{i-1,1} = \frac{1}{2}\left(\frac{u_{i,1}}{T^2_{i,1}}\right)(u_{i+1,1} - u_{i-1,1}) ,$$

$$\beta_{i-1,2} = 0 ,$$

$$\gamma_{i-1,0} = 0 ,$$

$$\gamma_{i-1,1} = -\frac{1}{2}\left(\frac{T_{i+1,1} - T_{i-1,1}}{T_{i,1}}\right) ,$$

$$\gamma_{i-1,2} = 0 ,$$

$$\delta_{i-1,0} = \frac{K_1}{\Delta r}\left(1 - \frac{\Delta r}{2r_i}\right) + \frac{1}{2}\left(\frac{u_{i,1}}{T_{i,1}}\right) ,$$

$$\delta_{i-1,1} = -2\left(\frac{K_1}{\Delta r}\right) + \frac{1}{2}\left(\frac{u_{i,1}}{T^2_{i,1}}\right)(T_{i+1,1} - T_{i-1,1}) - 4\sigma T^3_{i,1}\,(\Delta r) ,$$

$$\delta_{i-1,2} = \frac{K_1}{\Delta r}\left(1 + \frac{\Delta r}{2r_i}\right) - \frac{1}{2}\left(\frac{u_{i,1}}{T_{i,1}}\right) \qquad \text{(A.27)}$$

for $3 \le i \le M$; and

$$\alpha_{M,0} = -\frac{M_1}{\Delta r} ,$$

$$\alpha_{M,1} = \frac{M_1}{\Delta r} - 2\left(\frac{u_{M+1,1}}{T_{M+1,1}}\right)\left(1 - \frac{1}{T_{M+1,1}}\right) ,$$

$$\beta_{M,0} = 0 ,$$

$$\beta_{M,1} = \left(\frac{u_{M+1,1}}{T_{M+1,1}}\right)^2\left(1 - \frac{2}{T_{M+1,1}}\right) ,$$

$$\gamma_{M,0} = -1 + \frac{1}{T_{M+1,1}} ,$$

$$\gamma_{M,1} = 0 ,$$

$$\delta_{M,0} = -\frac{K_1}{\Delta r} ,$$

$$\delta_{M,1} = \frac{K_1}{\Delta r} - \frac{u_{M+1,1}}{T^2_{M+1,1}} . \qquad \text{(A.28)}$$

For $j \ge 2$, the derivation of relevant forms for $\vec{G}$ and $\vec{H}$ begins with a preliminary rewriting of Eqs. (A.1) in the following equivalent form:

$$\frac{1}{r}\frac{\partial}{\partial r}(r\rho u) + \frac{\partial}{\partial y}(\rho v) = 0 ,$$

$$\frac{1}{r}\frac{\partial}{\partial r}(r\rho u^2) + \frac{\partial P}{\partial r} + \frac{\partial}{\partial y}(\rho uv) = M_1\left(\frac{\partial^2 u}{\partial r^2} + \frac{1}{r}\frac{\partial u}{\partial r} - \frac{u}{r^2}\right) ,$$

$$\frac{\partial P}{\partial y} + A\rho = 0 \ ,$$

$$\frac{1}{r}\frac{\partial}{\partial r}(ru) + \frac{\partial v}{\partial y} \equiv \frac{1}{r}\frac{\partial}{\partial r}(r\rho uT) + \frac{\partial}{\partial y}(\rho vT) = K_1\left(\frac{\partial^2 T}{\partial r^2} + \frac{1}{r}\frac{\partial T}{\partial r}\right)$$

$$+ \dot{q}(r, y) - \sigma(T^4 - 1) \ ,$$

$$\rho T = 1 \ . \qquad \text{(A.29)}$$

Subject to Eqs. (A.13), this set is approximated at each interior grid point (r_i, y_j), $2 \le i \le M$, of line j, $2 \le j \le N + 1$ by the finite difference system

$$\frac{1}{4\,\Delta r}\left\{\frac{r_{i+1}}{r_i}\left(\left(\frac{u}{T}\right)_{i+1,j} + \left(\frac{u}{T}\right)_{i+1,j-1}\right) - \frac{r_{i-1}}{r_i}\left(\left(\frac{u}{T}\right)_{i-1,j} + \left(\frac{u}{T}\right)_{i-1,j-1}\right)\right\}$$

$$+ \frac{1}{\Delta y}\left(\left(\frac{v}{T}\right)_{i,j} - \left(\frac{v}{T}\right)_{i,j-1}\right) = 0 \ , \qquad \text{(A.30a)}$$

$$\frac{1}{4\,\Delta r}\left\{\frac{r_{i+1}}{r_i}\left(\left(\frac{u^2}{T}\right)_{i+1,j} + \left(\frac{u^2}{T}\right)_{i+1,j-1}\right) - \frac{r_{i-1}}{r_i}\left(\left(\frac{u^2}{T}\right)_{i-1,j} + \left(\frac{u^2}{T}\right)_{i-1,j-1}\right)\right\}$$

$$+ \frac{1}{4\,\Delta r}\left(P_{i+1,j} + P_{i+1,j-1} - P_{i-1,j} - P_{i-1,j-1}\right)$$

$$+ \frac{1}{\Delta y}\left(\left(\frac{uv}{T}\right)_{i,j} - \left(\frac{uv}{T}\right)_{i,j-1}\right)$$

$$= M_1\left(\frac{u_{i+1,j} - 2u_{i,j} + u_{i-1,j} + u_{i+1,j-1} - 2u_{i,j-1} + u_{i-1,j-1}}{2(\Delta r)^2}\right.$$

$$+ \frac{1}{r_i}\left(\frac{u_{i+1,j} - u_{i-1,j} + u_{i+1,j-1} - u_{i-1,j-1}}{4\,\Delta r}\right)$$

$$\left. - \frac{u_{i,j} + u_{i,j-1}}{2r_i^2}\right) \ , \qquad \text{(A.30b)}$$

$$\frac{1}{\Delta y}\left(P_{i,j} - P_{i,j-1}\right) = -\frac{A}{2}\left(\left(\frac{1}{T}\right)_{i,j} + \left(\frac{1}{T}\right)_{i,j-1}\right) , \qquad \text{(A.30c)}$$

$$\frac{1}{4\,\Delta r}\left(\frac{r_{i+1}}{r_i}\left(u_{i+1,j} + u_{i+1,j-1}\right) - \frac{r_{i-1}}{r_i}\left(u_{i-1,j} + u_{i-1,j-1}\right)\right)$$

$$+ \frac{1}{\Delta y}\left(v_{i,j} - v_{i,j-1}\right)$$

$$= K_1\left(\frac{T_{i+1,j} - 2T_{i,j} + T_{i-1,j} + T_{i+1,j-1} - 2T_{i,j-1} + T_{i-1,j-1}}{2(\Delta r)^2}\right.$$

$$\left. + \frac{1}{r_i}\left(\frac{T_{i+1,j} - T_{i-1,j} + T_{i+1,j-1} - T_{i-1,j-1}}{4\,\Delta r}\right)\right)$$

$$+ \frac{1}{2}\left(q(r_i, y_j) + q(r_i, y_{j-1})\right) + \sigma\left(\left(\frac{T_{i,j} + T_{i,j-1}}{2}\right)^4 - 1\right) ,$$

(A.30d)

ρ having been eliminated for convenience. This system is simplified by solving Eqs. (A.30a) and (A.30c) for $v_{i,j}$ and $P_{i,j}$ in terms of the various u and T on line j and variables on line j - 1 as

$$v_{i,j} = \left(\frac{v}{T}\right)_{i,j-1} T_{i,j} - \frac{1}{4}\left(\frac{\Delta y}{\Delta r}\right)\left\{\frac{r_{i+1}}{r_i}\left(\left(\frac{u}{T}\right)_{i+1,j} + \left(\frac{u}{T}\right)_{i+1,j-1}\right)\right.$$

$$\left. - \frac{r_{i-1}}{r_i}\left(\left(\frac{u}{T}\right)_{i-1,j} + \left(\frac{u}{T}\right)_{i-1,j-1}\right)\right\} T_{i,j} ,$$

$$P_{i,j} = P_{i,j-1} - \frac{A}{2}\left(\left(\frac{1}{T}\right)_{i,j} + \left(\frac{1}{T}\right)_{i,j-1}\right)\Delta y , \qquad \text{(A.31)}$$

and substituting those results into Eqs. (A.30b) and (A.30d) to generate (for $2 \le i \le M$)

$$G_i \equiv \frac{M_1}{2\,\Delta r}\left(u_{i+1,j} - 2u_{i,j} + u_{i-1,j}\right) - \frac{1}{4}\left(\frac{r_{i+1}}{r_i}\left(\frac{u^2}{T}\right)_{i+1,j} - \frac{r_{i-1}}{r_i}\left(\frac{u^2}{T}\right)_{i-1,j}\right.$$

$$\left. - \frac{M_1}{r_i}\left(u_{i+1,j} - u_{i-1,j}\right) + 2\left(\frac{M_1}{r_i^2}\right)u_{i,j}\,(\Delta r) - A\,\frac{\Delta y}{2}\left(\frac{1}{T_{i+1,j}} - \frac{1}{T_{i-1,j}}\right)\right)$$

$$- \left(\frac{\Delta r}{\Delta y}\right)u_{i,j}\left\{\left(\frac{v}{T}\right)_{i,j-1} - \frac{\Delta y}{4\,\Delta r}\left(\frac{r_{i+1}}{r_i}\left(\frac{u}{T}\right)_{i+1,j} - \frac{r_{i-1}}{r_i}\left(\frac{u}{T}\right)_{i-1,j}\right.\right.$$

$$\left.\left. + \frac{r_{i+1}}{r_i}\left(\frac{u}{T}\right)_{i+1,j-1} - \frac{r_{i-1}}{r_i}\left(\frac{u}{T}\right)_{i-1,j-1}\right)\right\} + R_i = 0\ ,$$

$$H_i \equiv \frac{K_1}{2\,\Delta r}\left(T_{i+1,j} - 2T_{i,j} + T_{i-1,j}\right) - \frac{1}{4}\left(\left(\frac{r_{i+1}}{r_i}\right)u_{i+1,j} - \left(\frac{r_{i-1}}{r_i}\right)u_{i-1,j}\right.$$

$$\left. - \frac{K_1}{r_i}\left(T_{i+1,j} - T_{i-1,j}\right)\right) - \left(\frac{\Delta r}{\Delta y}\right)T_{i,j}\left\{\left(\frac{v}{T}\right)_{i,j-1} - \frac{\Delta y}{4\,\Delta r}\right.$$

$$\left. \times\left(\frac{r_{i+1}}{r_i}\left(\frac{u}{T}\right)_{i+1,j} - \frac{r_{i-1}}{r_i}\left(\frac{u}{T}\right)_{i-1,j} + \frac{r_{i+1}}{r_i}\left(\frac{u}{T}\right)_{i+1,j-1} - \frac{r_{i-1}}{r_i}\left(\frac{u}{T}\right)_{i-1,j-1}\right)\right\}$$

$$+ \sigma\left(\left(\frac{T_{i,j} + T_{i,j-1}}{2}\right)^4 - 1\right)\Delta r + \Pi_i = 0\ , \qquad \text{(A.32)}$$

where

$$R_i = \frac{M_1}{2\,\Delta r}(u_{i+1,j-1} - 2u_{i,j-1} + u_{i-1,j-1}) - \frac{1}{4}\left(\frac{r_{i+1}}{r_i}\left(\frac{u^2}{T}\right)_{i+1,j-1}\right.$$

$$- \frac{r_{i-1}}{r_i}\left(\frac{u^2}{T}\right)_{i-1,j-1} - \frac{M_1}{r_i}(u_{i+1,j-1} - u_{i-1,j-1}) + 2\left(\frac{M_1}{r_i^2}\right)u_{i,j-1}\,\Delta r$$

$$\left. + 2(P_{i+1,j-1} - P_{i-1,j-1}) - A\frac{\Delta y}{2}\left(\frac{1}{T_{i+1,j-1}} - \frac{1}{T_{i-1,j-1}}\right)\right)$$

$$+ \frac{\Delta r}{\Delta y}\left(\frac{uv}{T}\right)_{i,j-1},$$

$$\Pi_i = \frac{K_1}{2\,\Delta r}(T_{i+1,j-1} - 2T_{i,j-1} + T_{i-1,j-1}) - \frac{1}{4}\left(\left(\frac{r_{i+1}}{r_i}\right)u_{i+1,j-1}\right.$$

$$\left. - \left(\frac{r_{i-1}}{r_i}\right)u_{i-1,j-1} - \frac{K_1}{r_i}(T_{i+1,j-1} - T_{i-1,j-1})\right) + \frac{\Delta r}{\Delta y}v_{i,j-1}$$

$$+ \frac{1}{2}\left(q(r_i, y_j) + q(r_i, y_{j-1})\right)\Delta r\,. \tag{A.33}$$

As outlined in Fig. A.4, a recursive Crank-Nicolson scheme is employed in subroutine MSWEEP to generate a numerical solution to Eqs. (A.1), (A.2a), (A.2b), and (A.2d), subject to a given $P(r, 0)$. For $j = 2, 3, \ldots, N + 1$, the solution on line j is found using solution data on line $j - 1$, the solution for $j = 1$ being used to start the recursion. For each $j \geq 2$, the relevant forms of G_i and H_i (as components of $\vec{F}$), $2 \leq i \leq M$, are therefore exactly those in Eqs. (A.32) [cf. Eqs. (A.24)], variables with $j - 1$ suffices being known. From Eqs. (A.2b), (A.2d), and (A.14), we also have

$$u_{1,j} = 0 \ , \qquad T_{1,j} = T_{2,j} \ , \tag{A.34}$$

and

$$M_1 \left(\frac{u_{M+1,j} - u_{M,j} + u_{M+1,j-1} - u_{M,j-1}}{2\ \Delta r} \right) = \left(\frac{u_{M+1,j} + u_{M+1,j-1}}{T_{M+1,j} + T_{M+1,j-1}} \right)^2$$

$$\times \left(\frac{T_{M+1,j} + T_{M+1,j-1} - 2}{2} \right)$$

$$+ \left(\frac{P_{M+1,j} + P_{M+1,j-1}}{2} \right.$$

$$\left. + \frac{A}{2} (y_j + y_{j-1}) \right) \ ,$$

$$K_1 \left(\frac{T_{M+1,j} - T_{M,j} + T_{M+1,j-1} - T_{M,j-1}}{2\ \Delta r} \right) = \left(\frac{u_{M+1,j} + u_{M+1,j-1}}{T_{M+1,j} + T_{M+1,j-1}} \right)$$

$$\times \left(\frac{T_{M+1,j} + T_{M+1,j-1} - 2}{2} \right) \ .$$

(A.35)

Therefore, for $j \geq 2$,

$$G_{M+1} = \frac{M_1}{2\ \Delta r} (u_{M+1,j} - u_{M,j} + u_{M+1,j-1} - u_{M,j-1}) - E_j^2 \left(\frac{T_{M+1,j} + T_{M+1,j-1} - 2}{2} \right)$$

$$- P_{M+1,j-1} + \frac{A}{4} \left(\frac{1}{T_{M+1,j}} + \frac{1}{T_{M+1,j-1}} \right) \Delta y - \frac{A}{2} (y_j + y_{j-1}) \ ,$$

$$H_{M+1} = \frac{K_1}{2\ \Delta r} (T_{M+1,j} - T_{M,j} + T_{M+1,j-1} - T_{M,j-1})$$

$$- E_j \left(\frac{T_{M+1,j} + T_{M+1,j-1} - 2}{2} \right) \ , \tag{A.36}$$

where

$$E_j = \frac{u_{M+1,j} + u_{M+1,j-1}}{T_{M+1,j} + T_{M+1,j-1}} . \qquad (A.37)$$

From Eqs. (A.32), (A.34), and (A.36), the Jacobian elements in Eqs. (A.18) and (A.19) are then as follows for each $j \geq 2$:

$$\alpha_{11} = -\frac{3}{2}\left(\frac{M_1}{\Delta r}\right) - \left\{\frac{\Delta r}{\Delta y}\left(\frac{v}{T}\right)_{2,j-1} - \frac{2}{4}\left(\left(\frac{u}{T}\right)_{3,j} + \left(\frac{u}{T}\right)_{3,j-1}\right)\right\} ,$$

$$\alpha_{12} = \frac{3}{4}\left(\frac{M_1}{\Delta r}\right) - \frac{2}{4}\left(2\left(\frac{u}{T}\right)_{3,j} - \frac{u_{2,j}}{T_{3,j}}\right) ,$$

$$\beta_{11} = \frac{1}{4}\left(A\left(\frac{\Delta y}{2}\right)\left(\frac{1}{T_{2,j}}\right)^2\right) ,$$

$$\beta_{12} = \frac{1}{4}\left(2\left(\frac{u}{T}\right)^2_{3,j} - A\left(\frac{\Delta y}{2}\right)\left(\frac{1}{T_{3,j}}\right)^2 - 2u_{2,j}\left(\frac{u}{T^2}\right)_{3,j}\right) ,$$

$$\gamma_{11} = 0 ,$$

$$\gamma_{12} = -\frac{2}{4}\left(1 - \frac{T_{2,j}}{T_{3,j}}\right) ,$$

$$\delta_{11} = -\frac{3}{4}\left(\frac{K_1}{\Delta r}\right) - \left\{\frac{\Delta r}{\Delta y}\left(\frac{v}{T}\right)_{2,j-1} - \frac{2}{4}\left(\left(\frac{u}{T}\right)_{3,j} + \left(\frac{u}{T}\right)_{3,j-1}\right)\right\}$$

$$+ 2\sigma\left(\frac{T_{2,j} + T_{2,j-1}}{2}\right)^3 \Delta r ,$$

$$\delta_{12} = \frac{3}{4}\left(\frac{K_1}{\Delta r}\right) - \frac{2}{4}\left(T_{2,j}\left(\frac{u}{T^2}\right)_{3,j}\right) ; \qquad (A.38)$$

$$\alpha_{i-1,0} = \frac{M_1}{2\,\Delta r}\left(1 - \frac{\Delta r}{2r_i}\right) + \frac{1}{4}\left(\frac{r_{i-1}}{r_i}\right)\left(2\left(\frac{u}{T}\right)_{i-1,j} - \frac{u_{i,j}}{T_{i-1,j}}\right) ,$$

$$\alpha_{i-1,1} = -\frac{M_1}{2\,\Delta r}\left(2 + \left(\frac{\Delta r}{r_i}\right)^2\right) - \Bigg\{\frac{\Delta r}{\Delta y}\left(\frac{v}{T}\right)_{i,j-1}$$

$$- \frac{1}{4}\left(\frac{r_{i+1}}{r_i}\right)\left(\left(\frac{u}{T}\right)_{i+1,j} + \left(\frac{u}{T}\right)_{i+1,j-1}\right)$$

$$+ \frac{1}{4}\left(\frac{r_{i-1}}{r_i}\right)\left(\left(\frac{u}{T}\right)_{i-1,j} + \left(\frac{u}{T}\right)_{i-1,j-1}\right)\Bigg\} ,$$

$$\alpha_{i-1,2} = \frac{M_1}{2\,\Delta r}\left(1 + \frac{\Delta r}{2r_i}\right) - \frac{1}{4}\left(\frac{r_{i+1}}{r_i}\right)\left(2\left(\frac{u}{T}\right)_{i+1,j} - \frac{u_{i,j}}{T_{i+1,j}}\right) ,$$

$$\beta_{i-1,0} = -\frac{1}{4}\left(\frac{r_{i-1}}{r_i}\left(\frac{u}{T}\right)^2_{i-1,j} - A\left(\frac{\Delta y}{2}\right)\left(\frac{1}{T_{i-1,j}}\right)^2\right.$$

$$\left. - \frac{r_{i-1}}{r_i}\,u_{i,j}\left(\frac{u}{T^2}\right)_{i-1,j}\right) ,$$

$$\beta_{i-1,1} = 0 ,$$

$$\beta_{i-1,2} = \frac{1}{4}\left(\frac{r_{i+1}}{r_i}\left(\frac{u}{T}\right)^2_{i+1,j} - A\left(\frac{\Delta y}{2}\right)\left(\frac{1}{T_{i+1,j}}\right)^2\right.$$

$$\left. - \frac{r_{i+1}}{r_i}\,u_{i,j}\left(\frac{u}{T^2}\right)_{i+1,j}\right) ,$$

$$\gamma_{i-1,0} = \frac{1}{4}\left(\frac{r_{i-1}}{r_i}\right)\left(1 - \frac{T_{i,j}}{T_{i-1,j}}\right) ,$$

$$\gamma_{i-1,1} = 0 ,$$

$$\gamma_{i-1,2} = -\frac{1}{4}\left(\frac{r_{i+1}}{r_i}\right)\left(1 - \frac{T_{i,j}}{T_{i+1,j}}\right) ,$$

$$\delta_{i-1,0} = \frac{K_1}{2\,\Delta r}\left(1 - \frac{\Delta r}{2r_i}\right) + \frac{1}{4}\left(\frac{r_{i-1}}{r_i}\right)\left(T_{i,j}\left(\frac{u}{T^2}\right)_{i-1,j}\right) ,$$

$$\delta_{i-1,1} = -2\left(\frac{K_1}{2\,\Delta r}\right) - \left\{\frac{\Delta r}{\Delta y}\left(\frac{v}{T}\right)_{i,j-1} - \frac{1}{4}\left(\frac{r_{i+1}}{r_i}\right)\left(\left(\frac{u}{T}\right)_{i+1,j} + \left(\frac{u}{T}\right)_{i+1,j-1}\right)\right.$$

$$\left. + \frac{1}{4}\left(\frac{r_{i-1}}{r_i}\right)\left(\left(\frac{u}{T}\right)_{i-1,j} + \left(\frac{u}{T}\right)_{i-1,j-1}\right)\right\} + 2\sigma\left(\frac{T_{i,j} + T_{i,j-1}}{2}\right)^3 \Delta r ,$$

$$\delta_{i-1,2} = \frac{K_1}{2\,\Delta r}\left(1 + \frac{\Delta r}{2r_i}\right) - \frac{1}{4}\left(\frac{r_{i+1}}{r_i}\right)\left(T_{i,j}\left(\frac{u}{T^2}\right)_{i+1,j}\right) \qquad \text{(A.39)}$$

for $3 \le i \le M$; and

$$\alpha_{M,0} = -\frac{M_1}{2\,\Delta r} ,$$

$$\alpha_{M,1} = \frac{M_1}{2\,\Delta r} - 2E_j\left(\frac{1}{2} - \frac{1}{T_{M+1,j} + T_{M+1,j-1}}\right) ,$$

$$\beta_{M,0} = 0 ,$$

$$\beta_{M,1} = E_j^2\left(\frac{1}{2} - \frac{2}{T_{M+1,j} + T_{M+1,j-1}}\right) - \frac{A}{4}\left(\frac{1}{T^2_{M+1,j}}\right)\Delta y .$$

$$\gamma_{M,0} = 0 ,$$

$$\gamma_{M,1} = -\frac{1}{2} + \frac{1}{T_{M+1,j} + T_{M+1,j-1}} ,$$

$$\delta_{M,0} = -\frac{K_1}{2\,\Delta r} ,$$

$$\delta_{M,1} = \frac{K_1}{2\,\Delta r} - \frac{E_j}{T_{M+1,j} + T_{M+1,j-1}} . \qquad (A.40)$$

The detailed specification of $\vec{G}$, $\vec{H}$, and J (= $\partial\vec{F}/\partial\vec{x}$) is now complete for all cases. The equation $J\vec{\delta} = -\vec{F}$ is solved for $\vec{\delta}$ using Gaussian elimination [Isaacson and Keller, 1966]. For efficiency, standard sparse-matrix methods are employed: only nonzero elements of J [see Eq. (A.19)] are stored, and operations involving zero elements are automatically omitted.

PROGRAM LISTING

FORTRAN listings of all parts of the computer code are now presented. Table A.2 lists the main program, and Tables A.3, A.4, and A.5 list the subroutines BCFUNC, SPRINT, and MSWEEP, respectively.

Table A.2

LISTING OF MAIN PROGRAM

```
FORTRAN-VIID V0R-00                                                    09/30/82  11:04:00  PAGE  17

FORTRAN VIID: LICENSED RESTRICTED RIGHTS AS STATED IN LICENSE L-0450     ***, SEE DOCUMENTATION PACKAGE, 00-101999.

                $BATCH
                C
                C
     000000T          PROGRAM [illegible]
                C
                C
     000006T          COMMON [illegible](401,500),[illegible](41,500),[illegible],[illegible](401,500),
                    1       X(41),Y(500),
                    2       [illegible]
                    3       DX,DP,DX,DY,[illegible]
                    4       [illegible],[illegible],[illegible]
                    5       [illegible]
                    6       ALPHA,BETA,[illegible]
                    7       [illegible],ITTY,[illegible]
                C
                C
                C     READ AND WRITE THE INPUTS
                C
                C
     000006T          ITTY=1
     00000AT          [illegible]=2

     000016T          READ (ITTY,1)  [illegible]
     000040T          READ (ITTY,3)  [illegible]
     00006CT          READ (ITTY,2)  [illegible]
     000098T          READ (ITTY,1)  [illegible]
     0000C4T     1    FORMAT (3F10.0)
     0000D2T     2    FORMAT (2F10.0, 2I10)
     0000E4T     3    FORMAT (F10.0, 2I10,F10.0)
     0000F6T     4    FORMAT (3F10.0, I10)

     000106T          [illegible]
     00012AT          [illegible]

     000136T          WRITE(IPRINT,10)
     00015CT    10    FORMAT (//// [illegible]
                    1  'BOUNDARY VALUE PROBLEM' ////)
     00018AT          WRITE(IPRINT,12)[illegible]
     0001CCT    12    FORMAT('  SYSTEM PARAMETERS: [illegible]
                    1  [illegible] =' F8.3 [illegible] =' F [illegible]
     000216T          WRITE(IPRINT,14)[illegible]
     000240T    14    FORMAT(/ '  MESH: [illegible] =' I5 [illegible] =' F8.4 [illegible] =' I5
                    1          '   DY =' F8.5)
     00027AT          WRITE(IPRINT,16)[illegible]
     0002A4T    16    FORMAT(/ '  [illegible]
                    1          '  [illegible] =' I [illegible] =' F [illegible] =' I5)
     000302T          WRITE (IPRINT,18)  [illegible]
     00032AT    18    FORMAT (/ '  [illegible]  [illegible] =' F [illegible] =' 
                    1  F8.5 '  [illegible] =' F8.4)
                C
                C
                C     INITIALIZATION
                C
                C
     0003ACT          [illegible]
     0003B0T          [illegible]
     0003D2T          [illegible]
```

Table A.2--Continued

```
FORTRAN-VIIO R04-00                                                          09/20/82  11:09:06  PAGE   27

FORTRAN VIID: LICENSED RESTRICTED RIGHTS AS STATED IN LICENSE L-0336        ***, SEE DOCUMENTATION PACKAGE, 04-101399.

 0003A0I           NP=N+1

 0003A1I           X(1)=0.0
 0003BAI           Y(1)=0.0
 0003C6I           DO 30 I=2,N
 0003D4I           X(I)=DX*(FLOAT(I)-1.)
 00040AI   30      CONTINUE
 000422I           DO 32 I=2,N
 00043E6I          II=I-1
 00044AI           CMULT=1.0
 00045AI           IF(I.GE.262) CMULT=2.0
 00046CI           IF(I.GE.362) CMULT=4.0
 00048AI           IF(J.GE.352) CMULT=[illegible]
 0004AAI           IF(J.GE.402) CMULT=16.0
 0004C0I           Y(I)=Y(II)+CMULT*DY
 0004EAI   32      CONTINUE
           C       DO 33 I=4,7,N
           C       II=I-1
           C       Y(I)=Y(II)+1.0
           CC      CONTINUE
 00050AI           Y(MP)=1.0
 00051AI           Y(MP)=YMAX

 000528I           DO 35 I=1,MP
 00053CI           V(1,I)=0.0
 00055AI   35      CONTINUE

 00056AI           DO 40 I=1,NP
 00057CI           U(1,I)=0.0
 000596I   40      CONTINUE
           C
           C       MAKE INITIAL GUESSES ALONG X = 0.
           C
 0005AEI           IZERO=0
 0005B6I           KK=1
 0005BEI           CALL GCHECK(KK,IZERO,IZERO)
 0005DCI           KOUT = 1
           C
           C
           C
           C       OVERALL ITERATION: MARCH FROM X=0. TO
           C                          X=XMAX, ALTERNATELY SOLVING
           C                          SOLN. ON Y=Y(I+1) FROM SOLN.
           C                          ON Y=Y(I), AND REPEATING UNTIL
           C                          EVEN ON Y=YMAX
           C
           C


 0005F4I           NUM=0
 0005FCI   50      CONTINUE
 0005FCI           NUM=NUM+1
 0005FAI           IF(NUM.GE.MAXITER) GO TO 950


 000612I           CALL SPVIS(1)
 00063AI           CALL ASLEEP
```

Table A.2--Continued

```
FORTRAN-VIID R04-06                                                    09/20/82  11:04:06  PAGE  37
FORTRAN VIID: LICENSED RESTRICTED RIGHTS AS STATED IN LICENSE L-0356      ***, SEE DOCUMENTATION PACKAGE, 08-101-98,

0006381           CALL SP[illegible](NP)

00065[illegible]           IF (KOUNT .EQ. 1) GO TO 900
          C
          C        OVERALL CONVERGENCE CHECK
          C        [illegible] MODIFICATION
          C
00066[illegible]           P(NS)=AAY IAX
000680[illegible]           DO 110 I=1,N
00069[illegible]           IP=I+1
0006A2[illegible]           IF(ABS(PMAX-P(I), [illegible]) [illegible] GO TO 115
0006F2[illegible]   110    CONTINUE
0007041           IF(ABS(PMAX-P(N), [illegible]) [illegible] GO TO 115
00075A1           GO TO 900

00076[illegible]   115    CONTINUE
00076[illegible]           P(NS)=AAY IAY
00077A1           DO 120 I=1,N
00078E1           P(I,1)=P(I,1)*[illegible]
00070[illegible]   120    CONTINUE
00077[illegible]           GO TO 53
          C
          C
          C        STANDARD PRINTOUT
          C
          C
0007FC1   900    CONTINUE
0007FC1           WRITE(IPRINT,895) [illegible]
00080C1   895    FORMAT(///,I6)

00081A1           DO 898 J=2,NP
00082E1           DO 897 I=1,NP
000[illegible]           P(I,J)=P(I,J)+AAY(I)
000[illegible]   897    CONTINUE
000[illegible]   898    CONTINUE

000[illegible]           DO 920 I=1,NP
000[illegible]           IF(Y(I).LT.2.E) GOTO [illegible]
000[illegible]           DO 905 INDEX=3,100
000[illegible]           FINDEX=FLOAT(INDEX)
0009121           IF(ABS(Y(I)-FINDEX).LT.0.001) GO TO 915
000[illegible]   905    CONTINUE
000[illegible]           GO TO 920
000[illegible]   915    CALL SPRINT(I)
000[illegible]   920    CONTINUE
000[illegible]           GO TO 980
          C
          C
          C        ERROR PRINTOUT
          C
          C
000[illegible]   950    CONTINUE
000[illegible]           WRITE(IPRINT,960) MAXITR
000[illegible]   960    FORMAT(////,' NO CONVERGENCE IN ',I6,' [illegible]
                 1                [illegible],////)

000[illegible]           CALL SPRINT(I)
```

Table A.2--Continued

```
FORTRAN-VIIO [illegible]                                              [illegible]  PAGE  [illegible]

FORTRAN VIIO: [illegible]                               [illegible] PACKAGE, [illegible]

      000A[illegible]           CALL [illegible]
                     C          STOP 1
      000A5[illegible]  [illegible]  CONTINUE

                     CC         DO [illegible] J=2, [illegible]
                     CC         DO 995 I=1, [illegible]
                     CC         P(I,J)=P(I,J)+[illegible](I)
                     CC         CONTINUE
                     CC         CONTINUE

      000A5[illegible]          WRITE (6)  (P(I,J), I = 1, [illegible])
      000A[illegible]           WRITE (6)  ([illegible](I,J), I = 1, [illegible])
      000A[illegible]           WRITE (6)  (P(I,J), I = 1, [illegible])
      000[illegible]            WRITE (2)  A, SIG A, [illegible], [illegible], [illegible], [illegible], [illegible], [illegible], [illegible]
      000[illegible]            WRITE (2)  [illegible], [illegible], [illegible], [illegible], [illegible], [illegible]SS
      000[illegible]            DO 990  I = 1, [illegible]
      000[illegible]            WRITE (2)  [illegible](I,J), I = 1, [illegible]
      000[illegible]     990    CONTINUE
      000[illegible]            DO 991  I = 1, [illegible]
      000[illegible]            WRITE (2)  ([illegible](I,J), I = 1, [illegible])
      000[illegible]     991    CONTINUE
      000[illegible]            WRITE (9)  A, SIG A, [illegible], [illegible], [illegible], [illegible], [illegible], [illegible], [illegible]
      000[illegible]            WRITE (9)  [illegible], [illegible], [illegible], [illegible], [illegible], [illegible]SS
      000[illegible]            DO 99[illegible]  I = 1, [illegible]
      000[illegible]            WRITE (9)  ([illegible](I,J), I = 1, [illegible])
      000[illegible]     99[illegible]   CONTINUE
      000[illegible]            DO 993  I = 1, [illegible]
      000[illegible]            WRITE (9)  ([illegible](I,J), I = 1, [illegible])
      000[illegible]     99[illegible]   CONTINUE
                     C          WRITE (7)  A, SIG A, [illegible], [illegible], [illegible], [illegible], [illegible], [illegible], [illegible]
                     C          WRITE (7)  [illegible], [illegible], [illegible], [illegible], [illegible], [illegible]SS
                     C          DO 900  I = 1, [illegible]
                     C          WRITE (7)  ([illegible](I,J), I = 1, [illegible])
                     C900       CONTINUE
      000[illegible]            STOP
      000[illegible]            END

NO  ERRORS[illegible]  [illegible]  [illegible]  [illegible]  [illegible]  [illegible]  [illegible]
STATEMENT BUFFER: [illegible]  [illegible]
SINGLE PRECISION FLOATING [illegible]
```

Table A.3

LISTING OF SUBROUTINE BCFUNC

```
FORTRAN-VIIO [illegible]                                                   [illegible]  PAGE  17

FORTRAN VIIO: LICENSED RESTRICTED [illegible]                              [illegible]

0000001          SUBROUTINE BCFU (IKEY,II,III)


0000041          COMMON  [illegible]
                1       [illegible]
                2       A,SIGMA,[illegible]
                3       [illegible]
                4       [illegible]
                5       [illegible]
                6       ALPHA,[illegible]
                7       [illegible]


0000041          [illegible]
0000101          IF(Y(II).GT.0.A) [illegible]
0000541          IF(Y(II).[illegible]
          C       IF(Y(II).LE.0.5) [illegible]
          C        [illegible]
          C        IF(Y(II).EQ.[illegible]
          C        IF(Y(II).EQ.[illegible]
          C        IF(Y(II).EQ.[illegible]
          C        IF(Y(II).EQ.[illegible]
          C        IF(Y(II).EQ.[illegible]
          C        [illegible]
          C        IF(Y(II).GE.0.AND.Y(II).[illegible]
          C        IF(Y(II).GE.1.) [illegible]
          C        IF(Y(II).GE..25.AND.Y(II).[illegible]
          C        IF(Y(II).GE..50.AND.Y(II).[illegible]
          C        [illegible]

0000091          GO TO (100, 200, 300, 400, 500) [illegible]
          C
          C
          C       INITIAL GUESSES FOR [illegible]
          C
          C
0000CA1   100    GO TO (125, 150, 175) [illegible]

0000E21   125    DO 126  I = 1, [illegible]
0001001          READ (IITY, 127) [illegible]
0001491   126    CONTINUE
0001AC1   127    FORMAT (3E10.0)
0001DA1          GO TO 900

          C150   CONTINUE
          C      DO 160  I = 1, [illegible]
          C      READ (IITY,161) [illegible]
          C160   CONTINUE
          C161   FORMAT (E10.0)

0001C01   150    CONTINUE
0001C91          DO 149  I = 1, [illegible]
0001D41          IF ([illegible]
0001E51          [illegible] = 1.43-0.5*X(I)
000222I          CC = 1.[illegible]
00022FI          CIC=1.0
00023AI          EP = EXP(CC*X(I))
```

Table A.3--Continued

```
FORTRAN-VIID R04-00                                              09/20/82  11:04:06  PAGE  27      6

FORTRAN VIID: LICENSED RESTRICTED RIGHTS AS STATED IN LICENSE L-0336       ***, SEE DOCUMENTATION PACKAGE, 04-101M99.

 000272I         EM = EXP(-CC*X(I))
 0002A2I         U(I,1) = -CCC*(EP-EM)/(EP+EM)


 0002E8I         FSIG=UO*0.25/SIGMA
 000300I         XNU=0.5

 00030CI         U(I,1)=-A*FSIG*X(I)/XNU
 000342I         T(I,1)=1.0+FSIG
 00035CI         P(I,1)=-A*FSIG*(1.0+BETA*UO*(1.0-X(I)**2))

 0003BEI          BBETAA=A/(8.*SIGMA)
 0003D8I         U(I,1)=-BBETAA*X(I)
 000402I         T(I,1)=1.10
 000416I          BBLOSS=A/(40.*SIGMA)
 000430I         P(I,1)=-BBLOSS

 00044AI    180  CONTINUE
 000462I         GO TO 900

 000468I    175  CONTINUE
 000468I         READ (4)  (U(I,1), I = 1, MP)
 0004E4I         READ (4)  (T(I,1), I = 1, MP)
 0005A0I         READ (4)  (P(I,1), I = 1, MP)
 0005DCI         DO 177 I=1,MP
 0005F0I         P(I,1)=P(I,1)-BLOSS
 000612I    177  CONTINUE
 00062AI         GO TO 900

            C
            C
            C    Q(X,Y) PRESCRIPTION - CAN BE CHANGED
            C
            C
 000630I    200  CONTINUE
 000630I         IF(JJ.EQ.1)TAVG=T(II,JJ)
 00066OI         JJM=JJ-1
 00066EI         IF(JJ.GE.2)TAVG=0.5*(T(II,JJ)+T(II,JJM))

 0006BEI         QVAL=QO-SIGMA*(TAVG**4-1.0)

 0006F6I         IF(Y(JJ).GT.1.0) QVAL=QVAL-QO
            C
            C
            C    NU(X,Y) PRESCRIPTION - CAN BE CHANGED
            C
            C
 000712I    300  CONTINUE
 000712I         XNU = XNUIN
 00071EI         CNU=0.0
 00072AI         XNU=XNU*EXP(-CNU*X(II))
 000770I         IF(X(II).GT.1.0)XNU=0.0
 000796I         GO TO 900
            C
            C
            C    K(X,Y) PRESCRIPTION - CAN BE CHANGED
            C
```

Table A.3--Continued

```
FORTRAN-VIID R04-00                                                      09/20/82  11:04:00   PAGE  57

FORTRAN VIID: LICENSED RESTRICTED RIGHTS AS STATED IN LICENSE L-0356        ***, SEE DOCUMENTATION PACKAGE, 04-101099.

                    C
0007 9C1     400    CONTINUE
0007 9C1            YK = AKIN
0007 AB1            CK=0.0
0007 B81            YK=YK*EXP(-(K*Y(II))
0007 FA1            IF(Y(II).GT.1.0)YK=0.0
0008 1E1            CK2=ALOSS
0008 2A1            IF(Y(II).GT.1.0) YK=ALOSS*(2.0-Y(II))*(CK-ALOSS)
0008 721            IF(Y(II).GT.2.0) YK=ALOSS
0008 F91            YK=YKIN
0009 AA1            GO TO 900
                    C
                    C       OPTIME COMPUTATION - CALL [illegible]
                    C
0008 AA1     500    CONTINUE
0008 AA1            IF(II.EQ.1)TAVG=T(II,II)
0008 DA1            IJ=IJ-1
0008 FA1            IF(IJ.GE.2)TAVG=(T(IJ,II)+T(IJ,II))/2.

0009 3A1            OPTIME=A.*SIGMA*(TAVG**3)

0009 621     900    CONTINUE
0009 621            RETURN
0009 681            END

NO ERRORS:F7D  R04-00     SUBROUTINE  [illegible]    09/20/82  11:04:00  TABLE SPACE:  4 KB
STATEMENT BUFFER:  20 LINES/1321 BYTES     STACK SPACE: [illegible]
SINGLE PRECISION FLOATING PT SUPPORT REQUIRED FOR EXECUTION.
```

Table A.4

LISTING OF SUBROUTINE SPRINT

```
FORTRAN-VIID R04-00                                                        09/20/82  11:04:06  PAGE  17     A
FORTRAN VIID: LICENSED RESTRICTED RIGHTS AS STATED IN LICENSE L-0336      ***, SEE DOCUMENTATION PACKAGE, 04-101899.

 0000001          SUBROUTINE SPRINT(II)                                             546
                                                                                    547
                                                                                    548
 0000041          COMMON X(41,500),V(41,500),P(41,500),T(41,500),                   549
                 1      Z(41),Y(500),                                               550
                 2      A, SIGMA,XMOLC,XKIN,Y AX, Y,                                551
                 3      IP, JP,DX,DT,DYDY,DAPY,DYJ,                                 552
                 4      FILTNE,MAXIT,ETOLC, ACLIP,                                  553
                 5      UVAL,XOP,XK,JPOTL,                                          554
                 6      ALPHA,BETA,PLOSS,TLOSS,                                     555
                 7      IPRINT,ITTY,KOUT                                            556
                                                                                    557
 0000041          DIMENSION  PX(41), VISC(41), DIFF(41), HEAT(41)                   558
            C                                                                       559
            C                                                                       560
            C     COMPUTE PX, DDY, THE AND DIFF TERMS                               561
            C                                                                       562
            C                                                                       563
 0000041          DO 50  I = 1, M                                                   564
 0002801          IP = I + 1                                                        565
 00029E1          IM = I - 1                                                        566
 0002CC1          DO 10  KK = 2, 4                                                  567
 0002D41          CALL SCHUIC (KK, I, II)                                           568
 0002F41   10     CONTINUE                                                          569
 00030A1          IF (I .EQ. 1)  GO TO 20                                           570
 0003201          IF (I .EQ. M)  GO TO 30                                           571
                                                                                    572
 0003341          PX(I) = (P(IP,II)-P(IM,II))/(2.*DX)                               573
 0003461          VISC(I) = (V(IP,II)-2.*V(I,II)+V(IM,II))*XK/(DX*DX)               574
 0003FC1          DIFF(I) = (T(IP,II)-2.*T(I,II)+T(IM,II))*XK/(DX*DX)               575
 0004721          HEAT(I) = UVAL                                                    576
 0004841          GO TO 50                                                          577
                                                                                    578
 0004AA1   20     PX(I) = 0.                                                        579
 00049C1          VISC(I) = 0.                                                      580
 0004AE1          DIFF(I) = 2.*(T(IP,II)-T(I,II))*XK/(DX*DX)                        581
 0005041          HEAT(I) = UVAL                                                    582
 00051A1          GO TO 50                                                          583
                                                                                    584
 0005201   30     P(I) = (P(I,II)-P(IM,II))/DX                                      585
 0005661          VISC(I) = VISC(IM)                                                586
 00057E1          DIFF(I) = DIFF(IM)                                                587
 0005961          HEAT(I) = UVAL                                                    588
                                                                                    589
 0005A31   50     CONTINUE                                                          590
            C                                                                       591
            C                                                                       592
            C     STANDARD PRINTOUT                                                 593
            C                                                                       594
            C                                                                       595
 0005C01          WRITE(IPRINT,100)J,Y(II)                                          596
 0005FA1  100     FORMAT(//// ' FOR  J =' I5 '   (Y =' F4.5 '):')                    597
 0006201          WRITE(IPRINT,120)                                                 598
 00063C1  120     FORMAT(//,'      I      X       U       V        T',              599
                 1  '     XOO      P' 2IX 'PX      DXHURW   KATRR   DIFF' /)        600
 0006A21          DO 140 I=1,MP                                                     601
 0006A61          WRITE(IPRINT,140)I,X(I),U(I,II),V(I,II),T(I,II),1./T(I,II),       602
```

Table A.4--Continued

```
FORTRAN-VIID R04-00
                                                                          09/20/82  11:04:06  PAGE   27        9
FORTRAN VIID: LICENSED RESTRICTED RIGHTS AS STATED IN LICENSE L-0336        ***, SEE DOCUMENTATION PACKAGE, 05-101-99.
 58                    1              P(I,11), PX(I), VISC(I), DIFF(I), HEAT(I)
 59  00060CI    140    FORMAT(5X,I6,6E8.3, 15X, 1E6.3)                                      403
 60  00052AI    160    CONTINUE                                                             404
 61  00083CI           RETURN                                                               405
 62  0003A2I           END                                                                  406
                                                                                            407
NO  ERRORS:F7D  R04-00      SUBROUTINE  SPV[illegible]     09/20/82  11:04:25  TABLE SPACE:    5 KB
STATEMENT BUFFER:    20 LINES/1321 BYTES     STACK SPACE: 171  [illegible]
SINGLE PRECISION FLOATING PT SUPPORT REQUIRED FOR EXECUTION
```

Table A.5

LISTING OF SUBROUTINE MSWEEP

```
FORTRAN-VIID R00-00                                                    09220252  1120216  PAGE  17     10

FORTRAN VIID: LICENSED RESTRICTED RIGHTS AS STATED IN LICE SE L-0536        ***, SEE DOCUMENTATION PACKAGE, 00-101 00,

 0000000T        SUBROUTINE MSWEEP


 0000004T        COMMON  R(41,500),Z(41,500),P(41,500),T(41,500),
                1        X(41),Y(500),
                2        A,SIGMA,RHO,DELTA,[illegible],
                3        DP,DR,DX,DY,DXDY,DXDX,[illegible],
                4        EPSILON,MAXITE,ETORP,MAXITR,
                5        DPAL,XCO,XK,[illegible],
                6        ALPHA,BETA,[illegible],
                7        [illegible],IITY,[illegible]

 0000004T        DIMENSION XX(82),EE(82),AZ(41),A1(41),
                1          A2(41),[illegible](41),B1(41),B2(41),
                2          C2(41),C1(41),C2(41),D2(41),
                3          D1(41),E2(41),[illegible],
                4          DUF(82)


 0000004T        [illegible]
 0014 9A1        [illegible]
 0014 A8T        [illegible] = [illegible] - 1
 0014 B6T        [illegible] = [illegible] - 2
 0014 C4T        [illegible] = [illegible] - 3

 0014 D2T        DO 800 I=1,[illegible]
 0014 E6T        I1=I-1
 0014 F4T        I2=I-2
       C
       C
       C         INITIAL GUESSES FOR [illegible]
       C
       C
 0015 02T        DO 20 I=2,[illegible]
 0015 16T        I1=2*(I-1)-1
 0015 2CT        II=2*(I-1)
 0015 40T        IF(I.EQ.1) GO TO 14
 0015 56T        IF(I .EQ. 2) GO TO 12
       C
       C         LINEAR EXTRAPOLATION USED [illegible]
       C
 0015 6CT        P(I,1)=2.*P(I,I1)-P(I,I12)
 0015 C0T        T(I,1)=2.*T(I,I1)-T(I,I12)
 0016 14T        GO TO 14
       C
       C         PREVIOUS VALUES [illegible] INITIAL GUESSES [illegible] USED FOR I = 1 OR I = 2
       C
 0016 1AT   12   P(I,1)=P(I,I1)
 0016 4ET        T(I,1)=T(I,I1)
 0016 82T   14   CONTINUE
 0016 82T        XX(I1)=P(I,1)
 0016 A0T        XX(II)=T(I,1)
 0016 CET        IF(I.EQ.2)T(I,1)=T(I,1)
 0017 0CT   20   CONTINUE
       C
       C
 0017 24T        DT=DY
```

Table A.5--Continued

```
FORTRAN-V110 R04-06                                                        09/20/82  11:04:06  PAGE   27     11

FORTRAN VIIDI LICENSED RESTRICTED RIGHTS AS STATED IN LICENSE L-6336       ***, SEE DOCUMENTATION PACKAGE, 04-101199,

 0017301          DXDY=DX/DY
 0017421          DYDX=DY/DX
 0017541          CMULT=1.0
 0017601          IF(J.GE.202) CMULT=2.0
 00177C1          IF(J.GE.302) CMULT=4.0
 0017931          IF(J.GE.352) CMULT=8.0
 0017941          IF(J.GE.402) CMULT=16.0
 0017D01          DY=DY*CMULT
 0017F21          DXDY=DXDY/CMULT
 0017F41          DYDX=DYDX*CMULT
 0018061          IF(J.LT.427) GOTO 22
 00181C1          DY=1.0
 0018281          DXDY=DX
 0018341          DYDX=1.0/DX
 0018461   22     CONTINUE
           C
           C
           C
           C      OVERALL VECTOR SOLUTION ITERATION
           C      USING GAUSS ELIMINATION OF LINEAR EQNS.
           C
           C
           C
 0018461          NOUTIT = 0
 00184E1   100    NOUTIT=NOUTIT+1
 00185C1          IF(NOUTIT.GT.MAXIT)GO TO 960


 0018741          DO 200 I=2,NP
 0018861          IM=I-1
 0018961          IP=I+1
 00188A1          IM2=2*(I-1)-1
 00188A1          II=2*(I-1)
 0018CE1          IF(J.EQ.1) JM=1

 0018F61          YMR=Y(IM)/Y(I)
 0019081          XPR=X(IP)/X(I)

 00192A1          KK=2
 0019321          CALL ACFUNC(KK,I,J)
 0019501          KK=3
 0019581          CALL ACFUNC(KK,I,JM)
 0019781          YNUV=XNU
 0019841          KK=4
 00194C1          CALL ACFUNC(KK,I,J)
 0019AC1          KK=4
 0019841          CALL ACFUNC(KK,I,J)
 0019D41          XKP=XK
 0019F01          KK=6
 0019F81          CALL ACFUNC(KK,I,J)
 001A081          KK=5
 001A1G1          CALL ACFUNC(KK,I,J)

 001A301          IF(I.GE.2) GO TO 116
           C
           C
           C      SECTION SETUP FOR I = 1
```

Table A.5--Continued

```
FORTRAN-VIIP R08-00                                                              09/20/82  11:04:06  PAGE   57     12
FORTRAN VIIP: LICENSED RESTRICTED RIGHTS AS STATED IN LICENSE L-0336        ***, SEE DOCUMENTATION PACKAGE, 00-101999.

                C
                C
001A46T                IF(I.GE.IP) GO TO 107
001A5ET                R=0.5*(P(IP,1)-P(IM,1))
001A86T                PI=0.

001A92T                X-I=0.0
001A9ET                DXI=0.0
001AAAT                DXP=X[illegible]/X(I)
001AC4T                DZX[illegible]=[illegible]/X(I)
001AF4T                FF(IP)=(U(IP,1)-2.*U(I,1)+U(IM,1))*[illegible]/DX
                      1        -0.5*(U(IP,1)-U(IM,1))*(U(I,1)/T(I,1)-DX[illegible])-[illegible]
                      2          -D2X*U(I,1)

0010921T               X1=X/X(I)
0014ACT                FF(IT)=(T(IP,1)-2.*T(I,1)+T(IM,1))*XX/D
                      1        -0.5*(T(IP,1)-T(IM,1))*(U(I,1)/T(I,1)-[illegible])*[illegible]

001C4CT                IF(IM.GE.2) GO TO 103
001C62T                AZ(1)=0.0
001C6CT                A1(1)=-2.*X(U/DX-0.5*U(3,1)/T(2,1)-D2X)
001C44T                A2(1)=X[illegible]/DX-0.5*U(2,1)/T(2,1)+0.5*[illegible]
001CD6T                BZ(1)=0.0
001CE0T                B1(1)=0.5*U(3,1)*U(2,1)/(T(2,1)**2)
001D06T                B2(1)=0.0
001D10T                CZ(1)=0.0
001D1AT                C1(1)=-0.5*(T(3,1)/T(2,1)-1.0)
001D3FT                C2(1)=0.0
001D48T                DZ(1)=0.0
001D52T                D1(1)=-XM/DX+0.5*T(3,1)*U(2,1)/(T(2,1)**2)
                      1        +DX*DPR[illegible]-0.5*X0
001DAAT                D2(1)=XK/DX-0.5*U(2,1)/T(2,1)+0.5*X
001DDCT                GO TO 200

001DF2T         103    AZ(IM)=X[illegible]/DX+0.5*U(I,1)/T(I,1)-0.5*[illegible]
001E2CT                A1(IM)=-2.*X(U/DX-0.5*(U(IP,1)-U(IM,1))/T(I,1)-D2X)
001EAAT                A2(IM)=X[illegible]/DX-0.5*U(I,1)/T(I,1)+0.5*[illegible]
001FD4T                BZ(IM)=0.0
001EF6T                B1(IM)=0.5*(U(IP,1)-U(IM,1))*U(I,1)/(T(I,1)**2)
001F46T                B2(IM)=0.0
001F58T                CZ(IM)=0.0
001FAAT                C1(IM)=-0.5*(T(IP,1)-T(IM,1))/T(I,1)
001FAET                C2(IM)=0.0
001FC0T                DZ(IM)=XK/DX+0.5*U(I,1)/T(I,1)-0.5*[illegible]
00200AT                D1(IM)=-2.*XK/DX+0.5*(T(IP,1)-T(IM,1))*U(I,1)
                      1        /(T(I,1)**2)+DX*DPR[illegible]
002094T                D2(IM)=XK/DX-0.5*U(I,1)/T(I,1)+0.5*X)
0020DET                GOTO 200

0020F4T         107    EE=U(MP,1)/T(MP,1)
002106T                FF(IM)=(U(MP,1)-U( ,1))*XMU/DX
                      1        -(EE+0.0)*EE*(T(MP,1)-1.0)-U(MP,1)
0021721T               FF(II)=(T(MP,1)-T( ,1))*XK/DX-(EE*(T(MP,1)-1.0)

0021C2T                AZ(M)=-X[illegible]/DX
002[illegible]F2T              A1(M)=X[illegible]/DX-(2.*EE+0.0)*(1.0-1.0/T(MP,1))
00222CT                A2(M)=0.0
```

Table A.5--Continued

```
FORTRAN-VTIO R04-00                                                        09/20/82  11:04:06  PAGE  47      13

FORTRAN VTIO: LICENSED RESTRICTED RIGHTS AS STATED IN LICENSE L-0336        ***, SEE NOTICE [illegible], 69-101099.

0022AE1           U2(4)=0.0
0022501           U1(M)=F*FF*(1.0-2.0/T(MP,1))-0.0*FF/T(MP,1))
0022A21           W2(M)=0.0
0022A41           C2(M)=0.0
0022F61           C1(M)=-(1.0-1.0/T(MP,1))
0022F61           C2(M)=0.0
00230A1           D2(M)=-XK/DX
0023281           D1(M)=XK/DX-[illegible]/T(MP,1)
0023561           GOTO 200
            C
            C
            C     REGION SET-UP FOR I .GT. 2
            C
            C
00235C1     110   CONTINUE
00235C1           IF(I.GE.MP) GO TO 130
0023741           WW=(U(IP,JP)-2.*U(I,J)+U(IM,JP))*XV*XK
                 1   /(2.*DX)-VP*((U(IP,JP)**2)/T(IP,1))
                 1   -V[illegible]*(U(IP,J)**2)/T(IM,JM)+2.*(U(IP,J)
                 3   -U(IM,J))-0.5*A*DY*(1./T(IP,1))
                 4   -1./T(IM,JM))/4.
0025121           WW=-WW-U(I,JP)*V(I,JM)/T(I,JP)*DXDY
00257A1           PI=-((T(IP,J)-2.*T(I,JP)+T(IM,JP))*XK*
                 1   /(2.*DX)-(VP*U(IP,JP)-VM*U(IM,J))/4.*V(I,JP)*DXDY)

00265E1           X=0.0
00266A1           DX=0.0
0026761           DXO=XK/X(I)
0026901           D2XO=DX*DXO/X(I)
00269A1           FF(I)=(U(IP,J)-2.*U(I,J)+U(IM,J))*XK
                 1        /(2.*DX)-0.25*(VP*(U(IP,J)**2)/T(IP,J)
                 2        -VM*(U(IM,J)**2)/T(IM,J)-0.5*A*DY
                 3        *(1./T(IP,J)-1./T(IM,J))-U(I,J)*
                 4        (DXDY*V(I,JP)/T(I,JP)-0.25*U(IP,J)*VP*
                 5        /T(IP,J)*VP*U(IP,JP)/T(IP,JP)-U(IM,J)*VM
                 6        /T(IM,J)-VM*U(IM,JM)/T(IM,JM))-DX
                 7      *0.25*DXO*(U(IP,J)-U(IM,J)*U(IP,JP)-U(IM,J))
                 8          -0.5*D2XO*(U(I,J)*U(I,J))

002A321           XI=XK/X(I)
002AAC1           FF(II)=(T(IP,J)-2.*T(I,J)+T(IM,J))*XK
                 1        /(2.*DX)-0.25*(VP*U(IP,J)-VM*U(IM,J))
                 2        -T(I,J)*(DXDY*V(I,JP)/T(I,JP)-0.25
                 3        *(VP*U(IP,J)/T(IP,J)*VP*U(IP,JP)/T(IP,JP)
                 4        -VM*U(IM,J)/T(IM,J)-VM*U(IM,JM)/T(IM,JM)))
                 5        +DX*QVAL-P)
                 6       +0.25*XI*(T(IP,J)-T(IM,J)*T(IP,JP)-T(IM,J))


002CFA1           IF(MP.GT.2)GO TO 120
002CFA1           A2(1)=0.0
002D0A1           B1(1)=-2.*XK/(2.*DX)-(DXDY*V(2,JM)/T(2,J))
                 1        -0.25*(U(3,J)/T(3,J)*U(3,JP)/T(3,JP))-0.5*D2XO
002DC21           B2(1)=XK/(2.*DX)-0.25*VP*(2.*U(3,J)-U(2,J))/T(3,J)
                 1        +0.25*DXO
002E3A1           B2(1)=0.0
```

Table A.5--Continued

```
FORTRAN-VIID R0A-00
[illegible]
```

Table A.5--Continued

```
FORTRAN-VIID R04-00                                              09/20/82  11:03:06  PAGE  67      15

FORTRAN VIID: LICENSED RESTRICTED RIGHTS AS STATED IN LICENSE L-0336        ***, SEE DOCUMENTATION PACKAGE, 04-191990.

                          1        -2.0*D.DAFF/(T(IM,I)+T(MP,IM))
       003CC21               B2(IM)=0.0
       003CD41               C2(IM)=0.0
       003CF61               C1(IM)=2.0/(T(IM,I)+T(MP,IM))-1.0
       003D141               C2(IM)=0.0
       003D461               D2(IM)=-VK/DX
       003D661               D1(IM)=XK/DX-2.0*DAFF/(T(MP,I)+T(MP,IM))
       003DC21               D2(IM)=0.0

       003D041       200     CONTINUE
                      C
                      C
                      C      SPARSE (JACOBIAN) MATRIX COMPACTIFICATION
                      C
                      C
       003DFE1               DO 250 IM=1,M
       003E001               ID=2*IM-1
       003E101               II=2*IM
       003E1E1               VMAT(1,ID)=0.0
       003E361               VMAT(2,ID)=A2(IM)
       003E541               VMAT(3,ID)=B2(IM)
       003E721               VMAT(4,ID)=A1(IM)
       003E961               VMAT(5,ID)=B1(IM)
       003EAE1               VMAT(6,ID)=A2(IM)
       003ECE1               VMAT(7,ID)=B2(IM)
       003EFA1               VMAT(1,II)=C2(IM)
       003F0A1               VMAT(2,II)=D2(IM)
       003F261               VMAT(3,II)=C1(IM)
       003F441               VMAT(4,II)=D1(IM)
       003F621               VMAT(5,II)=C2(IM)
       003F801               VMAT(6,II)=D2(IM)
       003F9E1               VMAT(7,II)=0.0
       003FB61       250     CONTINUE
                      C
                      C
                      C      GAUSS ELIMINATION TO SOLVE  ID=-I
                      C
                      C
       003FCE1               DO 500 I=1,NM
       003FF21               KMAX=3
       003FFA1               IF(I.EQ.NM2) KMAX=2
       0040041               IF(I.EQ.NM) KMAX=1

       00401E1               DO 490 K=1,KMAX
       0040321               IK=I+K
       0040441               NMK=4-K
       0040521               PIVOT=VMAT(NMK,IK)/VMAT(4,I)

       0040621               DO 485 LL=4,7
       0040841               LL=LL-K
       00409C1               VMAT(L,IK)=VMAT(L,IK)-PIVOT*VMAT(LL,I)
       0040FC1       485     CONTINUE

       0041021               FF(IK)=FF(IK)-PIVOT*FF(I)
       00412E1       490     CONTINUE
       0041461       500     CONTINUE
```

Table A.5--Continued

```
FORTRAN-VIID R04-00                                                        09/20/82  11:04:06  PAGE  77     16

FORTRAN VIID: LICENSED RESTRICTED RIGHTS AS STATED IN TITLE ISP L-0336        ***, SEE DOCUMENTATION PACKAGE, 04-101299.

0041SEI          ZZZ=0.0
0041AAI          IF(I.GE.1000) GOTO 510
00418DI          WRITE(IPRINT,502)
0041BCI   502    FORMAT(/////)
0041AAI          DO 510 IR=1,NN
0041BEI          WRITE(IPRINT,505) XMAT(1,IR),XMAT(2,IR),XMAT(3,IR),
                1          XMAT(4,IR),XMAT(5,IR),XMAT(6,IR),XMAT(7,IR)
0042ACI   505    FORMAT(7F10.4)
0042BAI   510    CONTINUE

004202I          DDEX(IN)=-FF(I N)/XMAT(4,NN)
0043061          DDEX(NN+1)=-(FF(NN+1)*XMAT(5,NN)+DDEX(NN))/XMAT(4,NN)
004358I          DDEX(NN+2)=-(FF(NN+2)+XMAT(6,NN+2)*DDEX(NN)
                1                 +XMAT(6,NN+2)*DDEX(NN+1))/XMAT(4,NN+2)

0043CAI          DO 550 I=1,NN
0043DFI          IN=NN-2-I
0043E0I          XXX=FF(IN)
004404I          DO 540 K=5,7
00440CI          INP=IN+K-4
004420I          XXX=XXX+XMAT(K,IN)*DDEX(INP)
004450I   540    CONTINUE
004466I          DDEX(IN)=-XXX/XMAT(4,IN)
004492I   550    CONTINUE
          C
          C
          C      CHECK FOR MEMBER CONVERGENCE
          C
          C
0044AAI          IFLAG=0
004492I          DO 420 IN=1,NP
0044C6I          XX(IN)=XX(IN)+DDEX(IN)
0044FEI          IF(ABS(DDEX(IN)).GT.EPS)IFLAG=1
00452EI   420    CONTINUE

004584I          DO 450 I=2,NP
00455BI          IO=2*(I-1)-1
00456FI          II=2*(I-1)
004582I          P(I,J)=XX(IO)
0045AAI          T(I,1)=XX(II)
0045D2I          IF(I.LE.2)T(1,1)=T(I,1)
00461DI   450    CONTINUE

00462BI          IF(IFLAG.EQ.0)GO TO 700
00463EI          GO TO 100
          C
          C
          C      SUCCESSFUL LINKS FOR ITERATION
          C
          C
004682I   700    CONTINUE

004642I          DO 750 I=1,NP

004656I          IF (I .EQ. 1)  GO TO 750

00466CI          IP=I+1
```

Table A.5--Continued

```
FORTRAN-VIID R04-06                                                   09/20/82  11:04:06  PAGE   87     17

FORTRAN VIID: LICENSED RESTRICTED RIGHTS AS STATED IN LICENSE L-0336      ***, SEE DOCUMENTATION PACKAGE, R0-101009,

0046A7A1          IF(I.EQ.N)IP=1
0046A98I          I0=I-1
0046A6AI          IF(I.EQ.1) GO TO 730
0046A9C1          FRAC=0.25
0046ACA1          IF(I.EQ.1)FRAC=0.5
0046AE41          IF(I.EQ.N)FRAC=0.5

0047021           [illegible]
0047241           [illegible]


00474A61          V(I,1)=Z(I,IP)*Z(1,J)/Z(I,1) [illegible]
                1       [illegible]
                2       [illegible]
                3       /Z(IP,JP))

0048CA1    730    V(I,1)=V(I,JP)-0.5*A*(Y*(1./Z(I,1)+1./Z(I,1))

0049521    750    CONTINUE
00496A1           IF(I.EQ.1) GO TO 800
0049A01           V(1,1)=2.0*V(2,1)-V(3,1)

0049C21    800    CONTINUE
00490A1           GO TO 940
           C
           C
           C      ERROR RETURN - NO CONVERGENCE
           C
           C
0049E01    900    CONTINUE
0049F01           WRITE(IPRINT,905) I, [illegible]
004A081    905    FORMAT(///,' [illegible] CONVERGENCE [illegible]',
                1       [illegible]
004A601           [illegible]
004A681           DO 920 IA=1,I
004A7C1           CALL [illegible](IA)
004A941    920    CONTINUE
           C      STOP 1

004AAC1    940    CONTINUE
004AAC1           RETURN
004AB41           END

NO  ERRORS:F70  R04-00     SUBROUTINE  [illegible]    09/20/82  11:04:55  TABLE SPACE:   [illegible]
STATEMENT BUFFER:   [illegible] BYTES     STACK SPACE: [illegible] WORDS
SINGLE PRECISION FLOATING PT SUPPORT REQUIRED FOR EXECUTION
```

REFERENCES

Brode, H. L., D. A. Larson, and R. D. Small, *Time-Dependent Model of Flows Generated by Large Area Fires*, Pacific-Sierra Research Corporation, Note 483, July 1982.

Countryman, C. M., *PROJECT FLAMBEAU . . . An Investigation of Mass Fire (1964-1967)*, Vol. 1, U.S. Department of Agriculture, U.S. Forest Service, Berkeley, California, 1969.

DCPA Attack Environmental Manual, Chap. 3, "What the Planner Needs To Know about Fire Ignition and Spread," U.S. Defense Civil Preparedness Agency and U.S. Department of Defense, Washington, D.C., June 1973.

Isaacson, E., and H. B. Keller, *Analysis of Numerical Methods*, Wiley, New York, 1966.

Johnson, L. E., and D. A. Larson, *Neglected Effects in Nuclear Warfare Simulation*, Pacific-Sierra Research Corporation, Note 438, May 1982.

Keller, H. B., *Numerical Methods for Two-Point Boundary-Value Problems*, Blaisdell, Waltham, Massachusetts, 1968.

Morton, B. R., G. I. Taylor, and J. S. Turner, "Turbulent Gravitational Convection from Maintained and Instantaneous Sources," *Proc. Roy. Soc. A.*, Vol. 24, 1956, pp. 1-23.

Murgai, M. P., and H. W. Emmons, "Natural Convection above Fires," *J. Fluid Mech.*, Vol. 8, 1960, pp. 611-624.

Nielsen, H. J., and L. N. Tao, "The Fire Plume above a Large Free-Burning Fire," *Tenth Symposium (International) on Combustion*, The Combustion Institute, Pittsburgh, 1965, pp. 965-972.

Palmer, T. Y., "Large Fire Winds, Gases and Smoke," *Atmos. Environment*, Vol. 15, No. 10/11, 1981, pp. 2079-2090.

Small, R. D., D. A. Larson, and H. L. Brode, *Analysis of Large Urban Fires*, Pacific-Sierra Research Corporation, Report 1122, September 1981.

Smith, R. K., B. R. Morton, and L. M. Leslie, "The Role of Dynamic Pressure in Generating Fire Wind," *J. Fluid Mech.*, Vol. 68, 1975, pp. 1-19.

Thomas, P. H., "The Size of Flames from Natural Fires," *Ninth International Symposium on Combustion*, The Combustion Institute, Pittsburgh, 1963, pp. 844-859.

Yokoi, S., *Study on the Prevention of Fire-Spread Caused by Hot Upward Current*, Japanese Ministry of Construction, Building Research Institute, Report 34, November 1960.

DISTRIBUTION LIST

National Addresses

Air Force Weapons Laboratory
Attn: Civil Engineering Division
Kirtland Air Force Base
Albuquerque, NM 87117 (1)

Air Force Weapons Laboratory
Attn: SUL Technical Library
Kirtland Air Force Base
Albuquerque, NM 87117 (1)

Mr. Raymond Alger
SRI International
Menlo Park, CA 94025 (1)

Mr. Norman J. Alvares
Lawrence Livermore National Laboratory
University of California
P.O. Box 808, L-442
Livermore, CA 94550 (1)

Assistant Director
Energy and Natural Resources
Office of Science and Technology Policy
Executive Office Building
Washington, D.C. 20500 (1)

Assistant Secretary of the Army (RD&A)
Attn: Deputy ASA for RD&S
The Pentagon
Washington, D.C. 20301 (1)

Dr. Jana Backovsky
SRI International
Menlo Park, CA 94025 (1)

Mr. A. P. Brackebush
Forest Fire Research
Northern Forest Fire Laboratory
Missoula, MT 59801 (1)

Mr. Clay P. Butler
SRI International
Menlo Park, CA 94025 (1)

Center for Planning and Research, Inc.
Attn: Document Library
2483 East Bayshore Road, Suite 104
Palo Alto, CA 94303 (1)

Dr. Craig Chandler, Director
Forest Fire & Atmospheric Science Research
U.S. Forest Service
Department of Agriculture
Washington, D.C. 20013 (1)

Dr. Conrad Chester
Oak Ridge National Laboratory
P.O. Box X
Oak Ridge, TN 37830 (1)

Chief of Engineers
Department of the Army
Attn: DAEN-RDZ-A
Washington, D.C. 20314 (1)

Dr. William F. Christian
Underwriters' Laboratories, Inc.
333 Pfingsten Road
Northbrook, IL 60062 (1)

Civil Engineering Center/AF/PRECET
Wright-Patterson Air Force Base, OH 45433 (1)

Dr. John Cockayne
Senior Scientist
Science Applications, Inc.
1710 Goodridge Drive
McLean, VA 22102 (1)

Defense Technical Information Center (DTIC)
Cameron Station
Alexandria, VA 22314 (12)

Department of Defense
Command and Control Technical Center
Attn: Office of the Director
The Pentagon
Washington, D.C. 20301 (1)

Department of Energy
Attn: Director, Department of Military Application
Washington, D.C. 20545 (1)

The Dikewood Corporation
Attn: Document Library
1613 University Boulevard, N.E.
Albuquerque, NM 87102 (1)

Director
Defense Nuclear Agency
Attn: Michael Frankel
Washington, D.C. 20305 (1)

Director
Defense Nuclear Agency
Attn: LtCol. David H. Thomas, USAF
Washington, D.C. 20305 (1)

Director
Lovelace Foundation
5200 Gibson Boulevard, S.E.
Albuquerque, NM 87108 (1)

Director, U.S. Army Ballistic Research Laboratory
Attn: Document Library
Aberdeen Proving Grounds, MD 21005 (1)

Director, U.S. Army Ballistic Research Laboratory
Attn: Mr. William Taylor
Aberdeen Proving Grounds, MD 21005 (2)

Director, U.S. Army Engineer Waterways Experiment Station
Attn: Document Library
P.O. Box 631
Vicksburg, MS 39180 (1)

Director, U.S. Army Engineer Waterways Experiment Station
Attn: Mr. W. L. Huff
P.O. Box 631
Vicksburg, MS 39180 (1)

Director, U.S. Army Materials and Mechanics Research Center
Attn: Technical Library
Watertown, MA 02172 (1)

Mr. Marvin Drake
Science Applications, Inc.
1250 Prospect Street
La Jolla, CA 92037 (1)

Mr. Donald Drzewiecki
Calspan Corporation
P.O. Box 400
Buffalo, NY 14225 (1)

Factory Mutual Research Corporation
Attn: Dr. Ray Friedman
1151 Boston-Providence Turnpike
Norwood, MA 02062 (1)

Federal Emergency Management Agency
Attn: Assistant Associate Director for Research
National Preparedness Programs Directorate
Washington, D.C. 20472 (3)

Federal Emergency Management Agency
Attn: David W. Bensen
Office of Research
National Preparedness Programs Directorate
Washington, D.C. 20472 (45)

Dr. Francis E. Fendell
R1/1038
TRW
One Space Park
Redondo Beach, CA 90278 (1)

Fire Research Library
National Bureau of Standards
Building 224, Room A-246
Washington, D.C. 20234 (1)

Mr. Dick Foster
SRI International
1611 Kent Street
Arlington, VA 22209 (1)

Dr. Robert Fristrom
Johns Hopkins Applied Physics Laboratory
Johns Hopkins Road
Laurel, MD 20810 (1)

Dr. Matthew G. Gibbons
5424 Lawton Avenue
Oakland, CA 94618 (1)

Mr. Edward L. Hill
Research Triangle Institute
P.O. Box 12194
Research Triangle Park,
NC 27709 (1)

Dr. Dennis Holliday
R&D Associates
P.O. Box 9695
Marina del Rey, CA 90291 (1)

Hudson Institute
Attn: Library
Quaker Ridge Road
Croton-on-Hudson, NY 10520 (1)

Mr. Peter S. Hughes
Los Alamos Technical Associates,
Inc.
P.O. Box 410
Los Alamos, NM 87544 (2)

Mr. Robert G. Hutman
Nuclear Test Engineering
Division
Lawrence Livermore National
Laboratory
University of California
P.O. Box 808
Livermore, CA 94550 (1)

Professor A. Murty Kanury
Department of Aerospace and
Mechanical Engineering
University of Notre Dame
Notre Dame, IN 46556 (1)

Mr. Kenneth Kaplan
#30 White Plains Court
San Mateo, CA 94402 (1)

Mr. Samuel Kramer
National Bureau of Standards
Building 225, Room B-124
Washington, D.C. 20234 (1)

Mr. Richard Laurino
Center for Planning and
Research, Inc.
2483 East Bayshore Road,
Suite 104
Palo Alto, CA 94303 (1)

Dr. Anatole Longinow
IIT Research Institute
10 West 35th Street
Chicago, IL 60616 (1)

Los Alamos Scientific Laboratory
Attn: Document Library
Los Alamos, NM 87544 (1)

Mr. Stanley B. Martin
Stan Martin and Associates
860 Vista Drive
Redwood City, CA 94062 (1)

Dr. Clarence R. Mehl
Sandia National Laboratories
Division 7112
P.O. Box 5800
Albuquerque, NM 87185 (1)

Mr. Joseph E. Minor
Texas Technological College
Lubbock, TX 79408 (1)

Mr. H. L. Murphy
P.O. Box 1727
San Mateo, CA 94401 (1)

National Council on Radiation
Protection and Measurements
Attn: Library
7910 Woodmont Avenue
Bethesda, MD 20014 (1)

National Fire Protection Association
Library
Batterymarch Park
Quincy, MA 02269 (1)

Oak Ridge National Laboratory
Attn: Librarian
P.O. Box X
Oak Ridge, TN 37830 (1)

Oak Ridge National Laboratory
Attn: Emergency Technology Division
Librarian
P.O. Box X
Oak Ridge, TN 37830 (1)

Dr. Fred Offensend
SRI International
Menlo Park, CA 94025 (1)

Mr. William Parker
National Bureau of Standards
Building 224, Room A-345
Washington, D.C. 20234 (1)

Professor R. K. Pefley
University of Santa Clara
Santa Clara, CA 95053 (1)

Mr. Laurence Pietrzak
Mission Research Corporation
P.O. Drawer 719
Santa Barbara, CA 93102 (1)

President
International Association of Fire Fighters
1750 New York Avenue, N.W. (3rd Floor)
Washington, D.C. 20006 (1)

Chief Robert G. Purington
Lawrence Livermore National Laboratory
University of California
P.O. Box 808, L-519
Livermore, CA 94550 (1)

The Rand Corporation
Attn: Document Library
1700 Main Street
Santa Monica, CA 90406 (1)

Mr. John Rempel
Center for Planning and Research
2483 East Bayshore Road, Suite 104
Palo Alto, CA 94303 (1)

Dr. John Rockett
National Bureau of Standards
Center for Fire Research
Building 224, Room B-260
Washington, D.C. 20234 (1)

Mr. Harvey G. Ryland
Ryland Research, Inc.
5266 Hollister Avenue, Suite 324
Santa Barbara, CA 93111 (1)

Dr. Donald Sachs
Kaman Sciences Corporation
2001 Jefferson Davis Highway
Arlington, VA 22202 (1)

Mr. Fred Sauer
Physics International Company
2700 Merced Street
San Leandro, CA 94577 (1)

Dr. Don Scheuch
430 Golden Oak Drive
Portola Valley, CA 94025 (1)

Mr. Leo A. Schmidt
Institute for Defense Analyses
Program Analysis Division
1801 N. Beauregard Street
Alexandria, VA 22311 (1)

Mrs. Ruth W. Schnider
Center for Planning and Research, Inc.
2483 East Bayshore Road, Suite 104
Palo Alto, CA 94303 (1)

Southwest Research Institute
Department of Fire Technology
P.O. Drawer 2851D
San Antonio, TX 78284 (1)

Dr. Lewis V. Spencer
National Bureau of Standards
Center for Radiation Research
Building 245, Room C-313
Washington, D.C. 20234 (1)

Mr. Walmer E. Strope
Center for Planning and Research, Inc.
5600 Columbia Pike, Suite 101
Bailey's Crossroads, VA 22041 (1)

Technology & Management Consultants
330 Washington Street
Suite 613
Marina del Rey, CA 90291 (1)

U.S. Army Combined Arms Combat Development Activity
Fort Leavenworth, KA 66027 (1)

U.S. Army Training and Doctrine Command
Fort Monroe
Hampton, VA 23651 (1)

U.S. Forest Service
Attn: Dr. A. Broido
P.O. Box 245
Berkeley, CA 94710 (1)

Mr. Thomas Watermann
IIT Research Institute
10 West 35th Street
Chicago, IL 60616 (2)

Mr. Carl Wiehle
Defense Intelligence Agency
Attn: WDB-4C2
Washington, D.C. 20301 (1)

Dr. Forman Williams
Department of the Aerospace and Engineering Sciences
University of California at San Diego
La Jolla, CA 92037 (1)

Mr. C. Wilton
Scientific Service, Inc.
517 East Bayshore Drive
Redwood City, CA 94060 (2)

<u>International Addresses</u>

Almannavarnir Rikisins
Reykjavik, Iceland (1)

Bundesministerium des Innern
Graurheindorfer Strasse 198
5300 Bonn 1
West Germany (1)

Canadian Defence Research Staff
Attn: Dr. K. N. Ackles
2450 Massachusetts Ave., N.W.
Washington, D.C. 20008 (4)

Civil Defense Administration
Ministry of Interior
Ankara, Turkey (1)

Civil Emergency Planning Directorate
North Atlantic Treaty Organization
1110 NATO, Belgium (1)

Directeur Organisatie
Bescherming Bevoling
Ministry of Interior
Schedeldoekshaven 200
Postbus 20011
2500 The Hague, Netherlands (1)

Directeur de la Protection Civile
Ministere de l'Interieur
36 Rue J. B. Esch
Grand-Duche de Luxembourg (1)

Direction de la Securite Civile
Ministere de l'Interieur
18 Rue Ernest Cognac
92 Levallois (Paris) France (1)

Director
Civilforsvarsstyrelsen
Stockholmsgade 27
2100 Copenhagen O
Denmark (1)

Forest Fire Research Institute
The Information Center
331 Cooper Street
Ottawa, Ontario KIA 043
Canada (1)

Brigadier I.G.C. Gilmore
Director, Australian Counter Disaster College
Mount Macedon, Victoria 3441
Australia (1)

The Head of Sivilforsvaret
Sandakerveien 12
Postboks 8136
Oslo dep
Oslo 1, Norway (1)

Home Office
Scientific Advisory Branch
Horseferry House
Dean Ryle Street
London SW1P 2AW
England (1)

Jefe, Seccion de Estudios y
  Planification
c/Evaristo San Miguel, 8
Madrid-8
Spain (1)

Ministero dell Interno
Direzione Generale della
  Protezione Civile
00100 Rome, Italy (1)

Ministry of Social Services
11 Spartis Street
Athens, Greece (1)

Secretaire d'Administration
Ministere de l'Interieur
Direction Generale de la
  Protection Civile
Rue de Louvain, 1
1000 Brussels, Belgium (1)

Dr. Ing. P.G. Seeger
Forschungsstelle fur
  Brandschutztechnik
University of Karlsruhe (TH)
75 Karlsruhe 21
Postfach 63380
West Germany (1)

Servico National de
  Proteccao Civil
Rua Bela Vista a Lapa, 57
1200 Lisbon, Portugal (1)

Dr. Vilhelm Sjolin
Director of BRANDFORSK
The Swedish Fire Research Board
S-115 87 Stockholm
Sweden (1)

Stato Maggiore Difesa Civile
Centro Studi Difesa Civile
Rome, Italy (1)

ANALYSIS OF THE LARGE URBAN FIRE ENVIRONMENT
Part II. Parametric Analysis and Model City Simulations
Unclassified

D. A. Larson and R. D. Small
Pacific-Sierra Research Corporation
12340 Santa Monica Boulevard, Los Angeles, California 90025

PSR Report 1210, November 1982, 120 pp., Contract EMW-C-0747, Work Unit 2564E

This report considers the fire environment that would result from a megaton-yield nuclear weapon explosion. An analysis (developed in Part I) that treats the physics of the burning zone and the volume immediately above it (turning region) is used to predict the velocity, temperature, and pressure fields of large area fires.

A sensitivity study explores the influence of turbulence, radiation, fire size, and burning intensity on the mean temperature levels and velocity fields. The results show hurricane-force velocities developing as the fire size or burning rate is increased. A sample calculation illustrates the change in fire-wind velocities as the fire evolves over time.

Calculations of the burning region for three model urban areas show the influence of building density and urban sprawl on the resulting fire environment. An additional set of predictions accounts for reduction of the fire intensity by blast in the urban center. For the latter cases, the temperature distribution is changed markedly, though the magnitude of the induced fire winds is not appreciably reduced.

ANALYSIS OF THE LARGE URBAN FIRE ENVIRONMENT
Part II. Parametric Analysis and Model City Simulations
Unclassified

D. A. Larson and R. D. Small
Pacific-Sierra Research Corporation
12340 Santa Monica Boulevard, Los Angeles, California 90025

PSR Report 1210, November 1982, 120 pp., Contract EMW-C-0747, Work Unit 2564E

This report considers the fire environment that would result from a megaton-yield nuclear weapon explosion. An analysis (developed in Part I) that treats the physics of the burning zone and the volume immediately above it (turning region) is used to predict the velocity, temperature, and pressure fields of large area fires.

A sensitivity study explores the influence of turbulence, radiation, fire size, and burning intensity on the mean temperature levels and velocity fields. The results show hurricane-force velocities developing as the fire size or burning rate is increased. A sample calculation illustrates the change in fire-wind velocities as the fire evolves over time.

Calculations of the burning region for three model urban areas show the influence of building density and urban sprawl on the resulting fire environment. An additional set of predictions accounts for reduction of the fire intensity by blast in the urban center. For the latter cases, the temperature distribution is changed markedly, though the magnitude of the induced fire winds is not appreciably reduced.

ANALYSIS OF THE LARGE URBAN FIRE ENVIRONMENT
Part II. Parametric Analysis and Model City Simulations
Unclassified

D. A. Larson and R. D. Small
Pacific-Sierra Research Corporation
12340 Santa Monica Boulevard, Los Angeles, California 90025

PSR Report 1210, November 1982, 120 pp., Contract EMW-C-0747, Work Unit 2564E

This report considers the fire environment that would result from a megaton-yield nuclear weapon explosion. An analysis (developed in Part I) that treats the physics of the burning zone and the volume immediately above it (turning region) is used to predict the velocity, temperature, and pressure fields of large area fires.

A sensitivity study explores the influence of turbulence, radiation, fire size, and burning intensity on the mean temperature levels and velocity fields. The results show hurricane-force velocities developing as the fire size or burning rate is increased. A sample calculation illustrates the change in fire-wind velocities as the fire evolves over time.

Calculations of the burning region for three model urban areas show the influence of building density and urban sprawl on the resulting fire environment. An additional set of predictions accounts for reduction of the fire intensity by blast in the urban center. For the latter cases, the temperature distribution is changed markedly, though the magnitude of the induced fire winds is not appreciably reduced.

ANALYSIS OF THE LARGE URBAN FIRE ENVIRONMENT
Part II. Parametric Analysis and Model City Simulations
Unclassified

D. A. Larson and R. D. Small
Pacific-Sierra Research Corporation
12340 Santa Monica Boulevard, Los Angeles, California 90025

PSR Report 1210, November 1982, 120 pp., Contract EMW-C-0747, Work Unit 2564E

This report considers the fire environment that would result from a megaton-yield nuclear weapon explosion. An analysis (developed in Part I) that treats the physics of the burning zone and the volume immediately above it (turning region) is used to predict the velocity, temperature, and pressure fields of large area fires.

A sensitivity study explores the influence of turbulence, radiation, fire size, and burning intensity on the mean temperature levels and velocity fields. The results show hurricane-force velocities developing as the fire size or burning rate is increased. A sample calculation illustrates the change in fire-wind velocities as the fire evolves over time.

Calculations of the burning region for three model urban areas show the influence of building density and urban sprawl on the resulting fire environment. An additional set of predictions accounts for reduction of the fire intensity by blast in the urban center. For the latter cases, the temperature distribution is changed markedly, though the magnitude of the induced fire winds is not appreciably reduced.

PSR Report 1210

ANALYSIS OF THE LARGE URBAN FIRE ENVIRONMENT

Part II. Parametric Analysis and Model City Simulations

Summary

By
D. A. Larson
R. D. Small

November 1982

Final Report
Contract EMW-C-0747, Work Unit 2564E

For
Federal Emergency Management Agency
National Preparedness Programs
Washington, D.C. 20472

FEMA Review Notice

This report has been reviewed in the Federal Emergency Management Agency and approved for publication. Approval does not signify that the contents necessarily reflect the views and policies of the Federal Emergency Management Agency.

Approved for Public Release: Distribution Unlimited

PACIFIC-SIERRA RESEARCH CORP.
12340 Santa Monica Blvd. • Los Angeles, CA 90025 • (213) 820-2200

SUMMARY

This report considers the large-fire environment that would occur in an urban area subject to a nuclear weapon explosion. The effects of system parameters are explored in a sensitivity study, and results for three model cities are presented.

The examples are characterized by extensive areas simultaneously burning, strong buoyancy, and large temperature gradients. Several such fires occurred during World War II. Though those fires were dramatic in intensity and destructiveness, each involved a relatively small area. A nuclear weapon explosion could generate a far larger area fire and a more severe fire environment. This report is intended to define such large fires. The results should be applicable for damage evaluation, formulation of shelter requirements, and rescue planning.

The calculations are based on the theory developed in Part I of this report, which is applicable to the fire zone and the volume immediately above it (turning region). The effects of variable area heating, turbulence, strong buoyancy, large temperature changes, and radiation are treated. The induced fire winds and rapid temperature changes at the fire periphery are uniquely determined by the use of jump conditions. Simulations of the Hamburg firestorm and a large Flambeau fire agreed well with available data.

The parametric analysis considers a large area fire and the effects of fire size, heating rates, mixing coefficients, and hot gas/smoke radiation. The results show the influence of those variables on the induced fire winds, mean temperature, and pressure gradients. In general, an increase in either the fire size or heating rate raises the mean temperature levels and the induced fire-wind velocities. For the larger heat release rates or fire sizes, the attendant increases in mean temperature and velocity are limited by compressibility effects.

Fires such as may result from a megaton-yield explosion are analyzed for three model urban areas. Each city is characterized by

a high-density center, a surrounding belt of mixed residential/industrial construction, and a lower density suburban belt. Each model city portrays a different degree of building density and urban sprawl. The results illustrate how a particular city geometry affects the velocity and temperature fields for a given fire. An additional series of computations considers reduction of the fire area by severe blast damage and debris formation. For those calculations, complete burning was allowed in an annular area, with the fire intensity significantly reduced in the center.

Finally, the model is employed to estimate the behavior of the velocity and temperature fields as a function of fire evolution. Those calculations may indicate the most appropriate periods for effecting rescue operations as well as provide an estimate of time-dependent shelter loadings.